농학석사 학위논문

Thiol-ene/Thiol-epoxy Dual Curing Systems of Bio-based Epoxy Resins Modified with Soybean Oil Derivatives

대두유 유도체로 개질된 바이오 에폭시 수지의 싸이올-앤/싸이올-에폭시 이중경화 시스템

2022년 2월

서울대학교 대학원

농림생물자원학부 환경재료과학 전공

김 리 나

Thiol-ene/Thiol-epoxy Dual Curing Systems of Bio-based Epoxy Resins Modified with Soybean Oil Derivatives

지도교수 김 현 중

이 논문을 농학석사 학위논문으로 제출함
2021년 12월

서울대학교 대학원
농림생물자원학부 환경재료과학 전공
김 리 나

김리나의 석사 학위논문을 인준함
2022년 1월

위 원 장 윤 혜 정 (인)

부위원장 김 현 중 (인)

위 원 오 정 권 (인)

Abstract

Thiol-ene/Thiol-epoxy Dual Curing Systems of Bio-based Epoxy Resins Modified with Soybean Oil Derivatives

Li-Na Kim

Program in Environmental Materials Science

The Graduate School

Seoul National University

Diglycidyl ether of bisphenol A (DGEBA) is a representative epoxy resin based on petroleum resources and is mainly composed of bisphenol A, a substance that disturbs the endocrine system. It is known that epoxy curing agents used with epoxy resins as well as epoxy resins are highly toxic and negatively affect the human body and environment when exposed. As these environmental and health risks continue to be raised, demand for bio-based polymers to replace petroleum-based polymer materials is increasing.

Therefore, in this study, chemically deformable and commercially available soybean oil-based epoxy resins were proposed as DGEBA

substitutes for the purpose of developing sustainable epoxy networks. Furthermore, as an alternative to more sustainable epoxy curing agents, new thiol-functionalized polysiloxane oligomers that are non-toxic and do not depend on petroleum were synthesized using the sol-gel method.

The synthesized thiol-functionalized polysiloxane oligomer is composed of molecules having a siloxane (Si-O-Si) network structure, so it was intended to improve the low reactivity and non-selective reactivity of vegetable oil by forming an organic-inorganic hybrid network. As a result, the thiol-ene/thiol-epoxy network was obtained by adding stoichiometric equivalents of thiol-functionalized polysiloxane oligomers to acrylated epoxidized soybean oil (AESO) and epoxidized soybean oil (ESO), respectively, and then sequentially applying UV and thermal curing reactions.

In the dual curing systems, the combination of photopolymerization and thermal polymerization could improve the mechanical properties and crosslinking density of the formed thiol-ene/thiol-epoxy network. In particular, 75A/25E samples among the dual-cured samples showed superior crosslinking density, glass transition temperature, and storage modulus values than the cured thiol-ene and thiol-epoxy networks alone.

Among the synthesized epoxy curing agents, TSQ oligomers have been found to further improve the crosslinking density, mechanical properties, and antibacterial properties as well as thiol-ene polymerization rates compared to TSO oligomers. On the other hand, the amount of volatile organic compound (VOC) released by TSO oligomers was lower than that of TSQ oligomers. These attempts to overcome the limitations of soybean oil-based epoxy resins are

expected to build sustainable epoxy networks in the future.

Keywords : Thiol-ene/Thiol-epoxy, Dual curing, Polysiloxane, Epoxidized soybean oil, Organic-inorganic networks, Crosslinking density

Student Number : 2020-28661

Table of Contents

Synthesis of Thiol-functionalized Polysiloxane

Chapter 3

Formation of Thiol-ene/Thiol-epoxy Hybrid Networks

List of Tables

List of Figures

Chapter 1

Introduction,
Objectives and
Literature Review

1. Introduction

1.1. Problems of bisphenol A-based epoxy resins

Epoxy resin is one of the most important materials as thermosetting polymers widely used throughout the industry due to its excellent mechanical properties and excellent resistance to heat or corrosion (Graiver, D. et al., 2003). Epoxy networks generally consist of additives such as epoxy resins, curing agents, and curing accelerators or a reactive diluent, and is a typical thermosetting resin in which a linear structure is changed to a three-dimensional cross-linked structure through a thermal curing process (Karger-Kocsis, J. et al., 2014). Petroleum-based diglycidyl ether bisphenol A (DGEBA) epoxy resins are manufactured from a reaction between epichlorohydrin (ECH) and bisphenol A (BPA) (Radojčić, D. et al., 2016). The epoxy resins made with BPA polymers are used for the internal surface coatings of food and beverage packaging, such as almost all soda cans and various canned food cans, as well as baby bottles and powdered infant formula sample containers. But, BPA is one of the most harmful packaging materials worldwide recently (Vilarinho, F. et al., 2019).

BPA can be leached into food as its migration from food packaging coated with epoxy resins. When the heating process is performed for reasons such as heat disinfection for sterilization, the migration level of BPA increases significantly, resulting in significant side effects. BPA is a toxic endocrine-disrupting chemical that interferes with hormone biosynthesis, metabolism, and its resulting action even at

very low concentrations, resulting in changes in the normal homeostasis of exposed individuals or their descendants. In addition, because BPA can produce estrogen effects with its affinity for estrogen receptors, mothers and children exposed to drugs during pregnancy and breastfeeding are exposed to children's behavioral disorders, respiratory disorders and convulsions, hormonal imbalances, reproductive disorders, and infertility (Lee, J. et al., 2019; Estlander, T. et al., 1991, 1996, 1997). Furthermore, due to hand-me-down poison, ecotoxic effects can lead to the extinction of living organisms. Various materials, such as PETG, PP, Tritan, PES, and PCT, are used commercially to replace the BPA-based products. But some of them showed higher estrogen activity than BPA-containing epoxy resins (Radojčić, D. et al., 2016). These studies show that sales products labeled BPA-free are very likely to contain substances that exhibit estrogen-like activity, such as BPA, and that better research is needed. In addition, endocrine-disrupting chemicals (EDCs) do not decompose easily and have high stability, so they continue to remain in the environment. As for the movement of EDCs within the ecosystem, the cumulative concentration increases exponentially every time they go up according to the food chain. After all, the accumulation of pollution in the food chain has the most serious impact on humans at the top of the food chain (Vilarinho, F. et al., 2019). Therefore, previous studies are interested in replacing bisphenol A diglycidyl ether with monomers obtained from renewable resources. Among various eco-friendly materials, the use of renewable synthetic vegetable oils such as acrylated epoxy soybean oil (AESO) and epoxy soybean oil (ESO) is gradually increasing instead of petroleum-based epoxy resin (Williams, C. K. et al., 2008).

1.2. BPA-based epoxy resin vs Vegetable oil-based epoxy resin

Petroleum-based diglycidyl ether bisphenol A (DGEBA) produces strong toxic fumes during thermosetting as well as the risk of exposure to EDCs (Radojčić, D. et al., 2016; Vilarinho, F. et al., 2019). In addition, epoxy resins are extracted from petroleum resources and are difficult to decompose, causing serious environmental pollution such as hazardous waste and greenhouse gas emissions, and at the same time, fossil fuel depletion problems (Ahmad, M. et al., 2015). Therefore, previous studies are interested in replacing diglycidyl ether bisphenol A (DGEBA) with monomers obtained from renewable resources (Liu, Z. et al., 2002; Altuna, F. et al., 2011; Liu, X. et al., 2009, 2014; Li, R. et al., 2018). Among the various eco-friendly materials, vegetable oil has recently attracted the attention of not only academia but also industry researchers in terms of sustainability based on renewable resources as a promising substitute for DGEBA. Vegetable oil is one of the most important biological resources for producing polymeric materials, and its main component is a triglyceride containing glycerol ester-containing three fatty acids. Triglyceride has several high-response sites, including double bonds, allylic positions, and the ester groups, which can prepare a wide variety of polymers with different structures and functionalities (Li, R. et al., 2018; Mustapha, R. et al., 2019; Tran, T. et al., 2020).

Among vegetable oils, soybean oil is one of the most widely used starting materials in the polymer industry due to its wide availability, low toxicity, and relatively inexpensive among various sources of bio-based feedstock (Liu, X. et al., 2014; Han, J. et al., 2018). Acrylated epoxidized soybean oil (AESO) and epoxidized soybean oil

(ESO) are one of the popular vegetable oil derivatives with renewability. There are many studies to increase the bio-based content of the epoxy resin system and improve performance by mixing petroleum-based diglycidyl ether bisphenol A (DGEBA) and epoxidized vegetable oil (ESO). However, ESO generally has a problem that long and flexible aliphatic chains act as plasticizers in epoxy networks, resulting in reduced crosslinking density and low glass transition temperatures (Karger-Kocsis, J. et al., 2014; Tran, T. N. et al., 2020). In addition, the internal epoxy group of ESO has a long distance between reactors, resulting in low reactivity and non-selective reactions, which eventually leads to incomplete curing reactions and makes it difficult to use alone (Wang, Z. et al. 2017; Tran, T. et al., 2020). Due to this fact, the oxirane ring-opening reaction of ESO usually needs higher temperature and longer completion of reaction time than commercial petroleum-based diglycidyl ether bisphenol A (DGEBA) (Radojčić, D. et al., 2016). Therefore, it is important to select a curing agent or catalyst suitable for ESO in order to use ESO as a renewable and safer alternative to bisphenol A epoxy resin. Generally, there is a method of improving mechanical properties by forming organic-inorganic hybrid epoxy networks by applying polysiloxane) (Radojčić, D. et al., 2016).

In addition, since the hydroxyl group conducts better reactivity toward the epoxy groups, the use of the silanol group as a catalyst can efficiently promote the oxirane ring-opening reaction of internal epoxy groups (Liu, H. et al., 2008). Hydrogen atoms in silanol groups form thiolate anions through protonation of thiols, and the reaction of the protonated thiolate anions with hydroxyl group leads to oxirane ring-opening reaction (Acocella, M. R. et al., 2016). Therefore, since the hydroxy group acts as a catalyst to accelerate the curing rate of

the thiol-epoxy reaction, the oligomer synthesized in this study can act as reactants or catalysts. For industrial application, if a strong acid such as H_2SO_4 and H_3PO_4 is used as a catalyst for ESO, the formation of a hydroxy group in the fatty acid backbone may cause oxirane ring-opening reaction, but this causes corrosion problems of equipments and is accompanied by problems of purifying the products (Saithai, P. et al. 2013).

As another method, polymerizing the bio-based epoxy resin with thiol groups through thiol-click reactions can accelerate the curing rate and improve the mechanical properties of cured materials. This study synthesized thiol-functionalized polysiloxane oligomers containing silanol groups satisfying all of these and applied them as curing agents and catalysts.

1.3. Thiol-click reactions

The thiol-click reaction first produces thiolate anions by protonation of unreacted thiols and losing active hydrogen ions. Since thiolate anions are much more nucleophilic than unreacted thiols, the nucleophilic attack of thiolate anions on epoxy groups produces alkoxide anions (Hoyle, C. E. et al., 2010; Holmes, R. et a., 2017). And then, the unreacted thiols are protonated with the alkoxide anions to generate final materials and thiolate anions. The thiol-click reactions can be initiated thermally or photochemically. All thiol-click reactions are generally characterized by low energy consumption, time efficiency by rapid curing rate, insensitivity to oxygen, and environmentally friendly reaction by mild conditions than other normal UV irradiation or thermal curing processes (Konuray, A. O. et al., 2020).

1.3.1. Disadvantages of one-step curing system

In this study, AESO and ESO, bio-based alternatives of DGEBA, were combined with thiol-functionalized curing agents to produce dual-cured materials through sequential UV curing and thermal curing processes. Since AESO contains acrylate groups, a thiol-acrylate reaction, one of the thiol-acrylate reactions, is applied.

The thiol-acrylate reaction consists of a combination of chain-growth homopolymerization of acrylate groups and the step-growth mechanism of thiol-ene polymerization. Since the conversion of the acrylate groups is roughly twice that of the thiol groups, it leads to non-stoichiometric polymerization (Konuray, A. O. et al., 2020). This is because the thiol-acrylate reaction creates heterogeneous networks with very different mobility due to competition between the two mechanisms. As a result, the unreacted thiol functional groups partially remain, which leads to poor performance of the cured material (O'Brien, A. et al., 2006; Sahin, M. et al., 2017). That is, under such non-stoichiometric reaction conditions, the cured materials cause problems in that crosslinking density, thermal and mechanical properties are degraded due to the presence of unreacted thiol groups.

On the contrary, the thermal curing process of the thiol-epoxy reaction requires a higher temperature and longer completion of reaction time than the UV curing process of the thiol-acrylate reaction (O'Brien, A. et al., 2006; Jian, Y. et al., 2013; Sahin, M. et al., 2017). In addition, the thiol-epoxy reaction needs thiol-functionalized curing agents, thermal accelerators, and reactive diluents (Rostami, A. A. et al., 2015).

1.3.2. Advantages of dual curing system

In order to intentionally control unreacted residual thiol groups, secondary polymerization reactions can be applied to obtain fully cured materials. Also, since the thiol-epoxy reaction is a stoichiometric reaction between the thiols and the epoxy groups unlike the thiol-acrylate reaction, it is considered that the non-stoichiometric polymerization of the thiol-acrylate reaction can be overcome by controlling the ratio of the two types of thiol-click reactions (Grauzeliene, S. et al., 2021). Furthermore, many recent studies have focused on catalyst-free click chemistry without a catalyst of potential toxicity (Han, J. et al., 2018; Andreani, T. et al., 2020). In general, a photoinitiator is necessary to generate radicals in a UV curing process. However, the photoinitiator has a very small molecular weight, so if the inner coating of the food packaging is polymerized through a UV curing reaction, the photoinitiator is highly likely to be leached from internal coatings and migrated to food. Even if the inner coating does not come into direct contact with the food, it is very easy to migrate to the food through the blocking layer, and it is highly likely to penetrate the cells or tissues of our human body and exhibit toxicity in various forms (Holmes, R. et al., 2017).

On the other hand, the thiol-ene reaction can be said to be a safe reaction without health hazards because thiyl radicals are generated during UV irradiation even in the absence of a photoinitiator (Holmes, R. et al, 2017). Therefore, unlike the one-step thiol-epoxy reaction, the dual curing process can prevent the health hazards of workers and improve work efficiency. The formation of dual curing thiol-ene/thiol-epoxy networks based on vegetable oils is very useful from an eco-friendly point of view. In addition, the dual curing

process combined with UV curing and thermal curing may improve thermal and mechanical properties of the cured materials, and by applying a secondary thermal curing process later, curing of the shaded area, which was not applied in UV curing process (Belmonte, A. et al., 2016).

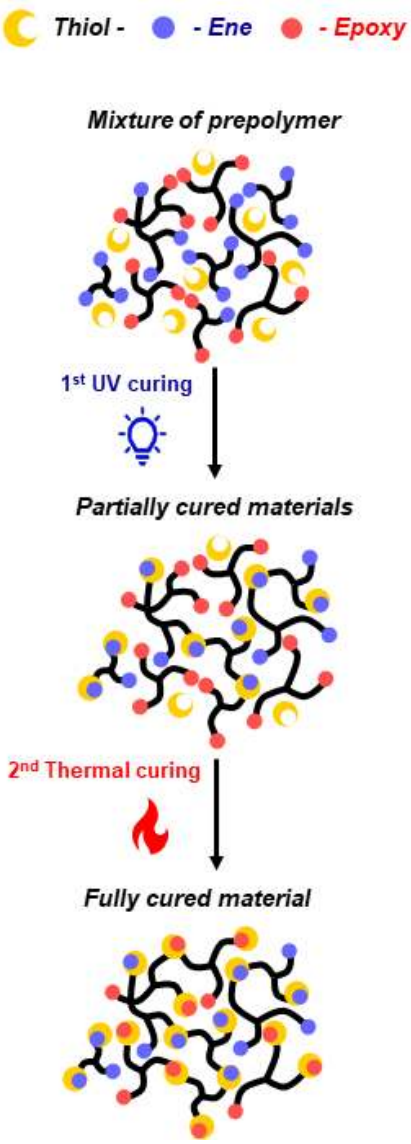

Figure 1. Scheme of thiol-ene/thiol-epoxy dual curing system

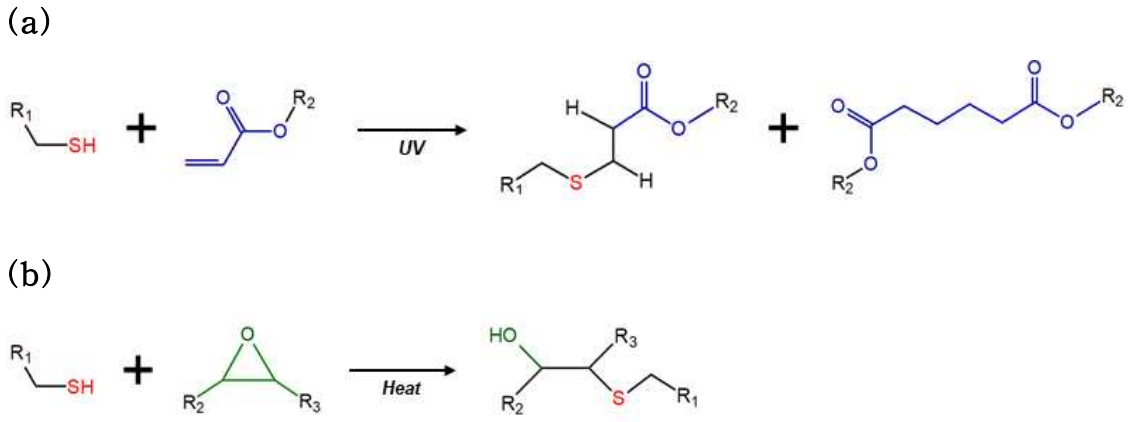

Figure 2. Mechanism of thiol-click reaction
(a) Thiol-ene reaction (b) Thiol-epoxy reaction

1.4. Necessities of polysiloxane

The epoxy curing agent is an essential reactant used with epoxy resin in the thermal curing process. In general, the final properties of the epoxy cured materials are determined according to the type of epoxy curing agent used. In order to solve environmental pollution and dependence on fossil fuels, it is necessary to form a sustainable epoxy network. Therefore, it is very important that both epoxy resin and curing agent are not based on petroleum resources and are not harmful to health (Lee, J. et al., 2019; Estlander, T. et al., 1991, 1996, 1997).

However, as with the epoxy resins, the curing agents commonly used today are derived from non-renewable petroleum resources. In addition, as commonly commercialized epoxy curing agents, polyamines, polyamides, and anhydrides usually generate quite high toxic gases harmful to human health (Ahmad, M. et al., 2015). The

main risks associated with the use of epoxy are related to the epoxy curing agents component rather than the epoxy resins themselves (Tavakoli, S. M. et al., 2003). A number of studies have been reported on irritating and sensitizing effects by epoxy curing agents (Kanerva, L. et al., 2013). Previous studies have shown that polyamine hardeners act stimulatingly and sensitively on the skin and respiratory tract. Anhydrides hardeners such as methylhexahydrophthalic anhydride (MHHPA) and methyltetrahydrophthalic anhydride (MTHPA) can also cause allergic rhinitis as well as immediate skin contact reactions. It was estimated that the cause of this symptom was estimated to be caused by airborne substances by strong toxic fumes from epoxy hardeners (Lee, J. et al., 2019; Estlander, T. et al., 1991, 1996, 1997). Also, among commercial epoxy curing agents, anhydrides are relatively less toxic than amines, but they are also a petrochemical and hazardous to the environment (Andreani, T. et al., 2020). And they have a large energy loss due to long-term curing due to their low curing reactivity (Mashouf Roudsari, G. et al., 2014). However, the blend ratio of epoxy curing agents can increase by up to 50 wt% across the entire epoxy network.

Recently, the research concerning the bio-based epoxy networks from plant oils is growing rapidly with the increasing requirements of the reduction of the VOCs emissions and non-toxicity of these materials (Mora, A. S. et al., 2019). More recently, the interest for bio-based amines is also increasing with the synthesis of amines from bio-based materials (Pelckmans, M. et al., 2017). However, the synthesis of bio-based amines often requires some toxic reactants or harsh reaction conditions (Wilhelm, K. et al., 1981). For instance, reductive amination of carbonyl functions is a process to synthesize

amines from vegetable oils and react with similar drawbacks (Miikka, V. et al., 2014). In addition, there is a limit to supplementing the poor physical properties of vegetable oil-based epoxy resins with these organic curing agents.

On the other hand, unlike the organic curing agent, since the polysiloxane curing agent may form an organic-inorganic network structure, the performance of the cured materials may be expected to be improved. As a component of sophisticated 3D oligomers, polysiloxane oligomers are integrated into the epoxy network to form an organic-inorganic structure combined with inorganic and organic properties, thereby expecting various performance improvements in the bio-based epoxy networks. Polysiloxane acts as a barrier that inhibits heat transfer over other organic curing agents, and thus vegetable oil-based epoxy siloxane coatings can extend temperature ranges and expect excellent thermal stability (Yue, S. et al., 2019). When polysiloxane is incorporated into bio-based epoxy resins, polysiloxane increases the crosslinking density, so the rigid crosslinked network protects the coating surface (Graiver, D. et al., 2003). In addition, the polysiloxane can prevent corrosive ion penetration by providing covalent and hydrogen bonds with the oxide layer on the surface. Optical transparency and gas permeability, which are disadvantages of epoxy resins, were also improved. Thiol-functionalized polysiloxane increases compatibility with epoxy resins due to the presence of organic functional groups (Vladimir, V. et al., 2015). Also, unlike most industrial epoxy curing agents, polysiloxane does not depend directly on petroleum resources, and silicon is one of the most abundant elements known to humans and does not pose a risk to the environment and health (Graiver, D. et al., 2003).

Among the representative industrial epoxy curing agents, thiol-functionalized curing agents that smell like garlic or rotten eggs, low-molecular amine curing agents that smell like ammonia, and high-molecular amine curing agents that smell like rotten fish have difficulty working with intense odors (Elisa, P. et al., 2020). If the epoxy curing agent is based on polysiloxane structure, this odor problem can be reduced and work efficiency can be improved (Liu, Z. et al., 2021). Previous studies have reported the synthesis of functional polysiloxane via the sol-gel reaction. However, these methods often require high temperatures, long reaction times, or a large number of excess mercaptans. However, in terms of eco-friendliness, the modification reaction of alkoxysilane may be performed in a short period of time under mild conditions by using ultra-sonication (Kim, J. S. et al., 2011). Compared with the traditional hydrolysis reaction, the reaction of this approach proceeds smoothly and gives quantitative yields. There is no need for complex protection/deprotection steps and heavy metal catalysts are also avoided. Thus, using this approach greatly simplifies the functionalization of polysiloxanes. Consequently, the resulting polysiloxane-based oligomers synthesized in green chemistry are characterized by low VOCs emission and no toxicity harmful to the human body. Furthermore, it is interesting that the performance of the cured materials can be improved by incorporating thiol-functionalized polysiloxane oligomers into bio-based epoxy resins.

2. Objectives

2.1. Sustainable epoxy networks

From an environmental point of view, epoxy networks need to develop polymer materials that are not based on petroleum resources to save petroleum resources. Recently, vegetable oil is increasingly used as a sustainable and safe alternative for petroleum-based diglycidyl ether bisphenol A (DGEBA) for producing polymers in the chemical industry as a bio-renewable raw material (Mashouf Roudsari, G. et al., 2014). The petroleum-based epoxy industry is transforming into a green industry by integrating eco-friendly technology such as UV curing, especially thiol-ene reactions, as well as the use of renewable raw materials (Chen, Q. et al., 2019).

In this study, AESO and ESO as chemically synthesized soybean oils are used as the main raw materials for epoxy resins to form thiol-ene/thiol-epoxy networks crosslinked with thiol-functionalized polysiloxane curing agents. However, since the thermal curing accelerator essential in the thermal curing process of the thiol-epoxy reaction is an additive that did not participate in the reaction, it remains in the cured material, which causes degradation of water resistance and corrosion resistance. Therefore, this study aims to form a sustainable epoxy network without toxic commercial catalysts by applying thiol-functionalized polysiloxane oligomers containing silanol groups into vegetable-based epoxy resins. Furthermore, the thiol-ene/thiol-epoxy networks formed in this study can prevent hazardous effects on health because toxic chemicals do not elute even

under external stress conditions such as heat and UV irradiation. This study aims to demonstrate the suitability of vegetable oil-based epoxy resin as a renewable and promising substitute for diglycidyl ether bisphenol A (DGEBA).

2.2. Dual curing system by thiol-click reactions

In this study, Acrylated epoxidized soybean oil (AESO) and epoxidized soybean oil (ESO) as their derivatives were used as derivatives for dual curing with thiols. However, ESO has a problem in that it is difficult to form a crosslinked polymer network due to its low and non-selective polymerization reactivity (Radojčić, D. et al., 2016). On the other hand, since AESO contains acrylate groups capable of crosslinking in fatty acid chains, it is very likely that the crosslinked polymer networks can be polymerized at a high curing rate (Saithai, P. et al., 2013). However, the thiol-acrylate reaction is a non-stoichiometric reaction, resulting in a problem in that the crosslinking density, thermal and mechanical properties are degraded dramatically due to the presence of unreacted thiol group by insufficient conversion. Therefore, this study aims to obtain a fully cured material by applying a secondary thermal polymerization reaction to remove unreacted thiol groups. In addition, the performance of cured materials is compared by varying the ratio between the thiol-ene reaction and the thiol-epoxy reaction, and optimal conditions are obtained. It would like to demonstrate the effectiveness of the thiol-ene/thiol-epoxy dual curing system.

2.3. Organic-inorganic hybrid networks

The low thermal stability of AESO and ESO, which are commercially modified soybean oils, has always limited their usage in the application, although it is bio-based renewable materials derived from soybean oil. This is because the inherent flexibility of the long aliphatic chain results in low curing reactivity and low thermal stability (Li, R. et al. 2018). For this reason, in this study, two types of thiol-functionalized polysiloxane oligomers are synthesized as sustainable epoxy hardeners to form organic-inorganic hybrid networks. The thiol-functionalized polysiloxane oligomers were synthesized through a sol-gel method with an acid-catalyst. In addition, silanol groups were grafted onto thiol-functionalized polysiloxane to promote the oxirane ring-opening reaction of vegetable oil-based ESO.

The polysiloxane structure satisfying the above conditions includes linear siloxane or partially silsesquioxane. Previous studies have shown that thermal stability with thermosetting polymers and completely condensed POSS is the same as thermal stability with incompletely condensed POSS (Duchateau, R. et al., 2002). Therefore, this study attempts to synthesize two types of polysiloxane oligomers, namely linear-structured polysiloxane and open-cage structured polysiloxane, including silanol groups.

This study attempted to compare the performance differences of polymers formed when two structurally different thiol-functionalized polysiloxane oligomers were incorporated into bio-based epoxy resins. It aimed at high curing reactivity and superior thermal stability of thiol-ene/thiol-epoxy resulting polymer composites by applying the thiol-functionalized polysiloxane oligomers. This is because it is

determined that the polysiloxane having excellent heat resistance absorbs heat introduced into the epoxy network and controls heat transfer and diffusion, thereby contributing to the improvement of thermal stability (Jia, M. et al., 2009).

3. Literature review

3.1. Vegetable oil-based epoxy resins

Epoxidized vegetable oil is a renewable and abundant feedstock with a wide range of availability and a promising future prospect as a DGEBA alternative (Tran, T. et al., 2020).

Previous studies synthesizing soybean oil and PLA through ring-opening polymerization and nucleophilic substitution reactions demonstrated superior antibacterial activity and biodegradability and found that the ester group of soybean oil can undergo enzymatic degradation faster than hydrolysis. From a sustainable point of view, These observations are significant in that the synthesized soybean oil with quaternary ammonium salt moieties has both antibacterial and biodegradable properties (Acik, G. et al., 2020).

There are also previous studies that use acrylated epoxy soybean oil (AESO) as a liquid resin to build a 3D biomedical scaffold and evaluate biocompatibility with human bone marrow mesenchymal stem cells (hMSC). AESO can be easily polymerized by ultraviolet laser, and the cured materials have an excellent shape memory effect, which has great potential for additional 4D effects. The processed

AESO scaffold showed significantly higher adhesion and proliferation of hMSC compared to PEGDA and demonstrated biocompatibility similar to clinically approved PLA and PCL. These observations are significant in that AESO is biocompatible and can be applied as a transdermal patch (Shida Mia et al. 2016).

In addition, modified vegetable oils such as epoxidized soybean oil (ESO) are widely used as reactive plasticizers to obtain highly compatible mixtures because they play a role in reducing interactions between the matrix and the filler. However, ESO may compete with silane in the reaction with the silanol group on the silica surface to interfere with the silanization process. It was confirmed that there was a chemical bond between ESO and the silica surface (Espósito, L. H. et al., 2020).

3.2. Thiol-ene/thiol-epoxy dual click reactions

Thiol-click reactions are very efficient in that they have high yields and fast reaction rates and are executed simply without additional additives. (Hoyle, C. E. et al., 2010)

Vegetable oils are low reactive due to long fatty acid chains, so there are various preceding studies to solve this problem using thiol-ene click reaction or thiol-epoxy click reaction. It has been proven that polymers crosslinked by thiol-click reactions improve glass transition temperature, stress, and storage modulus at breakage to help form polymers with rigid structures. Furthermore, dual-cured polymer showed higher rigidity, tensile strength, and storage modulus than the thiol-ene polymer to which UV curing was applied alone (Sigita Grauzeliene et al. 2021).

Some previous studies have applied sequential double curing

processes to obtain final materials with rare complex shapes, such as plate-shaped or spring-shaped materials. In the first curing step, a solid-like and stable intermediate material was obtained, and the shape of the material was fixed by complete curing in the second curing step. This study suggested that a dual curing process could be used in the development of various shape memory applications and complex mechanical actuators (Belmonte, A. et al., 2017).

In addition, it was proved through real-time IR analysis that the thiol-acrylate reaction is faster and more efficient than the thiol-epoxy reaction. In addition, it has been shown that integrating the thiol-epoxy reaction after the thiol-acrylate reaction can reduce polymerization shrinkage and stress due to low shrinkage factors in the thiol-epoxy process, and increase the glass transition temperature and physical characteristics as the thiol-epoxy content increases in the network (Jian, Y. et al., 2013).

3.3. Structural diversity of polysiloxane

Polyhedral oligomeric silsesquioxanes (POSSs) are characterized by structural diversity and the possibility of attachment of a variety of functional groups that significantly change their reactivity and solubility (Laine, R. M. et al., 2011). In scientific literature, the most widely described group is that of completely condensed silsesquioxanes, but an interesting alternative to cubic POSS cages may be incompletely condensed open-cage silsesquioxanes, which, thanks to their unique structure, may exhibit different physicochemical properties and different reactivity (Duchateau, R. et al., 2002). Liu et al. investigated the hydrogen-bonded interaction in POSS silanols and the possibility of their usage as anion receptors to form host−guest

complexes (Liu, H., et al. 2008). The scientific reports about open-cage silsesquioxanes are scarce. There are only a few examples of the synthesis and use of its functional derivatives, which, because of the presence of several functional groups protruding from the cage, can be as multifunctional precursors and nanofillers of many materials used, e.g., in electronics and hybrid materials (Lorenz, V. et al., 2001).

Chapter 2

Synthesis of Thiol-functionalized Polysiloxane

1. Introduction

Among bio-based polymers, vegetable oil-based polymers offer several important advantages in terms of excellent availability, biocompatibility, and low cost (Mustapha, R. et al., 2019). However, there is a problem that most vegetable oil-based epoxy resins have very low reactivity and non-selective reactions due to the influence of internal epoxy groups and long fatty acid chains (Wang, J. et al., 2017; Tran, T. et al., 2020). There have been many previous studies in which other epoxy resins are blended or additives such as curing agents or reactive diluents are used to obtain ideal materials having good processability, reactivity, high thermal stability, excellent mechanical properties, and durability (Jia, P. et al., 2015). However, typical epoxy curing agents and reactive diluents produce toxic gases during combustion and are harmful to the environment and the human body when exposed (Lee, J. et al., 2019; Estlander, T. et al., 1991, 1996, 1997).

In an effort to overcome the limitations of vegetable oil-based epoxy resins, this study synthesized thiol-functionalized polysiloxane oligomers with non-toxic linear structures and bulk structures without being based on petroleum resources (Wang, W. et al., 2014). In addition, a reactive hydroxyl group was introduced into the thiol-functionalized polysiloxane oligomers to promote the ring-opening reaction of the epoxy groups (Radojčić, D. et al., 2016).

The Si-O-Si structure of polysiloxane may improve heat resistance, mechanical characteristics, oxidation stability, water resistance, and crosslinking ability, and a siloxane-structured grafted thiol organic polymer may increase compatibility with vegetable oil-based epoxy resins (Jia, M. et al., 2009; Handke, M. et al., 2011). In this study,

through ^{29}Si NMR, ^{1}H NMR, ^{13}C NMR, FT-IR, and Raman analysis, the structures containing thiol groups, hydroxyl groups, methoxy groups, and siloxane groups were confirmed, and thermal stability was analyzed through TGA.

2. Experimental

2.1. Materials

Soybean oil, epoxidized acrylate (AESO, having an average of 2.7 acrylic groups and 0.3 epoxy groups per molecule) with acrylate equivalent weight 1,200 (g/eq.), (3-Mercaptopropyl)methyldimethoxysilane (MPMDMS, 95 %) and (3-Mercaptopropyl)trimethoxysilane (MPTMS, 95 %) were purchased from Sigma-Aldrich Co., Inc. Epoxidized soybean oil (ESO, SDB CIZER E-03) with epoxy equivalent weight 232 (g/eq.) was supplied by SAJOHAEPYO Co., Ltd. All materials were used as received without further purification.

(a)

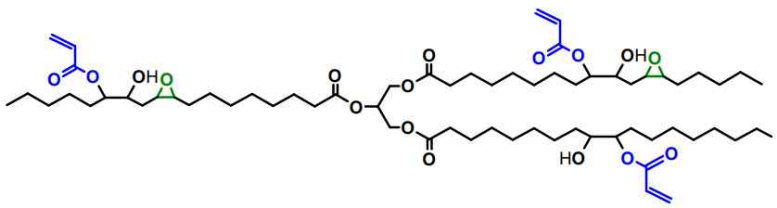

Acrylated epoxidized soybean oil (AESO)

(b)

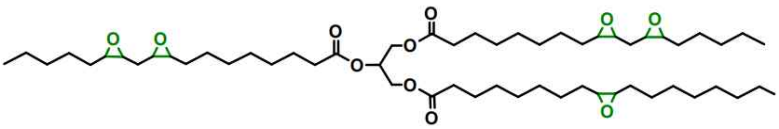

Epoxidized soybean oil (ESO)

(c)

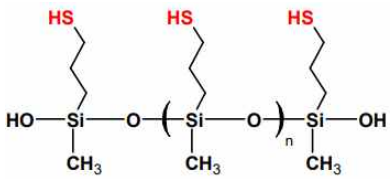

Thiol-siloxane oligomer (TSO)

(d)

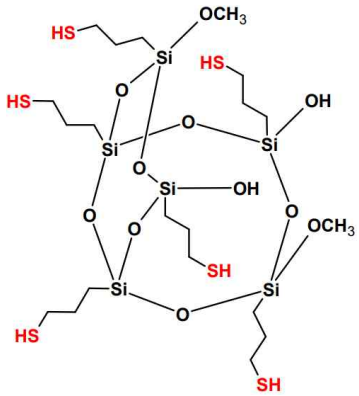

Thiol-silsesquioxane oligomer (TSQ)

Fig. 3. Chemical structures of materials
(a) Acrylated epoxidized soybean oil (AESO),
(b) Epoxidized soybean oil (ESO),
(c) Thiol-siloxane oligomer (TSO),
(d) Thiol-silsesquioxane oligomer (TSQ)

2.2. Methods

2.2.1. Synthesis of thiol-functionalized polysiloxane

(3-Mercaptopropyl)methyldimethoxysilane (MPMDMS) or (3-Mercaptopropyl)trimethoxysilane (MPTMS) 10 g was added to an one-neck flask and then mixed with 3 g of ethyl alcohol at a speed of 400 rpm for 5 minutes using a magnetic bar. To the hydrolysis reaction, the mixture was homogenized at 23 °C for 50 min in a sol state using an IKA Ultra-Turrax T25 digital homogenizer (IKA, Staufen, Germany) with a 10 mm dispersing tool operating at 20,000 rpm. To the condensation reaction, the distilled water (D.I water) 1 g and hydrochloric acid (0.01 mol/ℓ, HCl) 0.1 ㎖ were added in the flask using the ultra-sonication for 120 min. After the reaction, ethyl alcohol, H_2O, methyl alcohol as by-products and impurities were removed by a rotary evaporator and dried in a vacuum oven at 100 ℃ overnight to obtain a transparent viscous liquid.

TSO oligomer, Clear colorless liquid; yield, 70 %
^{1}H NMR (300 MHz, $CDCl_3$, ppm): δ = 0.69 (m, Si-CH_2), 1.66 - 1.76 (m, Si-CH_2-CH_2), 2.53 - 2.60 (t, Si-CH_2-CH_2-CH_2), 1.25-1.42 (m, Si-CH_2-CH_2-CH_2-SH), 3.77 (Si-OH), 0.06 - 0.19 (m, Si-CH_3). ^{13}C NMR (100.62 MHz, $CDCl_3$, ppm): δ = 16.19 (Si-CH_2), 27.85 (Si-CH_2-CH_2-CH_2-SH), 18.49 (Si-CH_2-CH_2-S), -0.62 (Si-CH_3)

TSQ oligomer, Clear colorless liquid; yield, 57.5 %

^{1}H NMR (300 MHz, $CDCl_3$, ppm): δ = 0.77 - 0.81 (s, $Si-CH_2$), 1.66 - 1.76 (d, $Si-CH_2-CH_2$), 2.53 - 2.60 (d, $Si-CH_2-CH_2-CH_2$), 1.25-1.42 (m, $Si-CH_2-CH_2-CH_2-SH$), 3.42 - 3.58 (d, $Si-OCH_3$), 3.81-3.87 (s, Si-OH). ^{13}C NMR (100.62 MHz, $CDCl_3$, ppm): δ = 11.16 ($Si-CH_2$), 27.51 ($Si-CH_2-CH_2-CH_2-SH$), 18.32 ($Si-CH_2-CH_2-S$), 58.39 ($Si-OCH_3$)

(a)

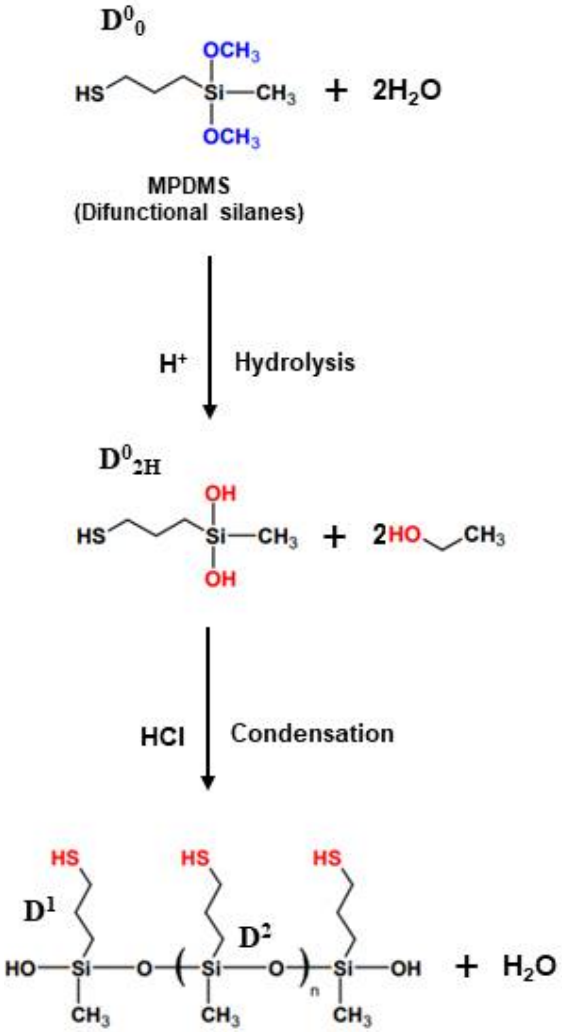

(b)

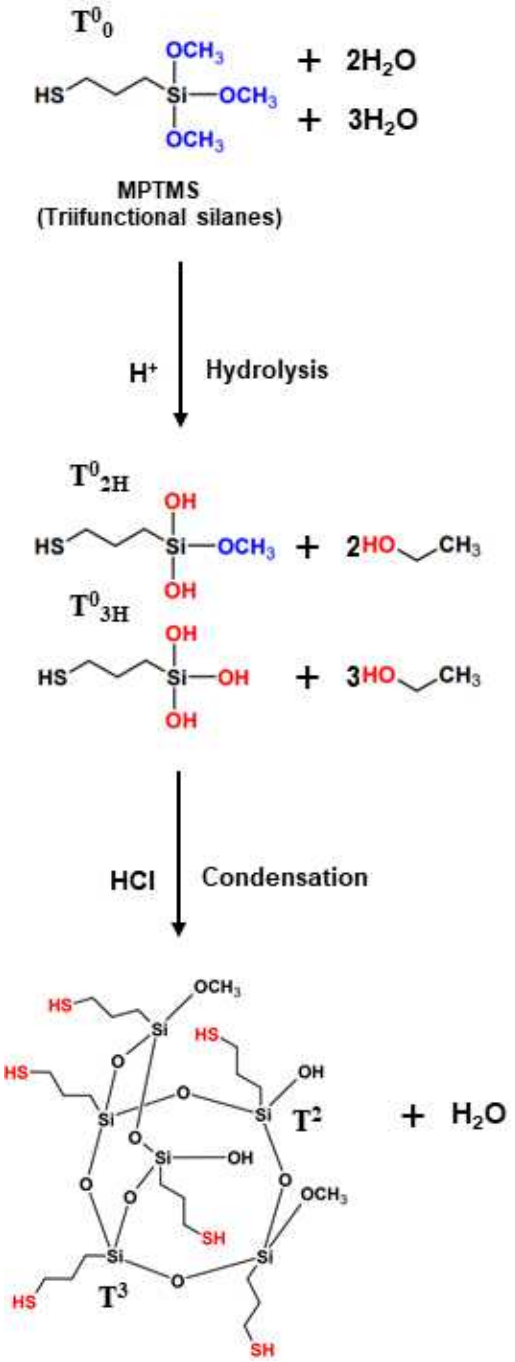

Figure 4. Two-step synthesis of thiol-functionalized polysiloxane oligomers (a) TSO oligomer (b) TSQ oligomer

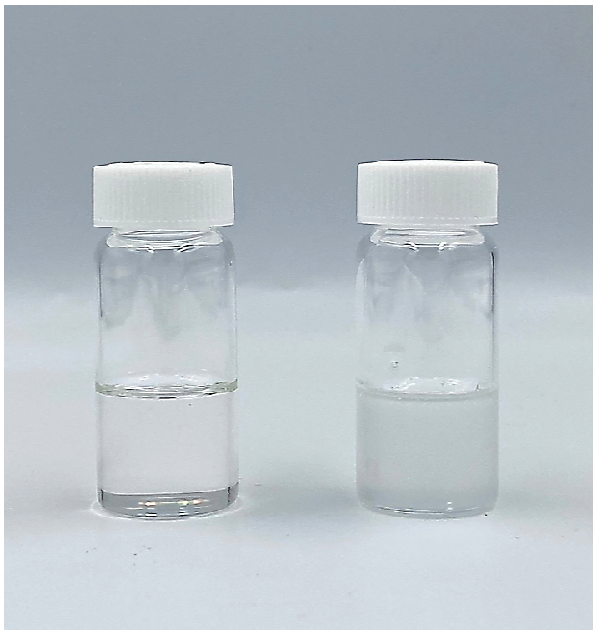

Figure 5. Appearances of thiol-functionalized polysiloxane oligomers TSO oligomer (left) TSQ oligomer (right)

2.3. Characterization of thiol-functionalized polysiloxane

2.3.1. Nuclear magnetic resonance (NMR)

^{1}H NMR and ^{13}C NMR spectra of the oligomers, the TSO (Thiol-siloxane oligomer), and TSQ (Thiol-silsesquioxane oligomer) were recorded in a 300-MHz NMR instrument (Bruker, Avance 300) at room temperature using $CDCl_3$ as a solvent. ^{29}Si NMR spectrum of the oligomers were performed on a 400-MHz NMR spectrometer (Bruker, Avance Ⅲ) and $CDCl_3$ was used as solvent in the measurements.

2.3.2. Gel permeation chromatography (GPC)

The molecular weights of the thiol-functionalized polysiloxane oligomers were measured by size exclusion chromatography using EcoSEC HLC-8320 GPC (TOSOH corporation). All samples were prepared with tetrahydrofuran (THF) at a concentration of 0.15% (wt/vol). The separation was performed on a set of Guard SuperMP(HZ)-M+2 and TSKgel Supermultipore HZ-M columns. The column dimension was 150 mm x 4.6 mm, the particle size of the packaging material was 3 μm, and 50 mL of the sample solution was injected into the GPC system. HPLC grade tetrahydrofuran was used as a mobile phase flowing at 0.35 ㎖/min. The column temperature was set to 40°C. A series of narrow polystyrene molecular weight standards of 580, 2,980, 9,960, 30,230, 69,650, 128,600, 325,600 and 660,500 Da were used to calibrate gel permeation chromatography (GPC) systems.

2.3.3. Fourier transform infrared (FT-IR) spectroscopy

The fourier transform infrared spectroscopy (FT-IR) of the structure analysis was recorded by a FT-IR spectrometer (Thermo-Nicolet iS10) with 32 scans and the wavenumber range of 500 - 4000 $㎝^{-1}$. All oligomers (10 μm) were dropped on ATR crystals and experiments were performed at room temperature. All spectra were corrected through CO_2 reduction, noise elimination, and baseline correction.

2.3.4. Raman spectroscopy

A DXR2xi Raman spectrometer (Thermo Scientific, USA) was used to record the Raman spectra of the synthesized thiol-functionalized polysiloxane oligomers. In measurements, the configuration was with the following experimental parameters that diode laser wavelength of 532 nm, laser power of 15 mW, and the range of 3400 - 50 cm^{-1}. Integration time for recording a Raman spectrum was 1 sec and 10 scans for any spectrum and no pre-treatment of the samples was necessary before Raman measurements.

2.3.5. Thermogravimetric analysis (TGA)

The thermal analyzer determines the thermal stability of the material by showing that the weight of the sample decreases as the physical and chemical properties of the material change as the temperature and time increase. The thermal stability of the TSO (Thiol-siloxane oligomer), and TSQ (Thiol-silsesquioxane oligomer) were conducted using a TGA 4000 thermal analyzer (Perkin Elmer). Samples were heated in a nitrogen atmosphere at a rate of 20°C/min from room temperature to 700°C, and 3 to 5 mg of samples were used for analysis. The weight loss changed as the temperature increased.

3. Results and discussion

3.1. NMR analysis

Fig. 6 (b) and Fig. 7 (b) show the ^{1}H NMR spectra of mercaptopropyl-terminated polysiloxane and polysilsesquioxane, respectively. The ^{1}H NMR spectra of synthesized TSO and TSQ oligomers were similar to each other and showed peaks that confirm the grafting of mercaptopropyl arms.

The repeating unit of the mercaptopropyl chain assigned four signals: methylene protons a, b, c and thiol protons d in all oligomers. Judging from the ratio of the integral values of the peaks, the protons of TSO and TSQ oligomers indicated a ratio of H_a : H_b : H_c : H_d = 1 : 1 : 1 : 0.5 and H_a : H_b : H_c : H_d = 1 : 1 : 1 : 0.8 at the mercaptopropyl chains, respectively.

Also, All the spectra of oligomers show the intensity of adsorbed water and hydrogen-bonded silanol groups (δ 3.5-5.0 ppm) and do not show the presence of isolated silanol groups (δ 1.1 ppm). The ^{1}H NMR spectrum of TSQ oligomers exhibits a peak at δ 3.56 ppm attributable to the Si-OCH_3 group which unhydrolyzed methyl protons, and that of TSO oligomers exhibits a peak at δ 0.15 ppm attributable to the Si-CH_3 group. The peak value of chemical shifts [δ] was 7.24 ppm, which was calibrated to the $CDCl_3$ solvent.

Fig. 6 (c) and Fig. 7 (c) represent the ^{13}C NMR spectra of mercaptopropyl-terminated polysiloxane and polysilsesquioxane, respectively. The ^{13}C NMR spectra of synthetic TSO and TSQ oligomers were also similar to each other like ^{1}H NMR and showed peaks confirming the grafting of mercaptopropyl arms. The repeating unit of the mercaptopropyl chain assigned three signals: methylene carbons a, b, and c in all oligomers. The ^{13}C NMR spectrum of TSQ oligomers shows peaks at 58.13 ppm due to the unhydrolyzed methyl carbons Si-OCH_3 group, and the spectrum of TSO oligomers shows

peaks at -0.63 ppm due to the Si-CH_3 group. In the ^{13}C NMR chemical shift measurement, the 77 ppm triple line peaks are peaks shown due to the coupling of carbon of solvent $CDCl_3$ with deuterium (I = 1).

Fig. 6 (a) and Fig. 7 (a) represent a series of ^{29}Si NMR spectra of mercaptopropyl-terminated polysiloxane and polysilsesquioxane, respectively. In this study, the existing D^n and T^n nomenclature proposed by Engelhardt was used to identify different silicon atoms present in the synthesized oligomers. The unit type D^n and T^n each mean two or three potential hydroxyl or alkoxy reactive groups, and the symbol 'n' means the number of other silicon atoms connected by bridging oxygen atoms. In other words, D^0 or T^0 species represent silicon atoms with two or three non-bridging oxygens, respectively. In these spectra, the D silicon sites [D^1 ($R_2Si(OSi)(Me)$ sites between −9 and -16 ppm and D^2 ($R_2Si(OSi)_2$) sites between −16 and -25 ppm] and T silicon sites [T^2 ($RSi(OSi)_2Me$) sites between −54 and -62 ppm, T^3 ($RSi(OSi)_3$) between −62 and -70 ppm] exhibit characteristic chemical shifts. Fig. 4 (a) indicates two types of D units in this spectrum; D^1 unit at −9 ppm and D^2 unit at −21 ppm. The polysiloxane linear bonding D^2 repeating units corresponds to a signals between δ -20 and -22 ppm. Therefore, the TSO oligomer has a linear siloxane structure of a repeating unit possessing mercapto groups. In the ^{29}Si NMR quantitative analysis, the integral area of the percentage of D^n units shows 8.14% and 91.86% in the D^1 and D^2 units, respectively. The degree of crosslinking of siloxane bonding was calculated through the following equation (1).

$$DC(\%) = \sum_{n}^{0-2} (n \times D^n/2) \quad (1)$$

* D^n units denotes the structure $Si(OSi)_n(OMe)_{2-n}$ (n=0-2)
* DC : Degree of crosslinking of siloxane bonding

As a result, the condensation density of siloxane bonding in TSO oligomer was 95.93%. This high condensation density indicated that the network structure of the oligomer is compact and that the Si-O binding energy is high. This could effectively improve the thermal stability of the final hybrid network.

Fig. 7 (a) indicates two types of T units in this spectrum: T^2 unit around −57 ppm bearing alkoxy groups and silanol groups and T^3 unit around −67 ppm, representing the resonance of 8 silicon atoms in the POSS cage. In the ^{29}Si NMR quantitative analysis, the integral area of the percentage of T^n units shows 69.44% and 30.56% in the T^2 and T^3 units, respectively. The degree of crosslinking of siloxane bonding was calculated through the following equation. Subsequently, the condensation density of siloxane bonding in the TSQ oligomer was calculated as 76.85% using the equation (2).

$$DC(\%) = \sum_{n}^{0-3} (n \times T^n/3) \qquad (2)$$

* T^n units denotes the structure $Si(OSi)_n(OMe)_{3-n}$ (n=0-3)
* DC : Degree of crosslinking of siloxane bonding

Like TSO oligomers, TSQ oligomers also show a compact network structure of oligomers with high condensation density, and Si-O bonds with high binding energy can effectively improve the thermal stability of the hybrid networks. T^2 and T^3 species suggest the presence of relatively large-sized structures such as oligomers, and oligomer trialkoxysiloxanes are known to form polyhedral silica

networks. The small signal around δ -67.3 ppm is attributed to the cage-like octamer of T_8 - POSS skeleton in T^3 silicon site (Handkea, M. et al., 2011). However, since the signal by the T^2 Si atoms exists with T^3 species, it can be seen that TSQ oligomer has an incompletely condensed POSS skeleton possessing mercapto groups.

(a)

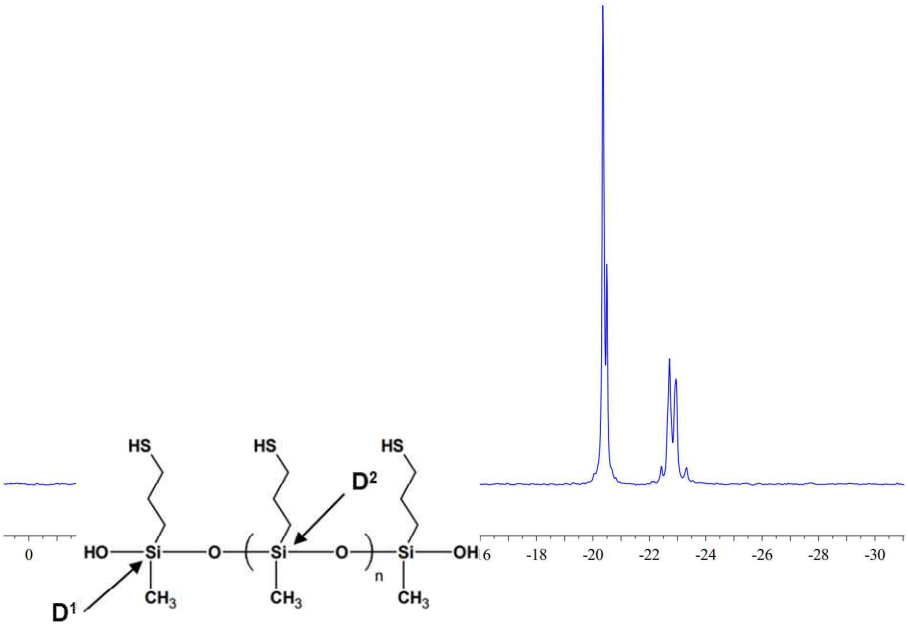

(b)

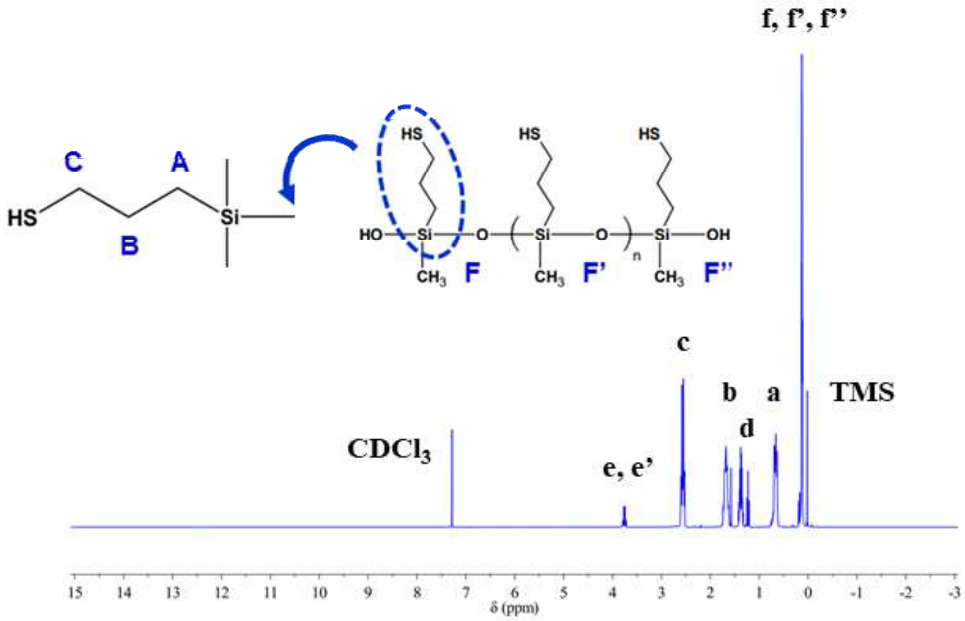

(c)

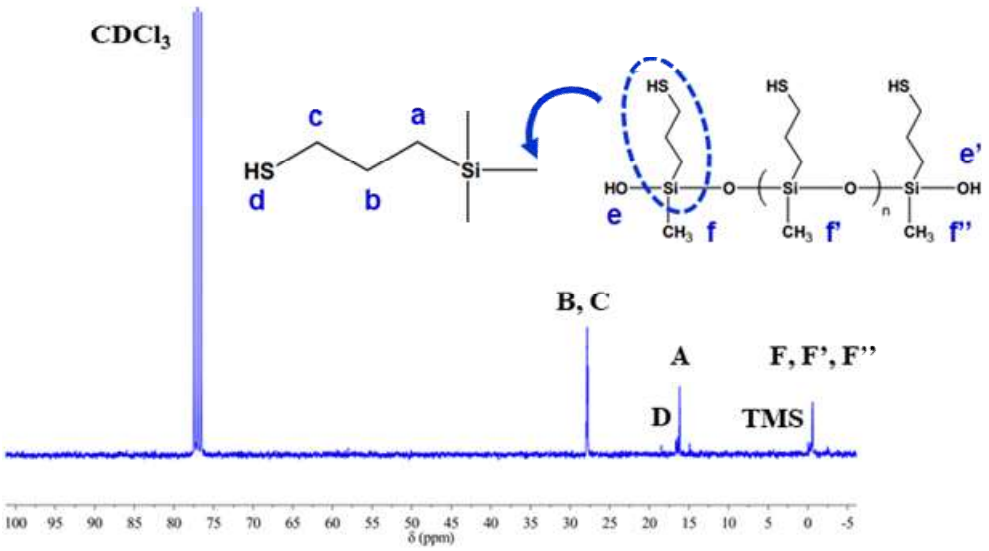

Figure 6. (a) ^{29}Si NMR, (b) ^{1}H NMR and (c) ^{13}C NMR spectra of TSO oligomer

(a)

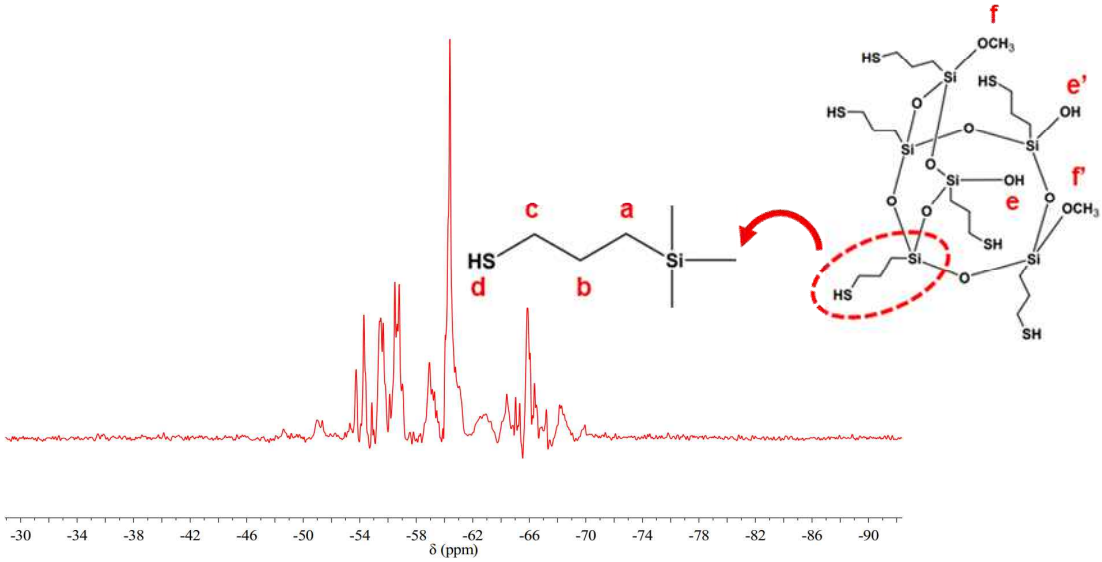
f
e'
f'
e
c
a
HS
d
b
Si
OCH3
OH
SH
-30 -34 -38 -42 -46 -50 -54 -58 -62 -66 -70 -74 -78 -82 -86 -90
δ (ppm)

(b)

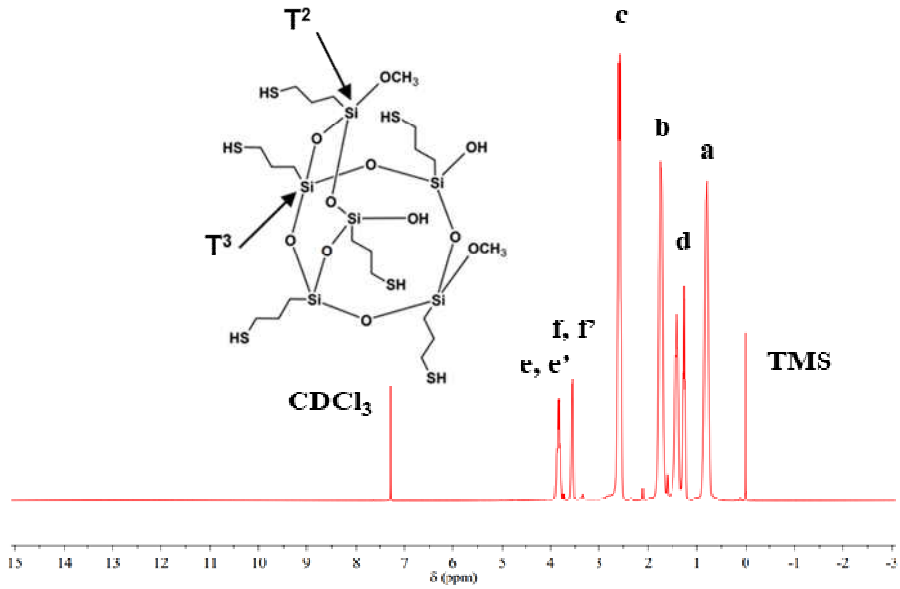
T2
T3
c
b
a
d
f, f'
e, e'
TMS
CDCl3
OCH3
OH
SH
15 14 13 12 11 10 9 8 7 6 5 4 3 2 1 0 -1 -2 -3
δ (ppm)

(c)

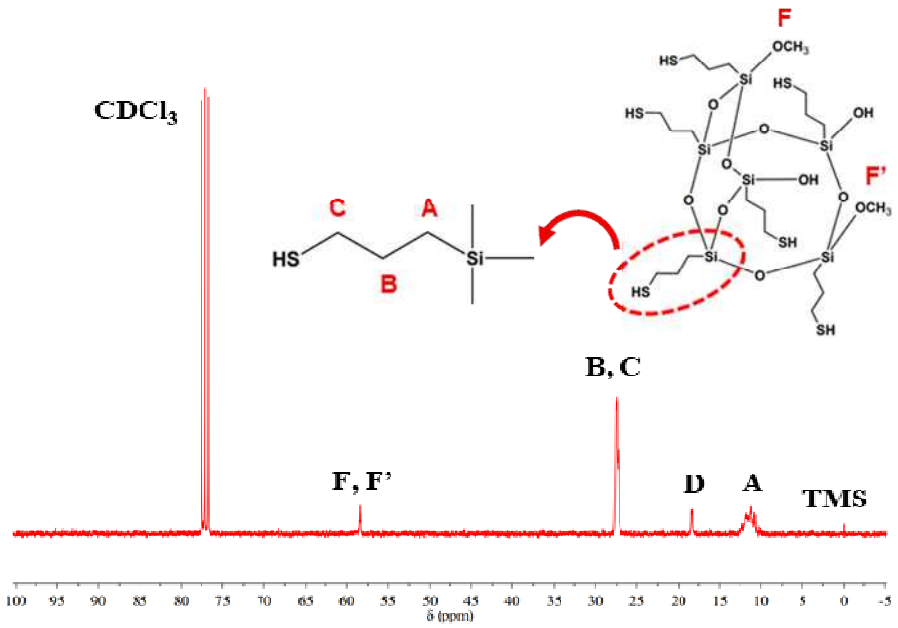

Figure 7. (a) ^{29}Si NMR, (b) ^{1}H NMR and (c) ^{13}C NMR spectra of TSQ oligomer

3.2. GPC analysis

The molecular weights of TSO and TSQ oligomers were measured by gel permeation chromatography (GPC). As shown in Fig, the weight average molecular weight of TSO and TSQ oligomers were 752 and 1447, respectively, with different molecular weight depending on the molecular structure. TSQ oligomer showed a higher MW than TSO in the homopolymer structure, and the result was influenced by the condensed silsesquioxane structure in TSQ oligomer. The poly diversity index (Mw/Mn) of TSQ and TSO oligomers had values of 1.451 and 1.251, respectively. Since TSO oligomer has fewer side branch structures than TSQ oligomer, it is considered that it has a relatively narrower molecular weight distribution.

3.3. FT-IR analysis

The ATR-FTIR spectra of the TSQ oligomers showed O-H stretching vibrations of the hydroxyl groups between 3700 and 3200 cm^{-1}, and the sharp band at 3675 cm^{-1} of TSO oligomers and the weak absorption peak at 920 cm^{-1} commons in both oligomers were associated with residual isolated Si-OH groups. And the FTIR spectra further confirmed the synthesis of showing the bands at 2967 and 2856 cm^{-1} from the asymmetric and symmetric C-H stretching mode of CH_3 groups and the bands between 3050 and 2780 cm^{-1} from the υas and υsym modes of CH_2 groups in the propyl arms. A weak signal is observed at 2556 cm^{-1} in all oligomers due to the S-H stretching mode of the mercapto groups.

The sharp single peak at 1257 cm^{-1} corresponding to the Si-CH_3 bending vibrations are only detected with high intensity in TSO oligomers. The absorption peak near 1400 cm^{-1} is the flexural vibration of O-H, which indicates that both TSQ and TSO have hydroxyl groups (Chen, Q. et al., 2019). A silsesquioxane having one Si-O-Si angle shows only one intense peak at 980 to 1080 cm^{-1} like TSQ oligomers. In contrast, a linear siloxane structure, which has two Si-O-Si angles in the perpendicular and horizontal directions, shows the two peaks like the TSO oligomers (Ivaldi, C. et al., 2019). Thus, It can be concluded that a cage-like silsesquioxane and linear siloxane structures were synthesized, respectively.

(a)

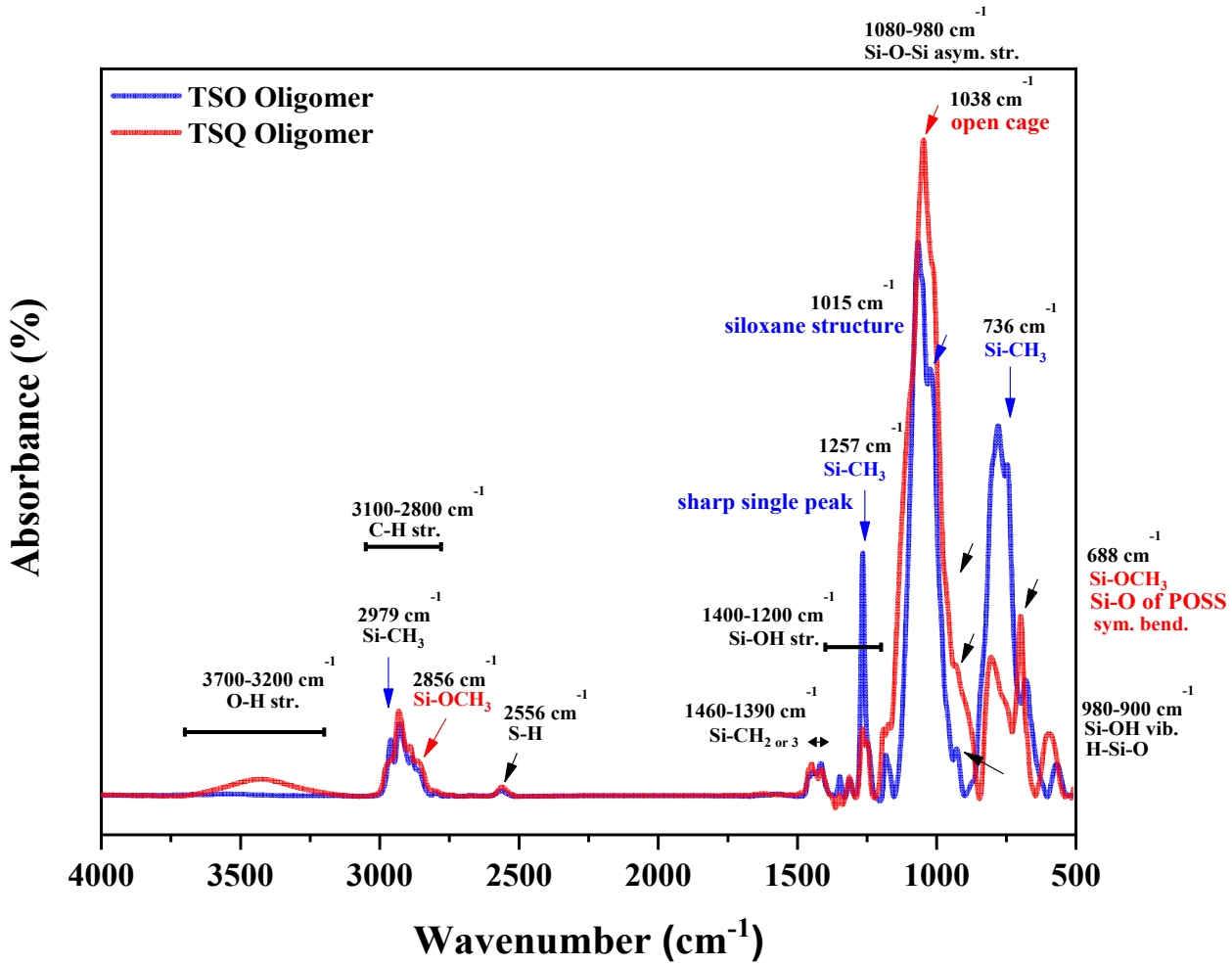
TSO Oligomer
TSQ Oligomer
Absorbance (%)
Wavenumber (cm-1)
4000
3500
3000
2500
2000
1500
1000
500
1080-980 cm-1
Si-O-Si asym. str.
1038 cm-1
open cage
1015 cm-1
siloxane structure
736 cm-1
Si-CH3
1257 cm-1
Si-CH3
sharp single peak
3100-2800 cm-1
C-H str.
2979 cm-1
Si-CH3
3700-3200 cm-1
O-H str.
2856 cm-1
Si-OCH3
2556 cm-1
S-H
1400-1200 cm-1
Si-OH str.
1460-1390 cm-1
Si-CH2 or 3
688 cm-1
Si-OCH3
Si-O of POSS
sym. bend.
980-900 cm-1
Si-OH vib.
H-Si-O

(b)

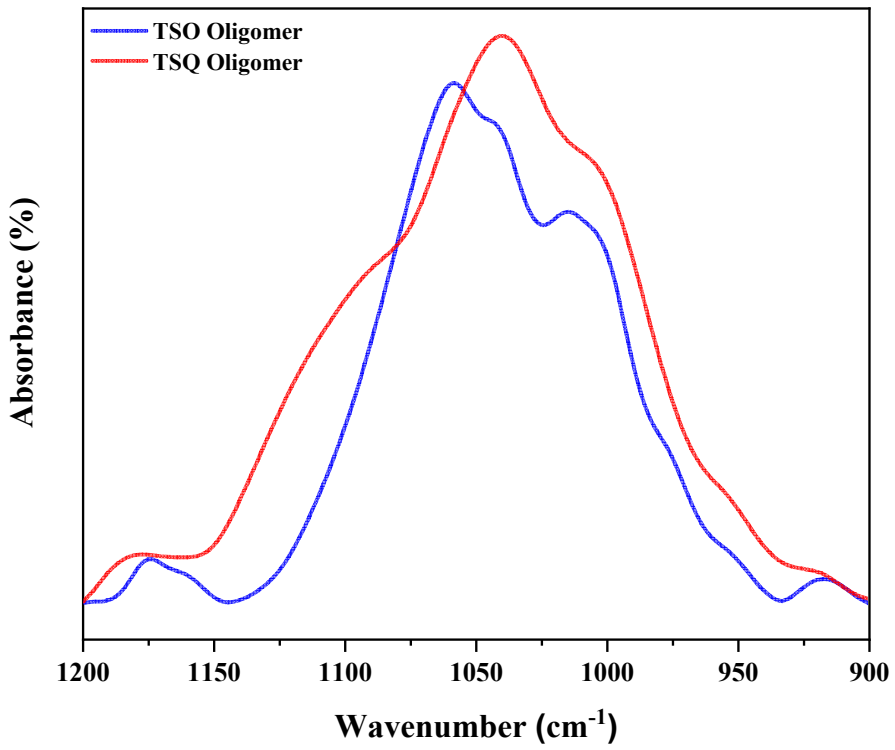

Figure 8. (a) FT-IR spectra of TSO/TSQ oligomers (b) Major IR bands of TSO/TSQ oligomers from 900 cm^{-1} to 1200 cm^{-1}

3.4. Raman analysis

In this study, Raman analysis was performed for a more detailed structure analysis of the thiol-functionalized polysiloxane oligomers. As the same of FT-IR spectra analysis, RAMAN shows the bands between 3050 and 2780 cm^{-1} from the C - H stretch from the propyl chains and the S-H stretching mode of the mercapto groups was assigned a strong band at 2565 cm^{-1} in all oligomers. The Si - O - Si bonds are formed by condensation of Si-OH groups, which are created by the hydrolysis of the MPDMS or MPTMS (Handke, M. et

al., 2011; Kim, J. S. et al., 2011). A small peak at 920 cm^{-1} refers to the stretching mode of the Si-O bond from non-bridging isolated silanol groups (Handke, M. et al., 2011). The existence of a signal at 920 cm^{-1} indicates the presence of uncondensed silanol groups remaining after the process of the sol-gel process (Maura, R. et al., 2013). The strong characteristic band located at 1080-1180 cm^{-1} in the TSO and TSQ oligomers is attributed to the asymmetric stretching vibrations of Si—O—Si associated with the formation of a condensed polysiloxane network (Wang, H. et al., 2012). At the intense signal at 1095 cm^{-1} of the Si-O-Si band, the higher frequency like TSQ oligomers could be attributed to silsesquioxane structure, while the lower frequency is due to linear siloxane structure. In other words, the Si-O-Si band intensity suggests the condensation reaction of hydrolyzed alkoxysilanes (Mariusz, S. et al., 2018).

In particular, RAMAN evidenced that the cage structure of TSQ oligomers at small bands at 510, 810 and 966 cm^{-1}. While for the TSO oligomers, Si-O-Si stretching vibrations of D^1 unit structure detected the bands between 550 and 460 cm^{-1} and O-Si-O stretching vibrations of D^2 unit structure detected the bands between 650 and 550 cm^{-1}. The Si - O - Si bonds are formed by condensation of Si-OH groups, which are created by the hydrolysis of the MPDMS or MPTMS (Handke, M. et al., 2011; Kim, J. S. et al., 2011). Small bands between 925 and 830 cm^{-1}, 1400 and 1200 cm^{-1} were assigned to the stretching mode of the Si - O bond from non-bridging silanol groups, respectively (Handke, M. et al., 2011). The Si - O bond indicates that there were uncondensed Si-OH bonds in the MPDMS or MPTMS (Handke, M. et al., 2011; Kim, J. S. et al., 2011).

(a)

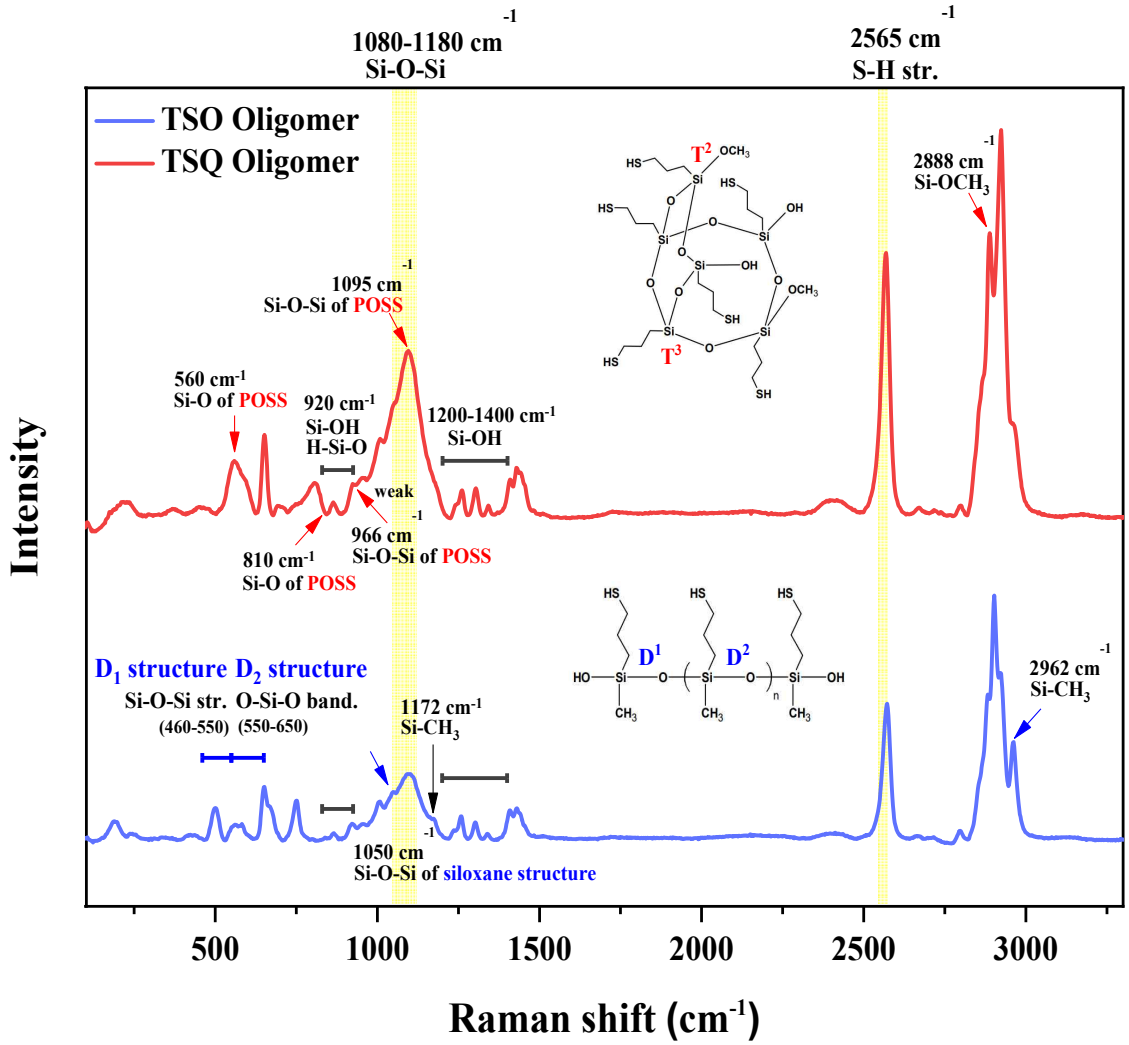
1080-1180 cm-1
Si-O-Si
2565 cm-1
S-H str.
TSO Oligomer
TSQ Oligomer
T2
T3
2888 cm-1
Si-OCH3
1095 cm-1
Si-O-Si of POSS
560 cm-1
Si-O of POSS
920 cm-1
Si-OH
H-Si-O
1200-1400 cm-1
Si-OH
weak
966 cm-1
Si-O-Si of POSS
810 cm-1
Si-O of POSS
D1 structure D2 structure
Si-O-Si str. O-Si-O band.
(460-550) (550-650)
1172 cm-1
Si-CH3
D1
D2
2962 cm-1
Si-CH3
1050 cm-1
Si-O-Si of siloxane structure
Intensity
500
1000
1500
2000
2500
3000
Raman shift (cm-1)

(b)

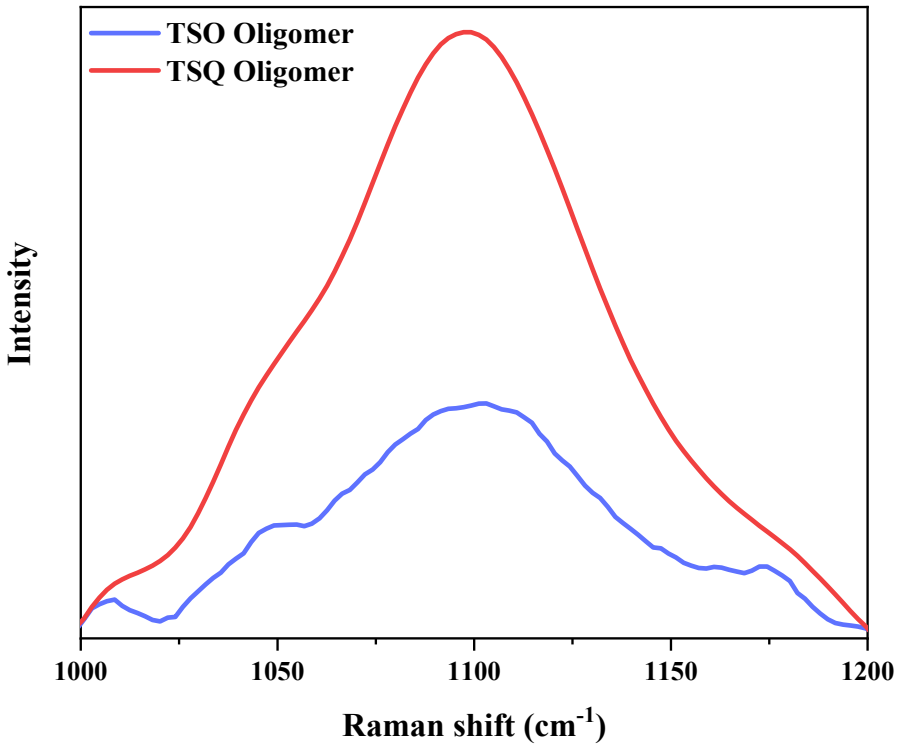

Figure 9. (a) RAMAN spectra of TSO/TSQ oligomers (b) Major RAMAN bands of TSO/TSQ oligomers from 1000 cm^{-1} to 1200 cm^{-1}

3.5. Thermal stability analysis

Fig. 10 (a, b) shows the changes in the decomposition curves. When the weight loss was 5 wt%, the temperature of the TSO monomer before the sol-gel reaction was 67.4 ℃, but the temperature of the synthesized TSO oligomer after the reaction was 249.2 ℃. Similarly,

the temperature of the TSQ monomer was 95.1℃ but the temperature of the synthesized TSQ oligomer after the sol-gel reaction was 310.4 ℃, showing a temperature increase of more than three times. Likewise, the temperature of maximum degradation was higher in oligomers than in monomers and higher in TSQ oligomers than in TSO oligomers, as shown in the following table. As a result of the measurement of residual mass, TSQ oligomer was 50 wt% higher than TSO of 8.5 wt%, which can be attributed to the polysiloxane structure. This is because around 5~15 wt% of residue, such as TSO oligomer, is explained by the formation of siloxane structures, and higher residues, from 30 to 50 wt%, such as TSQ oligomer, is explained by the formation of silsesquioxane structures (Kalia, S. et al., 2018).

IPDT provides a useful indicator of thermal stability because it is a quantitative value at the temperature proposed by Doyle. A^* is a simplified value consisting of residual mass and temperature and can be expressed as a ratio of the entire curved area including the area of the entire TGA thermal analysis curve and the residual mass. K^* is a value used as a coefficient of A^*, and $A^* \cdot K^*$ is a unique thermal stability index, and the larger the value, the higher the thermal stability. After calculating the area under the decomposition curve through the integration in the following figure, IPDT was calculated to measure the thermal stability of the oligomers. Here, the two main factors that influenced thermal stability were the initial decomposition temperature and residual mass (Liu, S. H. et al., 2019). The calculation was performed using the following equation (3) :

$$A^* = (S_1 + S_2)/(S_1 + S_2 + S_3)$$
$$K^* = (S_1 + S_2)/S_1 \quad (3)$$

where T_i is the initial temperature (30 ℃), and T_f is the final temperature (700 ℃). The IPDT can be obtained by substituting the calculated value of * T_i, T_f, A^* and K^* into the below equation (4).

$$IPDT(℃) = A^* K^* (T_f - T_i) + T_i \quad (4)$$

The IPDT value of TSQ oligomers was 1744.1 ℃ which was relatively higher than that of TSO oligomers of 458 ℃, indicating good thermal stability and heat resistance overall. This means that TSQ oligomer with a bulk structure has a better thermal stability factor value than TSO oligomer with linear structure. Although TSO oligomer has a higher condensation density than TSQ oligomer, the silsesquioxane structure of TSQ oligomer, which limits heat transfer from a polymer surface to an internal structure, is considered to have a greater impact on thermal stability (Xu, Y. et al., 2020).

Table 1. TGA data of thiol-functionalized polysiloxane oligomers

Formulation (AESO/ESO)	$T_{dec.-5\%}$ (℃)	T_{max} (℃)		$A^* \cdot K^*$	IPDT (℃)	Residual mass (%)
		1st	2nd			
TSO oligomer	249.2	329.6	391.7	0.6	458	8.5
TSQ oligomer	310.4	394.5	517.1	2.2	1744.1	50
TSO monomer	67.4	130.2	-	0.1	112.1	0
TSQ monomer	95.1	167.2	-	0.2	173	1.04

* $T_{dec.-5\%}$: Temperature at the weight loss of 5% obtained from TGA curve
* IPDT : Integral procedural decomposition temperature
* T_i : Initial temperature (30 ℃)
* T_f : Final temperature (800 ℃)
* A^* , K^* : Thermal stability index
* T_{max} : temperature of maximum rate of weight loss

(a)

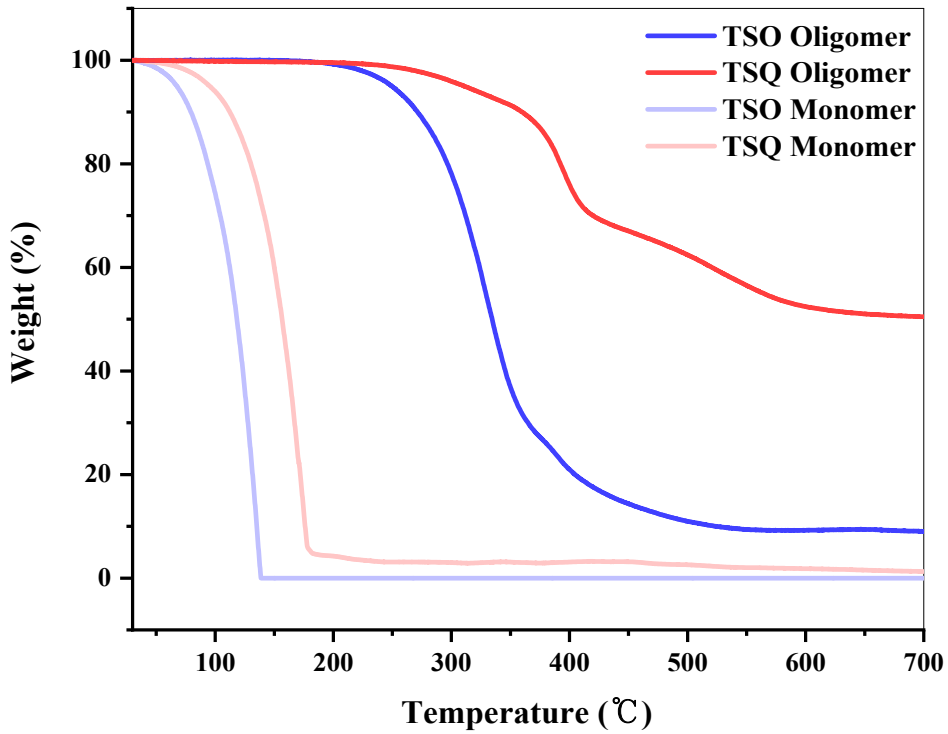

(b)

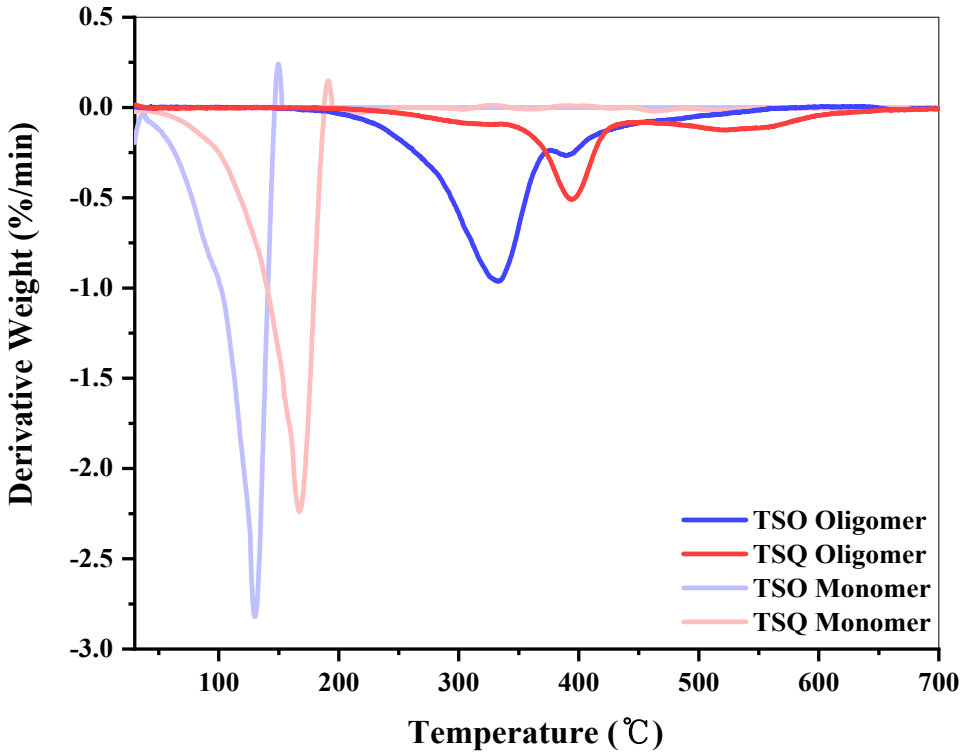

Figure 10. (a) TGA and (b) DTG curves of TSO/TSQ oligomers

4. Conclusions

In this study, thiol-functionalized polysiloxane oligomers were synthesized through a sol-gel process as a method to improve the low reactivity of the vegetable oil-based epoxy resins. Unlike other epoxy curing agents, the synthesized thiol-functionalized oligomers were suitable as sustainable epoxy curing agents because they were

not based on petroleum resources and were not toxic.

The formation of siloxane bonds of two structures was confirmed through ^{29}Si NMR, FT-IR, and RAMAN analysis, respectively, and the presence of hydroxy and methoxy groups was confirmed through ^{1}H NMR and ^{13}C NMR analysis. In addition, it was confirmed through TGA analysis that TSQ oligomers with silsesquioxane structure exhibit better thermal properties and thermal decomposition activation energy than TSO oligomers with linear siloxane structure. Therefore, the observed results show that the thiol-functionalized polysiloxane oligomers will serve as suitable epoxy curing agents and curing accelerators to contribute to the improvement of low thermal and physical properties of vegetable oil-modified epoxy resins.

Chapter 3

Formation of Thiol-ene/Thiol-epoxy Hybrid Networks

1. Introduction

In general, the thiol-click reaction is a simple and efficient method that may react under mild conditions without a solvent and has been widely used because the reaction is not delayed by oxygen in the air and shows a high conversion rate and rapid reaction rate (Hartmuth, C. et al., 2001). Since the thiol-ene and thiol-epoxy reactions are also efficient at high polymerization rates, the impact on the environment can be minimized with low energy consumption and high productivity.

However, the thiol-acrylate reaction, one of the thiol-ene reactions, is a non-stoichiometric reaction, so the unreacted thiol group remains, which eventually degrades the mechanical properties of the cured material (O'Brien, A. et al., 2006; Sahin, M. et al., 2017).

Therefore, in this study, the thiol-epoxy reaction was proposed as a second curing reaction for the purpose of decreasing the unreacted thiol group by the thiol-acrylate reaction (Jian, Y. et al., 2013). A thiol group can participate in both thiol-acrylate and thiol-epoxy reactions, and as a result, networks formed in the thiol-acrylate and thiol-epoxy reactions are connected. In addition, unlike the thiol-acrylate reaction, the thiol-epoxy reaction is a stoichiometric reaction, so it is easy to calculate the formulation ratio for network formation during the two-stage dual curing reaction (Belmonte, A. et al., 2017; Cengiz, N. et al., 2013).

This study analyzed the curing behavior, crosslinking density, mechanical and thermal properties of thiol-ene/thiol-epoxy networks formed by mixing thiol-functionalized polysiloxane oligomers with AESO and ESO in stoichiometric ratios, respectively. In addition,

various performances of the thiol-ene/thiol-epoxy networks formed by incorporating thiol-functionalized polysiloxane oligomers with two structures were also compared.

2. Experimental

2.1. Preparation of thiol-ene/thiol-epoxy networks

AESO and ESO were mixed in other ratios of 100/0, 75/25, 50/50, 25/75, and 0/100, respectively. All samples targeting a molar ratio of both acrylate/thiol and epoxy/thiol = 1:1 were fabricated from stoichiometric mixtures of AESO, ESO, and the thiol-functionalized polysiloxane oligomers.

The thiol-functionalized polysiloxane oligomers, TSO and TSQ synthesized in this study, are highly compatible with the AESO/ESO resin, so do not require a blending process using external chemical diluents. After blending at a rotation speed of 1000 rpm for 10 minutes at room temperature using a paste mixer, a synthesized oligomer, TSO or TSQ was added to the target equivalent ratio and further mixed at 1000 rpm for 5 minutes thoroughly. The prepared homogeneous mixture was filled in a silicon mold, degassed in a vacuum oven at 30 °C for 30 minutes, and then exposed to 200 mW/cm^2 365 nm irradiation using an LED UV lamp (area curing system) for 15 minutes in the presence of air. After UV curing, the primary-cured samples were moved to the vacuum oven and secondary thermally cured at 150 °C for 3 hours.

Consequently, two separate networks were formed sequentially by a two-step curing process that enables the production of interpenetrating polymer networks (IPN) resulting polymer composites. DMA measurement specimens were manufactured with dimensions of 40 mm width × 6 mm height × 2 mm thickness and TMA measurement specimens with dimensions of 20 mm width × 4 mm height × 0.7 mm thickness.

Table 2. Formulations of thiol-ene/thiol-epoxy resin blend

Formulation	Resins (wt%)		Curing agents (%)	
(AESO/ESO)	AESO	ESO	TSO	TSQ
TSO 100A/0E	75	-	25	-
TSO 75A/25E	49	16	35	-
TSO 50A/50E	28	28	44	-
TSO 25A/75E	12	38	50	-
TSO 0A/100E	-	46	54	-
TSQ 100A/0E	76	-	-	24
TSQ 75A/25E	50	17	-	33
TSQ 50A/50E	29	29	-	42
TSQ 25A/75E	13	39	-	48
TSQ 0A/100E	-	47	-	53

* All samples targeting a 1:1 M ratio of thiol to acrylate and epoxy functional groups were fabricated from stoichiometric mixtures

1 Step. Synthesis of Thiol Oligomers

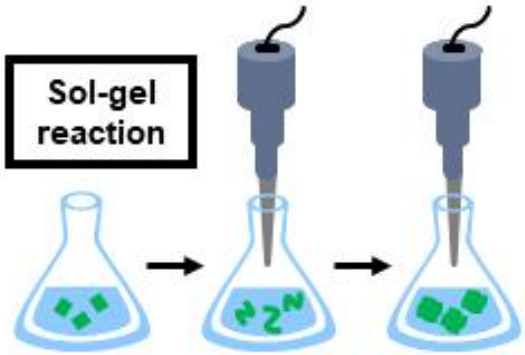

2 Step. Blending

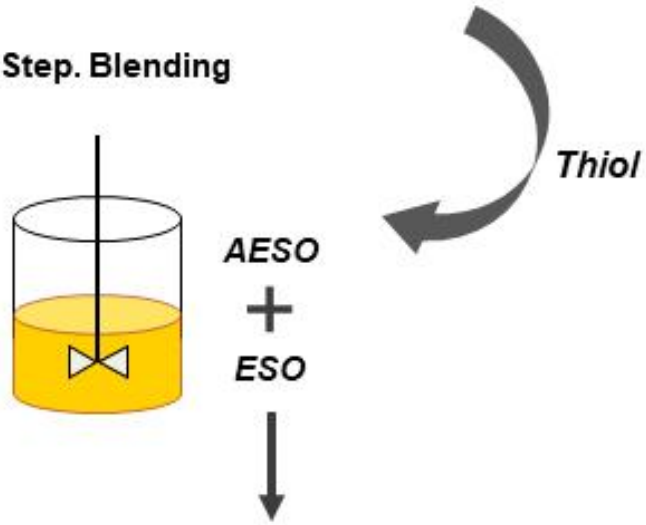

3 Step. UV Curing → Thermal Curing

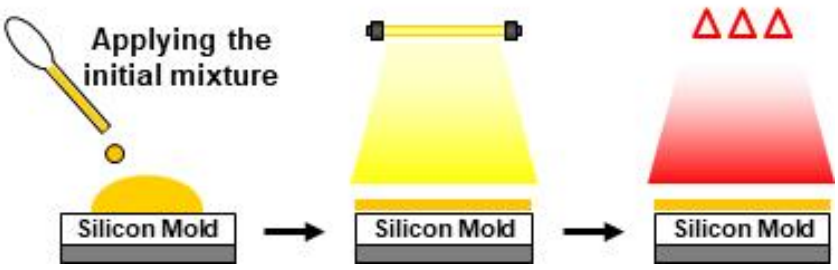

Figure 11. Manufacturing process of thiol-ene/thiol-epoxy composites

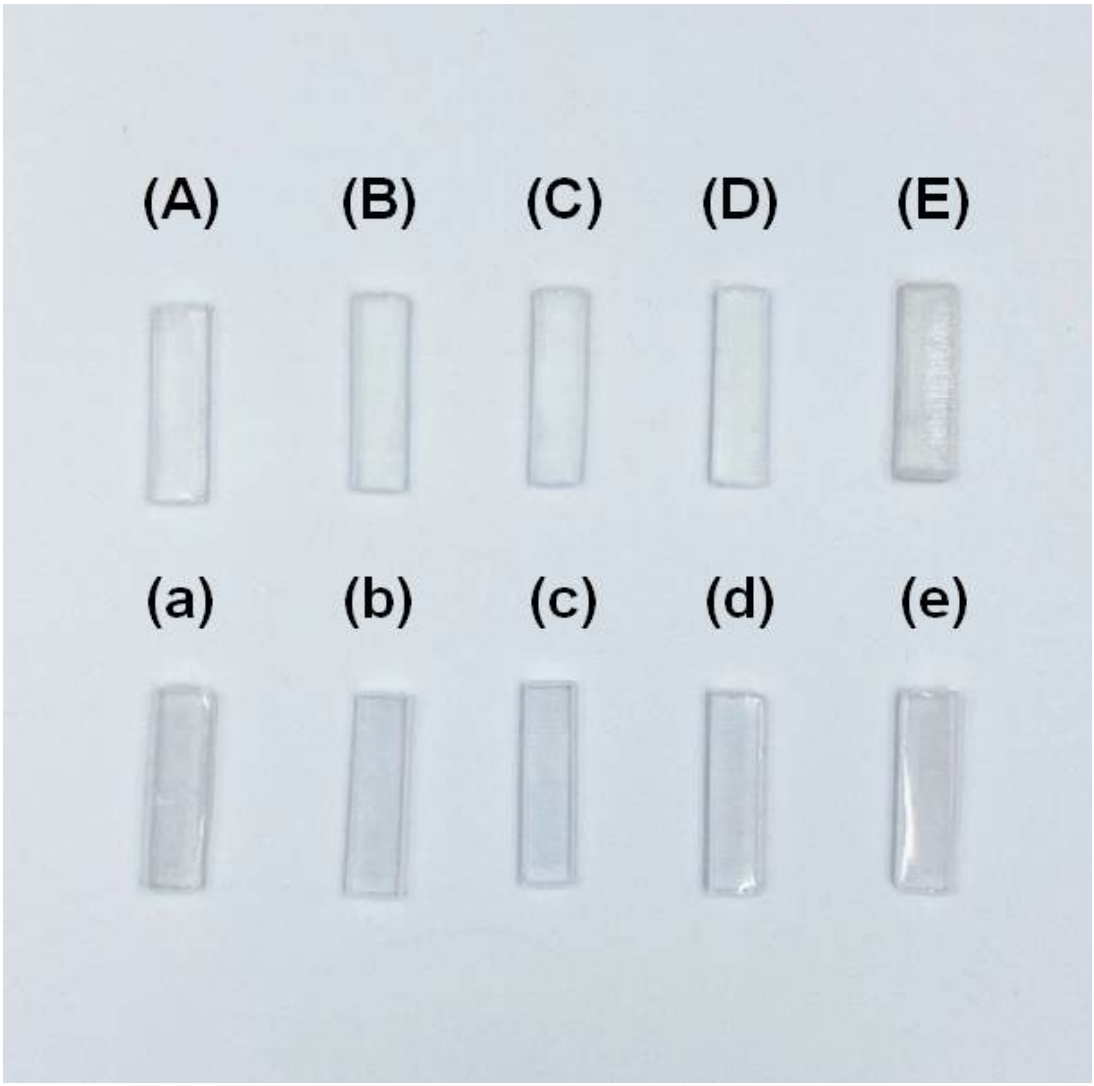

Figure 12. Specimens of thiol-ene/thiol-epoxy composite test samples (A) TSO 100A/0E (B) TSO 75A/25E (C) TSO 50A/50E (D) TSO 25A/75E (E) TSO 0A/100E (a) TSQ 100A/0E (b) TSQ 75A/25E (c) TSQ 50A/50E (d) TSQ 25A/75E (e) TSQ 0A/100 composite test samples

2.2. Characterization of thiol-ene/thiol-epoxy networks

2.2.1. Real-time fourier transform infrared (RT-FTIR) spectroscopy

A photopolymerization monitoring experiment was performed to measure the conversion rate of the acrylate and thiol groups in the thiol-ene reaction mechanism. These studies were performed by FT-IR spectrometer (Thermo-Nicolet iS10) equipped with an attenuated total reflectance (ATR) accessory and the wavenumber range of 500 - 4000 cm^{-1}. The initial mixtures TSO 100A/0E and TSQ 100A/0E were dropped about 10 μm on the ATR crystal, and the experiment was conducted at room temperature. The initial mixtures were irradiated by ultraviolet light from an SP-9-250UB (250 W lamp, 250-460 nm, USHIO Inc. System Company, Japan) equipment for 20 min. The conversion rate of acrylate and thiol groups according to the UV irradiation time could be measured by comparing the peaks at 1620-1640 cm^{-1} and 2550-2600 cm^{-1}, respectively. The peak intensity of the C=C and S-H stretching decreases with the UV Irradiation time. All spectra were corrected through CO_2 reduction, noise elimination, and baseline correction. The conversion rate of thiol-ene initial mixtures such as TSO 100A/0E and TSQ 100A/0E were calculated by applying the following equation (5) :

$$Acrylate\ Conversion(\%) = [1 - (A_{1635})_t / (A_{1635})_0] \times 100\,(\%) \quad (5)$$
$$Thiol\ Conversion(\%) = [1 - (A_{2570})_t / (A_{2570})_0] \times 100\,(\%)$$

where $(A_{1635})_0$ and $(A_{1635})_t$ are the intensity for 1635 cm^{-1} (C=C bond) at the initial time and after curing, respectively, and $(A_{2570})_0$ and $(A_{2570})_t$ are the intensity for 2570 cm^{-1} (S-H bond) at the initial time and after curing, respectively.

2.2.2. Advanced rheometric expansion system (ARES)

The kinetics of the crosslinking process in thiol-ene/thiol-epoxy hybrid networks were monitored with an ARES rheometer (MCR 302, Anton Paar Ltd.) using shear mode. The mixtures of thiol-ene/thiol-epoxy hybrid networks were prepared and blended together by other ratios (100/0, 75/25, 50/50, 25/75, and 0/100 of wt.%). The crosslinking process occurred over the 1 mL mixture of thiol-ene/thiol-epoxy hybrid networks on a disposable parallel plate (diameter of 25 mm).

The UV curing procedure for the thiol-ene reaction was carried out under the conditions with a 0.1 mm gap, 0.3 % shear strain, and frequency of 10 Hz. The samples were irradiated at room temperature (20 ± 2 °C) using ultraviolet light from a SPOT-CURE SP-9 (200 W light source, wavelength 250 - 460 nm, Ushio Co., Inc.) device for 15 min. The thermal curing procedure for the thiol-epoxy reaction was performed at 150°C for 3 hours under conditions of 0.1 mm interval, 1% shear deformation, and 1 Hz frequency. The dual curing for the thiol-ene/thiol-epoxy hybrid networks was processed by combining

UV and thermal curing sequentially including the heating time from room temperature to 150 °C. The gel point (G′=G″) was determined as the crossover point of storage (G′) and loss (G″) modulus.

2.2.3. Gel fraction measurement

The gel fraction was measured to compare the crosslinking of the dual-cured samples. First, 2-3 mg of samples were immersed in toluene at room temperature for 24 hours (W_0). The insoluble part of the sample was filtered through a 200 mesh wire net and the oven was dried at 70°C for 24 hours by constant weight. The weight was then measured (W_1). The gel fraction was calculated by applying the following equation (6) :

$$Gel\ fraction(\%) = (W_1/W_0) \times 100 \quad (6)$$

where W_0 and W_1 are the sample weights before and after filtration in toluene, respectively. The test was replicated three times.

2.2.4. Contact angle measurement

The contact angles of the water droplets have been measured on the thiol-ene/thiol-epoxy films.

All measurements were performed in the static contact angle mode measured using a contact angle analyzer (Poenix 300, Surface & Electro-Optics Corp, Republic of Korea). The temperature and relative humidity were 25 ± 3 and 50 ± 3 %, respectively. An average of five

measurements was taken here for reporting the water contact angle.

2.2.5. Dynamic mechanical analysis (DMA)

The dynamic mechanical behaviors of tested sample, including storage modulus and tan δ values, was measured using the TA Instruments DMA Q800 analyzer through tension mode with an oscillation frequency of 1 Hz. The testing temperature ranged from -50 to 120 °C at a heating rate of 5 °C/min. Cured samples with dimensions of 40 mm × 6 mm × 2 mm (length × width × thickness) were used for testing. The glass transition temperature (T_g) was measured as the maximum peak of the tan δ curve (K). The crosslinking density (v_e) was calculated according to Flory's rubber elasticity theory [30] by applying the following equation (7),

$$\nu_e = E_{high}/3RT_{high} \quad (7)$$

where v_e is the crosslinking density (mol/m^3), E_{high} is the storage modulus (Pa) at rubbery plateau regime determined at T_g + 50 °C, R is the gas constant (8.314 J/K·mol), and T_{high} is the absolute temperature at E_{high}.

2.2.6. Thermogravimetric analysis (TGA)

The thermal stability and thermal decomposition temperature of the dual cured samples were measured using a TGA 4000 thermal analyzer (Perkin Elmer). The weight of the TGA sample was about

3-5 mg. The sample was loaded on a ceramic pan, and heated in a nitrogen atmosphere at a constant heating rate of 20°C/min from 30 °C to 800 °C to prevent unwanted oxidation.

2.2.7. Antimicrobial test

Escherichia coli MG1655, *Cronobacter sakazakii* ATCC29544, and *Staphylococcus aureus* RN4220 were used for antimicrobial test in this study. *E. coli* and *C. sakazakii* were cultured in Luria-Bertani (LB) media (Difco, USA), and *S. aureus* was grown in Tryptic Soy broth (TSB) (Difco, USA). Overnight cultures of bacteria were diluted to approximately 10^4 colony-forming units (CFU) mL^{-1} in fresh 3 ml each broth. The sample was cut into a 1 x 1 cm square with a razor, and sterilized with 70% ethanol. After transferring sample into bacterial cultures, the cultures were incubated in 37°C at 220 rpm for 6 hours. Viable cell counts were determined by 10-fold serial dilution in PBS and plating on each agar plates.

2.2.8. Volatile organic compounds (VOCs) test

A thermal extractor (TE, Gerstel) capable of flow control (10~300 ㎖/min) was used to measure TVOCs emission of various specimens. In this study, VOCs was released by carrier gas at the flow rate of 134 ㎖/min, and gas collection was possible using an adsorption tube. The thermal extractor consists of an adjustable oven (room temperature) that heats the glass tube (length 178 mm, diameter 13.6 mm) where the sample is located inside. Each sample 25 ㎎ was placed in a glass extraction tube. The VOCs was purged under a

pure nitrogen gas stream at a constant flow on a Tenax TA adsorption tube (Supelco, USA) and mini pump (MP-Σ30, SIBATA, Japan) (Villberg, K. et al., 1997; Wrona, M. et al., 2017).

The thermal extraction process was applied at 25 ± 1 °C for 30 min and the total volume of gas sampling was 1 L. As for the VOCs analysis, Gas sampling was performed using 'Methods for Measuring VOCs Emissions from Indoor and Building Materials-Solid Absorber Tubes and GC-MS / FID Method' ES 02603.1. As for the substances to be analyzed by VOCs, qualitative analysis was conducted using quantitative analysis items (TVOC, Benzene, Toluene, Ethyl-benzene, o,m,p-Xylene, Stylene) and peak area% using individual calibration lines. The TVOCs concentration ($\mu g/m^3$) was calculated using the Toluene calibration curve for the total area of the chromatogram between n-Hexane and n-Hexadecane (Kim, K. R. et al., 2020).

3. Results and discussion

3.1. Monitoring of thiol-acrylate photopolymerization kinetics

As the C=O bond and the C=C bond of the conjugated acrylate group are broken by UV irradiation, it can be seen that the C=O vibration motion ester peak of the triglyceride near 1720 cm^{-1} moves to a higher frequency, which is divided into two peaks. When the C=C bond of the acrylate group breaks, the 1635cm^{-1} peak of C=C

stretching and 810cm^{-1} peak of C-H out-of-plane bending in the C=C double bond decrease. In addition, it can be observed that the S-H peak around 2570 cm^{-1} is reduced by the thiol-ene reaction but does not completely disappear, indicating that the unreacted thiol group remains. Supplementary Fig. S1 shows the results of real-time monitoring experiments of real-time monitoring of the reduction of the 1635 cm^{-1} peak of the acrylate group and the 2570 cm^{-1} peak of the thiol group in TSO 100A/0E and TSQ 100A/0E, respectively.

As a result of calculating the conversion rates of acrylate and thiol groups according to the UV irradiation time, the Figure shows that the conversion of all samples did not complete 100 % in this study due to the thiol-acrylate system. In a thiol-acrylate system, non-stoichiometric polymerization occurs when the conversion of the acrylate functional group is approximately twice that of the thiol functional group. This is because there is competition between the step-growth mechanism of the radical thiol-ene polymerization and the chain-growth homopolymerization of the acrylate groups. The UV curing rate of acrylate generally becomes faster as the number of functional groups increases. Likewise, since the number of functional groups per unit mass of TSQ oligomers is relatively higher than that of TSO oligomers, it was confirmed that TSQ 100A/0E has a faster crosslinking rate than TSO 100A/0E. For other reasons, TSO 100A/0E is slower than TSQ 100A/0E because the methyl group of TSO oligomers has a greater steric hindrance than the methoxy group of TSQ oligomers, and the steric hindrance affects the rate of reaction (Stefan, E. et al., 2000). Since photocuring behavior determines manufacturing time and production cost, it is very important to analyze the curing behavior of photocuring polymer materials.

(A)

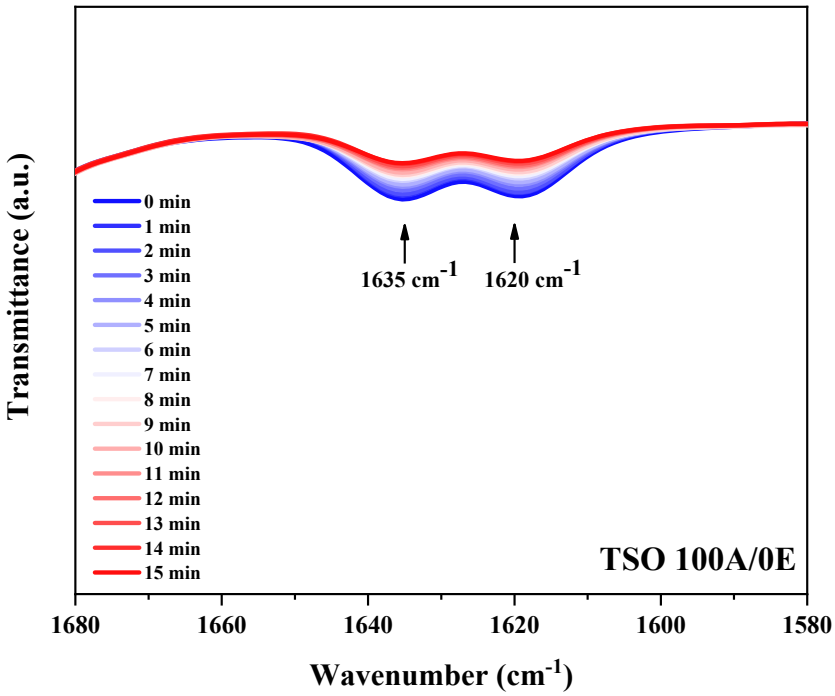
Transmittance (a.u.)
0 min
1 min
2 min
3 min
4 min
5 min
6 min
7 min
8 min
9 min
10 min
11 min
12 min
13 min
14 min
15 min
1635 cm-1
1620 cm-1
TSO 100A/0E
1680
1660
1640
1620
1600
1580
Wavenumber (cm-1)

(B)

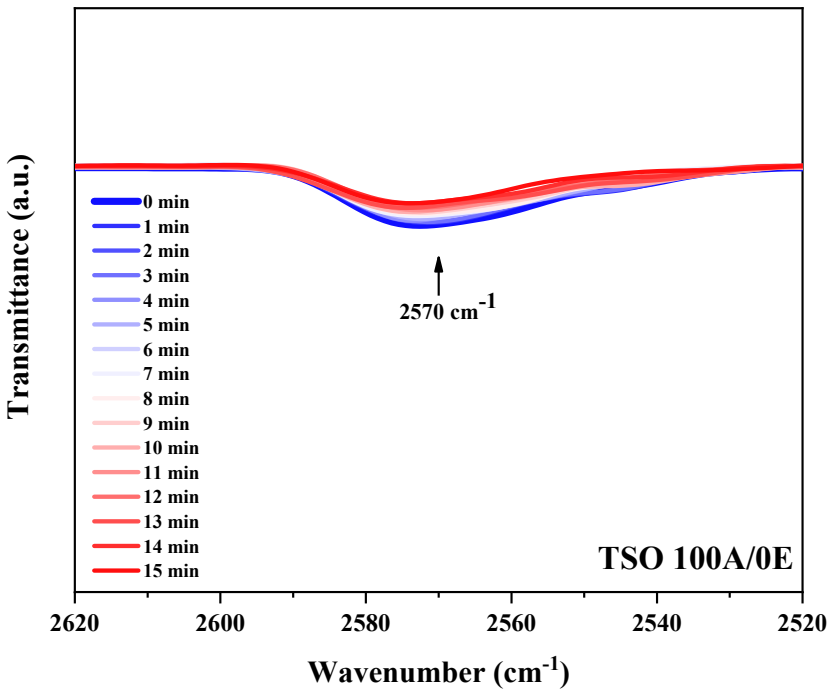
Transmittance (a.u.)
0 min
1 min
2 min
3 min
4 min
5 min
6 min
7 min
8 min
9 min
10 min
11 min
12 min
13 min
14 min
15 min
2570 cm-1
TSO 100A/0E
2620
2600
2580
2560
2540
2520
Wavenumber (cm-1)

(a)

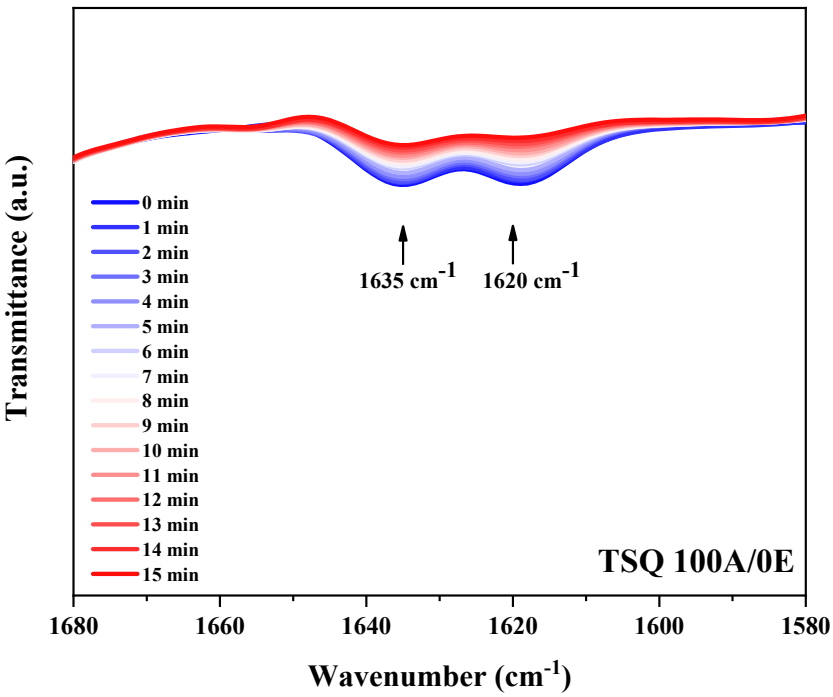
Transmittance (a.u.)
0 min
1 min
2 min
3 min
4 min
5 min
6 min
7 min
8 min
9 min
10 min
11 min
12 min
13 min
14 min
15 min
1635 cm-1
1620 cm-1
TSQ 100A/0E
1680
1660
1640
1620
1600
1580
Wavenumber (cm-1)

(b)

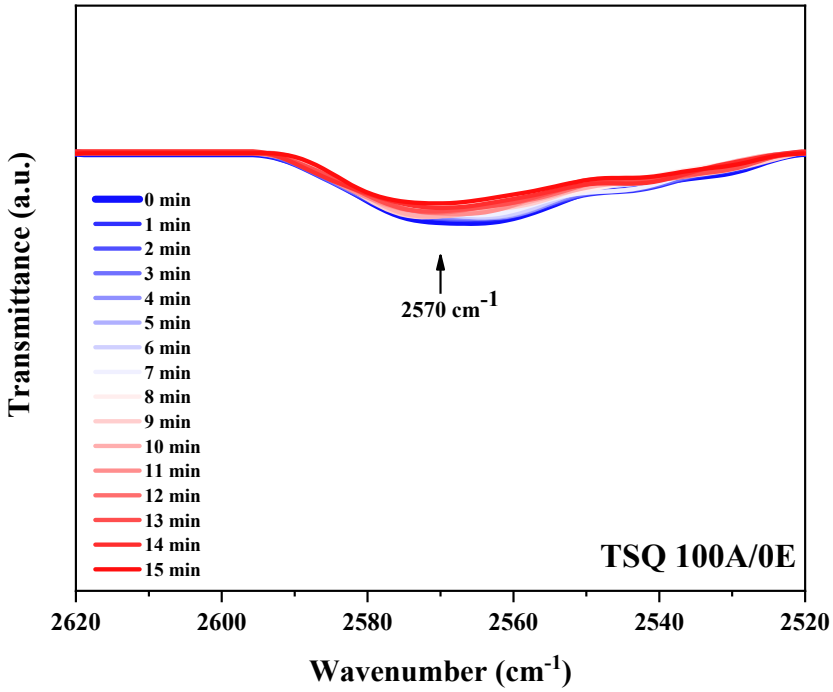

Figure 13. FT-IR spectra of thiol-acrylate polymerization depending on UV irradiation time
(A) Acrylate groups of TSO 100A/0E,
(B) Thiol groups of TSO 100A/0E,
(a) Acrylate groups of TSQ 100A/0E,
(b) Thiol groups of TSQ 100A/0E

(a)

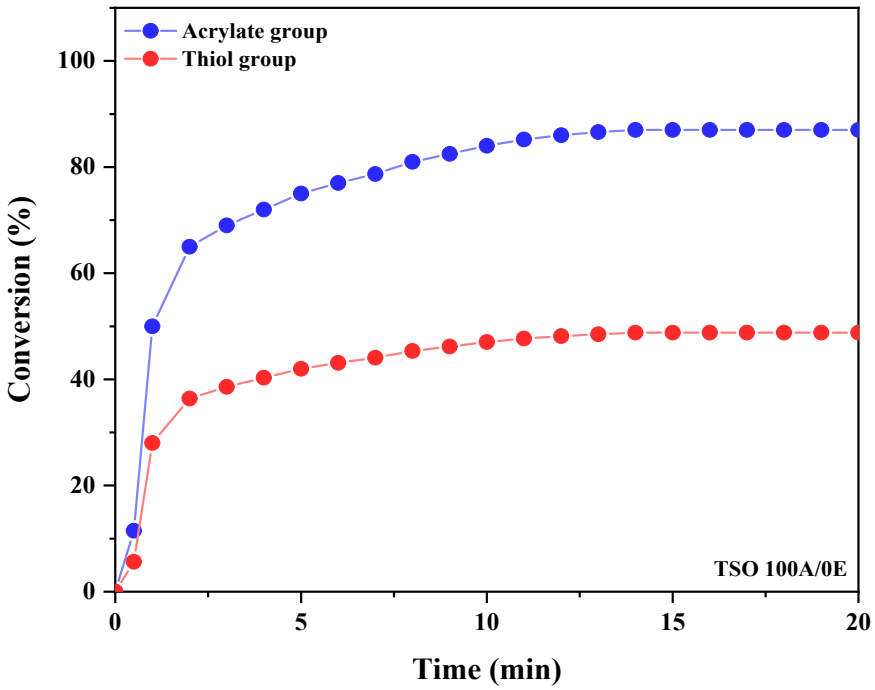
Acrylate group
Thiol group
Conversion (%)
Time (min)
TSO 100A/0E
0
20
40
60
80
100
0
5
10
15
20

(b)

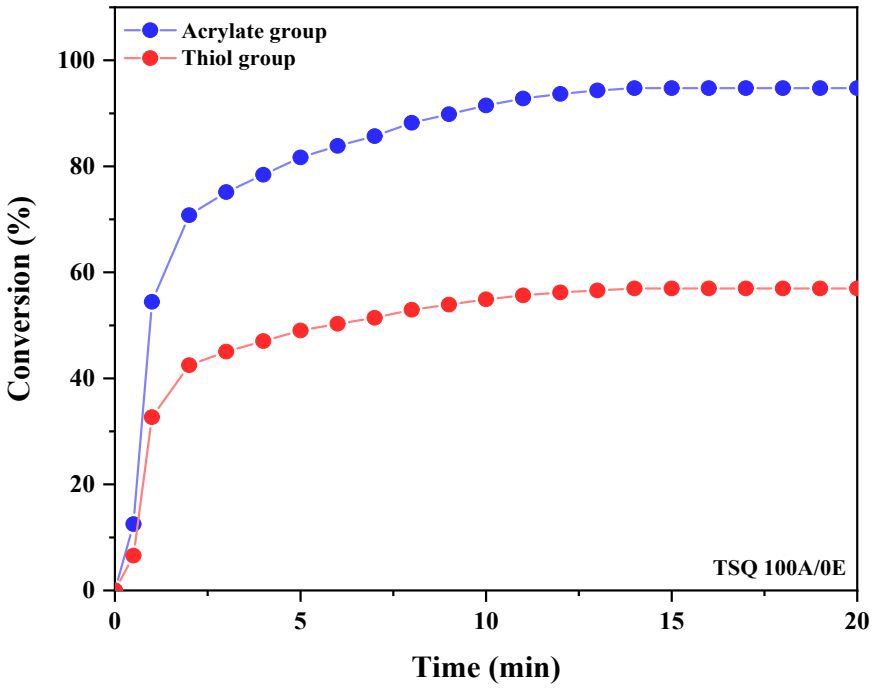

Figure 14. Conversion rate of acrylate and thiol functional groups (a) TSO 100A/0E, (b) TSQ 100A/0E

3.2. Monitoring of crosslinking kinetics

As curing progresses, the crossover point of storage modulus G′ and loss modulus G′′, that is, the gelation time is defined as the required time for the curing system to reach G′ = G′′ (Holmes, R. et al., 2017). It means that the viscoelastic fluid is transferred to the viscoelastic solid due to sufficient entanglement of the polymer chain. It is very important to know the gelation time of the cured material in the actual process because it is almost impossible to process due to its high viscosity after the gelation time. Table 4 shows the gelation time according to the different blend ratios of thiol-ene/thiol-epoxy resin and the type of curing agent, and it can

be seen that the gelation time increases rapidly as the ratio of thiol-ene reaction in thiol-ene/thiol-epoxy resins with different blend ratios increases.

The gelation time of dual-cured TSO 75A/25E or TSQ 75A/25E is 81s, 33s, respectively, which is as short as the only thiol-ene polymerization like TSO 100A/0E or TSQ 100A/0E with gelation time of each 27s, 21s. It supports the fact that thiol-ene by photopolymerization shows much faster curing and higher crosslinking density than thiol-epoxy by thermal curing. Furthermore, the dual-cured TSO 75A/25E or TSQ 75A/25E have the highest storage modulus value, 1,112 kPa and 2,358 kPa than the only thiol-ene or thiol-epoxy polymerization samples like 100A/0E or 0A/100E, respectively. Overall, TSQ cured samples have a better crosslinking density than those of TSO in the thiol-ene/thiol-epoxy hybrid network. However, the gelation times of TSQ 25A/75E and TSQ 0A/100E are longer than those of TSO due to steric hindrance by the protruding interfacial hydroxyl group. On the other hand, as the ratio of the thiol-epoxy reaction increases, an incomplete curing reaction occurs due to the internal epoxides of the long aliphatic chain that exhibits low and non-selective reactivity, resulting in an increase in gelation time (Tran, T. et al., 2020).

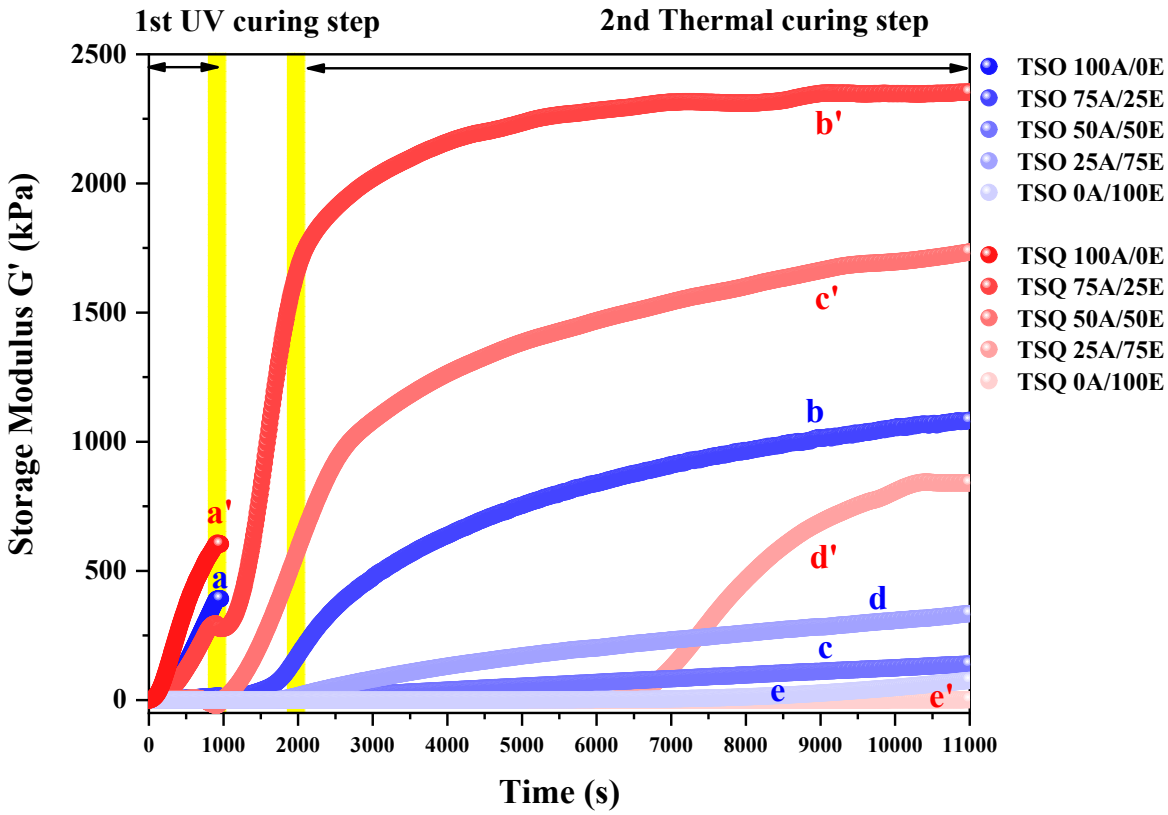

Figure 15. Storage modulus G′ versus curing time of thiol-ene/thiol-epoxy networks

Table 3. Rheological characteristics of thiol-ene/thiol-epoxy mixtures

Formulation (AESO/ESO)	Storage Modulus G′ (kPa)	Complex Viscosity η* (Pa·s)	Gel Point T_{gel} (s)
TSO 100A/0E	393	6,266	27 ±3
TSO 75A/25E	1,112	177,010	81 ±3
TSO 50A/50E	150	23,857	704.7 ±3
TSO 25A/75E	351	55,802	1303.2 ±6
TSO 0A/100E	76.6	13,816	4115.6 ±7.5
TSQ 100A/0E	604	9,630	21 ±3
TSQ 75A/25E	2,358	375,310	33 ±3
TSQ 50A/50E	1,781	282,610	81 ±3
TSQ 25A/75E	840.7	19,148	6090.7 ±6
TSQ 0A/100E	1.1	160	8676.9 ±7.5

* Including the heating time from room temperature to 150 ℃.

3.3. Gel fraction of thiol-ene/thiol-epoxy networks

Fig. 16 shows that the crosslinking density of the samples cured with TSQ oligomer is superior to that of samples containing TSO oligomer. This is because it has the high crosslinking density and stiffness segments by the polysilsesquioxane structure of TSQ oligomer as well as the influence by the number of functional groups (Lin, Y. et al., 2018; Mariusz, S. et al., 2018; Magdalena, G. et al., 2020). Furthermore, In the case of increasing thiol-epoxy reaction ratio compared to the thiol-ene reaction, the crosslinking density is lowered due to an incomplete curing reaction by the internal epoxy group of the long aliphatic chain that exhibits much poorer and non-selective reactivity than those terminal epoxy groups, indicating

the lowest degree of crosslinking in the 0A/100E sample (Liu, Z. et al., 2014). The degree of crosslinking of 75A/25E, which is a dual curing sample, was similar to that of 100A/0E polymerized by a thiol-acrylate reaction, but showed a higher value.

This is because the thiol-acrylate reaction, one of the thiol-ene reactions, is a non-stoichiometric polymerization that occurs together with chain-growth homopolymerization of the acrylate group and step-growth mechanism of the thiol-ene reaction, and thus an unreacted residual thiol group exists in 100A/0E. The elution of residual unreacted thiol groups due to the insufficient conversion results in a lower crosslinking density (Yue, S. et al., 2019).

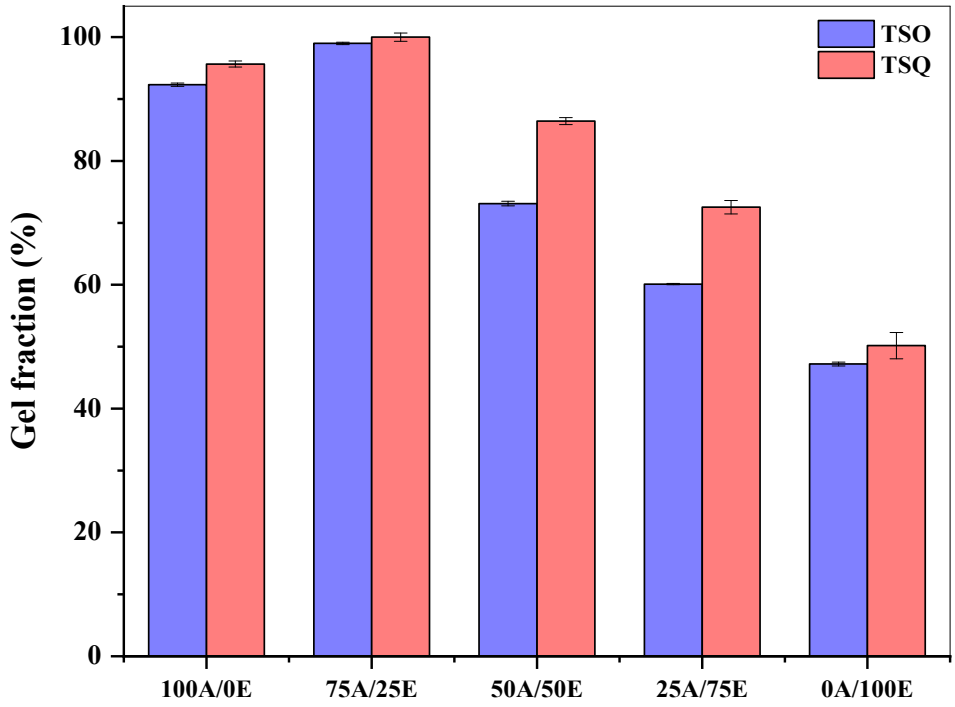

Figure 16. Gel fraction of thiol-ene/thiol-epoxy composites

3.4. Contact angle of thiol-ene/thiol-epoxy networks

In this research, two types of thiol-functionalized polysiloxane oligomers used as epoxy curing agents were separately applied to prepare film samples by varying mixing ratios of AESO and ESO. Fig. 14 shows the water contact angle of the prepared film.

In the 25A/75E films, the TSO film had a slightly higher contact angle than the TSQ film, but in general, the TSQ film showed a higher contact angle than the TSO film. This means that TSQ oligomers have a better ability to build epoxy networks than TSO oligomers. This is because the stronger the binding force between molecules, the higher the surface energy tends to be. In addition, TSQ 75A/25E films showed the highest contact angle value among TSQ samples, and TSO 50A/50E films showed the highest contact angle among TSO samples, indicating that the most suitable epoxy network was built at each corresponding blend ratio.

Comparing the contact angle values according to the blend ratio, the overall angle slope increased as the thiol-functionalized polysiloxane oligomers content added during film production increased. However, since the higher the ESO content, the lower the degree of crosslinking of the cured films due to the influence of the internal epoxy groups, the lowest contact angle value was found in the 0A/100E sample composed ESO only.

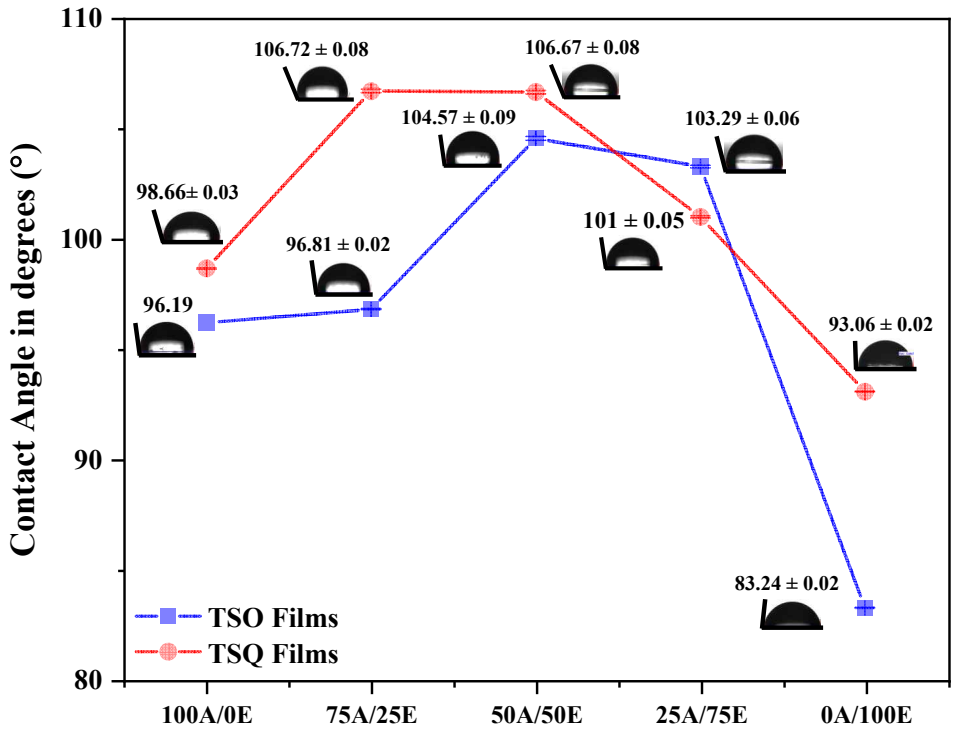

Figure 17. Water contact angles of thiol-ene/thiol-epoxy films

3.5. Mechanical properties of thiol-ene/thiol-epoxy networks

The damping factor (tan δ) of the thiol-ene/thiol-epoxy composites can be observed one peak in all cured samples, indicating that the soybean oil-based resins and the thiol-functionalized polysiloxane oligomers have good compatibility. However, compared to samples cured with a TSO oligomer, the width and height of the damping factor (tan δ) peak tend to be wider and lower, which is believed to be a phenomenon caused by an increase in the heterogeneity of the resins and TSQ oligomer (Unsworth, J. et al., 1992). This is because

the TSQ oligomer has unreacted dangling chains such as -OH and $-OCH_3$, and thus the distribution of crosslinking points is relatively more heterogeneous than the TSO oligomer. In addition, when the peak shapes of 100A/0E and 0A/100E were compared, it was found that the inhomogeneity with TSQ oligomer was greater in ESO than in AESO because the internal expoxides of ESO in a thermal polymerization have non-selective reactivity. Also, as the molecular chain of the long and flexible ESO increases, the distance between the reactors increases, and the crosslinking density decreases due to incomplete curing (Matsumoto, A. et al., 1998). For the reasons, it was observed that the glass transition temperature, storage modulus, and crosslinking density were all the lowest in the 0A/100E sample.

However, Fig. 14 shows that the storage modulus of a thiol-acrylate polymerized 100A/0 without ESO rapidly decreases as the temperature increases than the dual curing sample 75A/25E. This is because the unreacted thiol functional groups remain due to the influence of non-stoichiometric polymerization of thiol-acrylate, dramatically reducing the performance of cured 100A/0E (Allison, K. et al., 2006). Also, the presence of residual unreacted thiol groups due to the insufficient conversion results in a lower crosslinking density (Su, Y. et al., 2019). Therefore, it may be seen that the dual curing sample has a higher mechanical strength than the sample to which only photo-curing or thermal-curing is applied. Meanwhile, TSQ oligomer has a silsesquioxane structure as well as an effect by the number of functional groups, so they form a more dense crosslinking network than that of TSO oligomer with a linear structure (Ma, Y., et al., 2017; Xu Y. et al., 2020). In addition, as mentioned above, when unreacted dangling chains exist such as TSQ oligomer and the distribution of the crosslinking points is uneven, more physical

crosslinking is included, resulting in a higher glass transition temperature. Therefore, in the same content of the sample, as shown in Table 4 the samples cured with TSQ oligomer has a higher glass transition temperature, storage modulus, and crosslinking density than those of TSO oligomer.

(a)

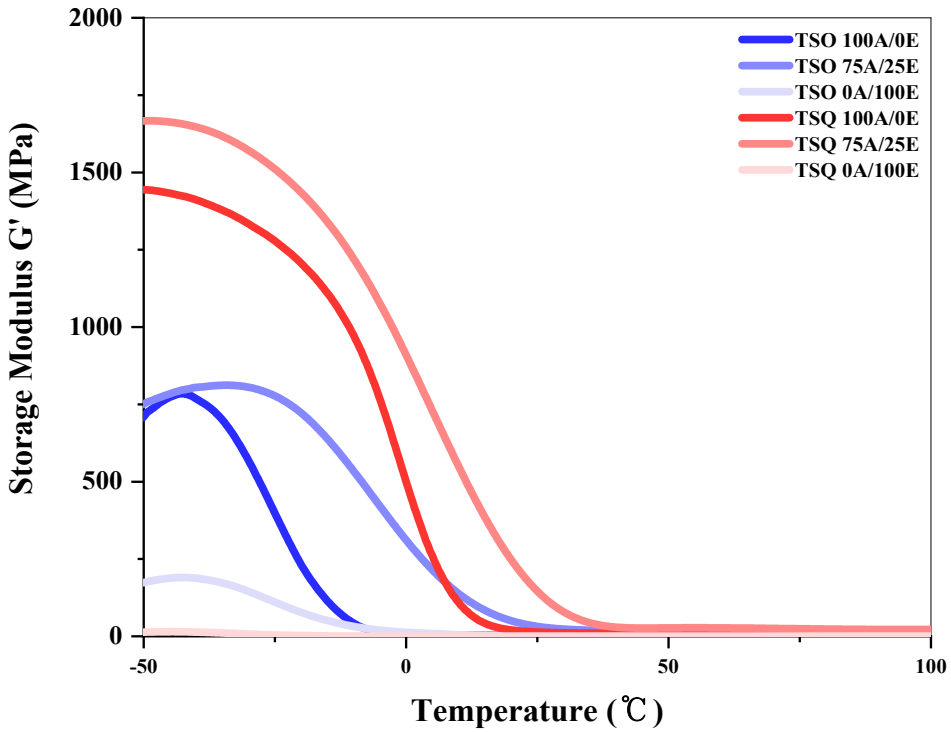

(b)

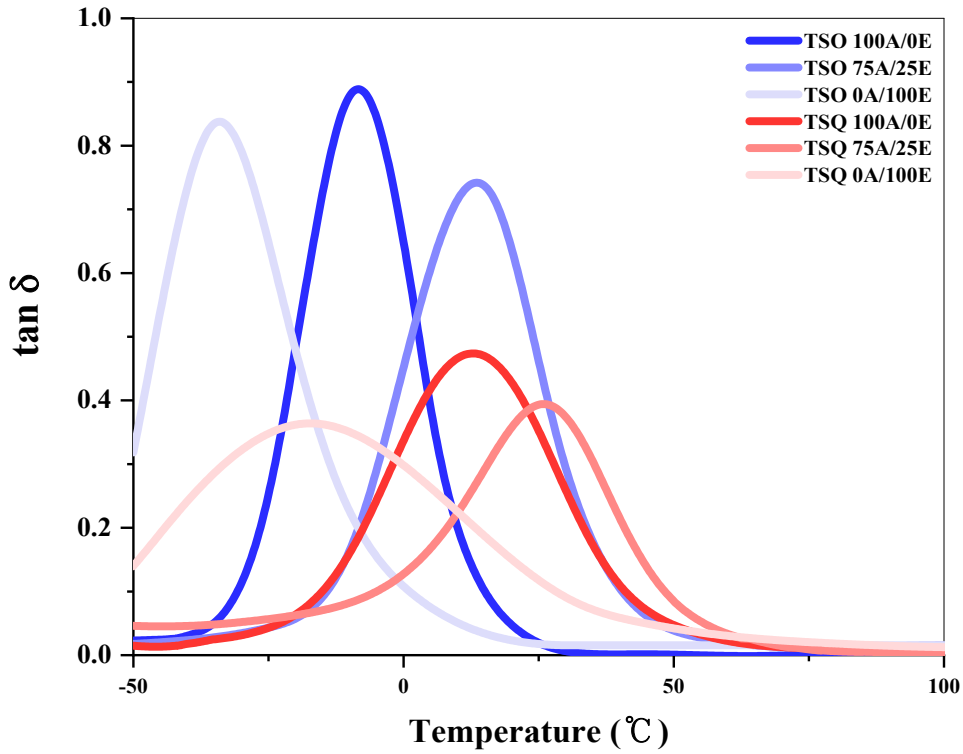

Figure 18. (a) Storage modulus (G′) of thiol-ene/thiol-epoxy composites (b) Tan δ curves versus temperature for thiol-ene/thiol-epoxy composites

Table 4. DMA data of thiol-ene/thiol-epoxy composites

Formulation (AESO/ESO)	T_g (℃)	E_{high} (MPa)	T_{high} (K)	v_e (mol/m^3)
TSO 100A/0E	-8.3	3.2	314.7	412.8
TSO 75A/25E	13.6	18.3	336.6	2177.4
TSO 0A/100E	-34.2	1.8	288.8	251.2
TSQ 100A/0E	12.8	7.7	335.8	921.5
TSQ 75A/25E	26	24.2	349	2780.9
TSQ 0A/100E	-17.5	0.5	305.5	63.6

* T_g : Temperature of the maximum of tanδ estimated by DMA
* E_{high} : Storage modulus at rubbery plateau regime determined at T_g + 50 ℃
* T_{high} : Temperature at E_{high}
* v_e : Cross-linking density calculated according to the Flory's rubber elasticity theory

3.6. Thermal stability of thiol-ene/thiol-epoxy networks

All samples were made of a stoichiometric mixture of acrylate and epoxy groups per thiol in a molar ratio of 1:1. According to this, as a result, the content of the added thiol oligomer increases as the content of the epoxy group relative to acrylate group in the total mixture increases. According to Table 5, for samples cured with TSO oligomers, except for 0A/100E, there was no significant difference in temperature at the weight loss of 5 wt% obtained from TGA curves of 399.7~407.3 ℃ and the temperature of maximum decomposition was

481.7~504.7 ℃, and the highest value was 75A/25E, a dual-cured sample. In the case of samples cured with TSQ oligomers, the temperature at the weight loss of 5 wt% was 352.2 to 357.8 ℃ and the temperature of maximum decomposition was 413 to 420℃, which were not significantly different in all samples, and among them, likewise, the highest value was 420 ℃ in 75A/25E, a dual-cured sample.

These results were found to have no significant effect on the tendency according to the amount of thiol-functionalized polysiloxane oligomers added. It was found that the higher thermal decomposition temperature was not shown despite an increase in the content of thiol-functionalized polysiloxane oligomers with excellent thermal stability due to the decrease in crosslinking density as the epoxy group content increased. In addition, unlike the thermal decomposition temperature of the oligomers themselves, the thermal decomposition temperature was higher than that of the sample cured with TSO oligomer to TSQ oligomer. It is thought to be due to the steric hindrance caused by the protruding interfacial hydroxyl group of TSQ oligomer.

On the other hand, the Integral procedural decomposition temperature (IPDT) represented by a quantitative value obtained by the area ratio was proposed by Doyle as below equation.

$$A^* = (S_1 + S_2)/(S_1 + S_2 + S_3)$$
$$K^* = (S_1 + S_2)/S_1 \quad (3)$$

$$IPDT(℃) = A^* K^* (T_f - T_i) + T_i \quad (4)$$

Here, T_i and T_f were represented initial and final experimental temperatures, 30 ℃ and 800 ℃ in this study, respectively. S_1, S_2, and S_3 show the product of mass and temperature intervals. S_2 is defined by multiplying the residual mass amount by the temperature interval, S_1 is defined by subtracting S_2 from the area below the thermal decomposition curve, and S_3 is defined by the area outside the area below the thermal decomposition curve. As the content of the epoxy group in the thiol-ene/thiol-epoxy hybrid network increases, the total thiol-functionalized polysiloxane oligomers content increases, and thus the IPDT, which represents thermal stability as a quantitative value obtained by the area ratio, gradually increased. This showed results contrary to the thermal decomposition temperature. Both of the above factors correspond to indicators showing thermal stability, but the thermal decomposition temperature is somewhat insufficient to exhibit practical thermal stability as a value obtained by simply using a reaction rate process according to the shape of a decomposition curve.

On the other hand, IPDT is considered to be more suitable because it reflects the entire thermal decomposition process, starting from the beginning of thermal decomposition and including data on residual mass after the reaction is completed (Xie, Y. et al. 2010). As the degree of the residual mass increased, which showed that the thermal stability of the thiol-ene/thiol-epoxy resulting polymers improved gradually. As the amount of thiol-functionalized polysiloxane oligomers increased in the thiol-ene/thiol-epoxy resulting polymer networks, the IPDT value increased due to the increase in thermal stability index A* and K*. That is, the thiol-functionalized polysiloxane oligomers act as a factor that increases thermal stability by preventing local thermal decomposition. In addition, since the silsesquioxane structure of the TSQ oligomer restricts heat transfer

from a polymer surface to an internal structure, the samples cured with the TSQ oligomer showed higher IPDT values than those of the TSO oligomer (Arkadiusz, N. et al., 2019).

(A)

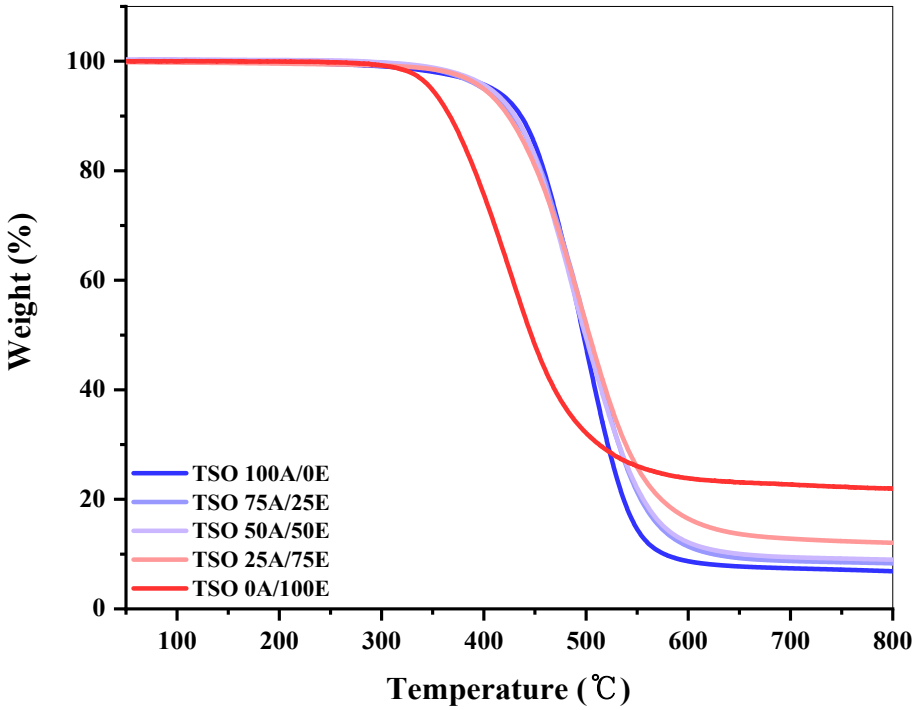

(B)

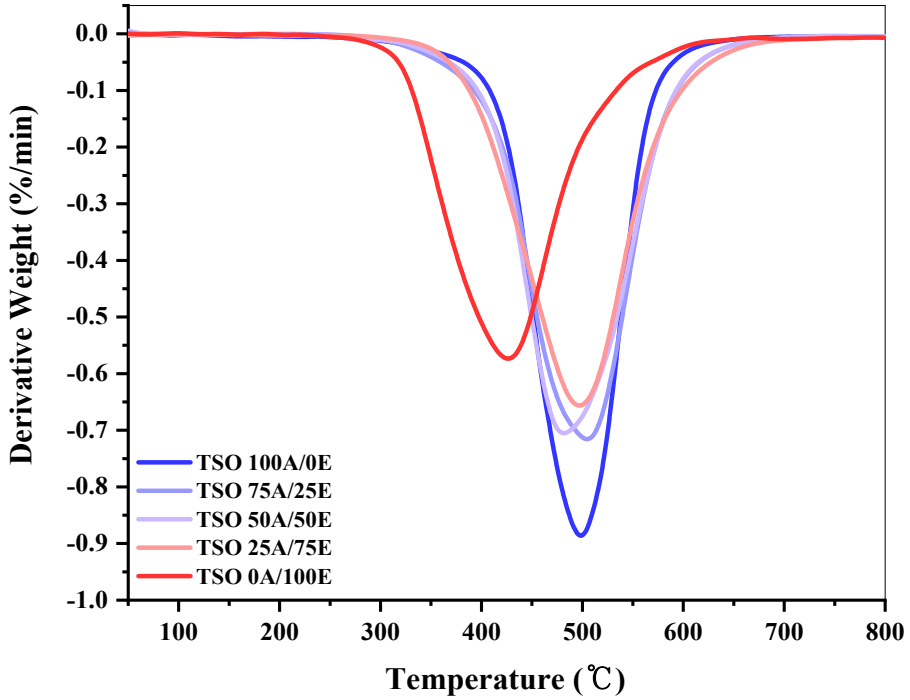
Derivative Weight (%/min)
0.0
-0.1
-0.2
-0.3
-0.4
-0.5
-0.6
-0.7
-0.8
-0.9
-1.0
100
200
300
400
500
600
700
800
Temperature (℃)
TSO 100A/0E
TSO 75A/25E
TSO 50A/50E
TSO 25A/75E
TSO 0A/100E

(a)

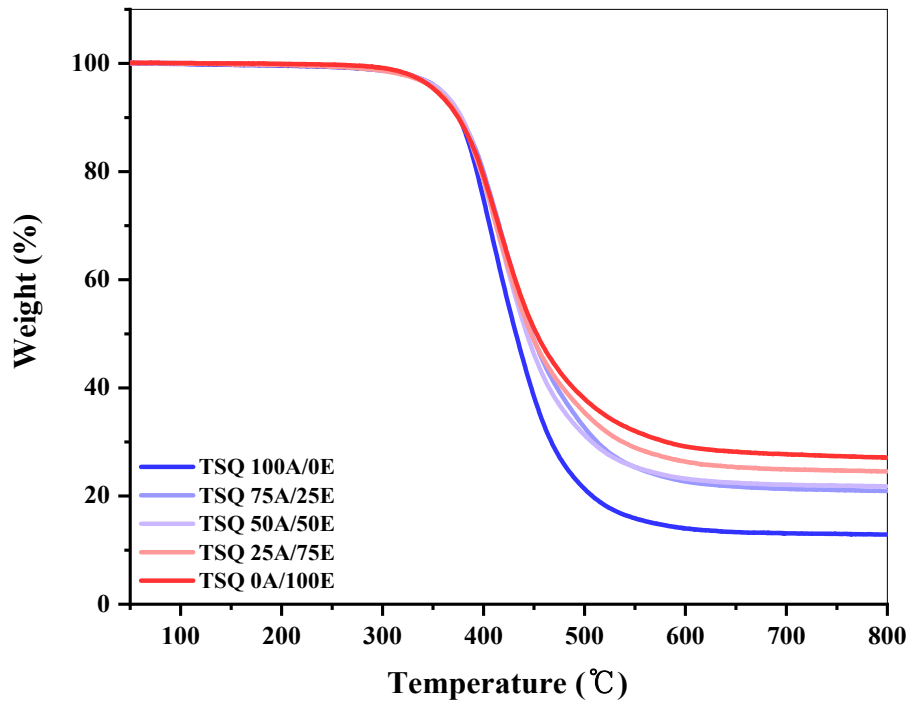
Weight (%)
100
80
60
40
20
0
100
200
300
400
500
600
700
800
Temperature (℃)
TSQ 100A/0E
TSQ 75A/25E
TSQ 50A/50E
TSQ 25A/75E
TSQ 0A/100E

(b)

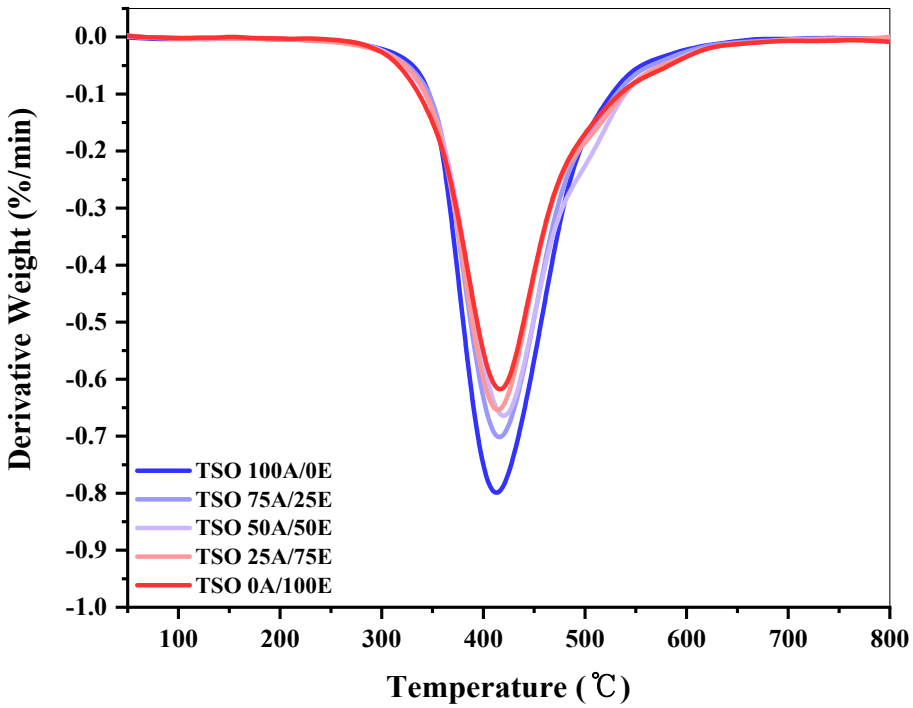

Figure 19. TGA and DTG curves of thiol-ene/thiol-epoxy composites (A, B) for cured with TSO oligomer, (a, b) for cured with TSQ oligomer

Table 5. TGA data of thiol-ene/thiol-epoxy composites

Formulation (AESO/ESO)	$T_{dec.-5\%}$ (℃)	T_{max} (℃)	$A^*·K^*$	IPDT (℃)	Residual mass (%)
TSO 100A/0E	407.3	498.7	0.5	418.42	6.9
TSO 75A/25E	399.7	504.7	0.51	424.85	8.3
TSO 50A/50E	405	481.7	0.52	430.84	9
TSO 25A/75E	400.2	496.9	0.56	460.81	12.1
TSO 0A/100E	348.8	426.3	0.8	648.69	22
TSQ 100A/0E	357.5	413	0.63	513.8	12.9
TSQ 75A/25E	355.2	420	0.77	622.81	20.9
TSQ 50A/50E	357.8	415.7	0.8	644.05	21.8
TSQ 25A/75E	353.8	414.3	0.9	722.58	24.6
TSQ 0A/100E	352.2	416.7	1	823.2	27

* $T_{dec.-5\%}$: Temperature at the weight loss of 5% obtained from TGA curve
* IPDT : Integral procedural decomposition temperature
* T_i : Initial temperature (30 ℃)
* T_f : Final temperature (800 ℃)
* A^* , K^* : Thermal stability index
* T_{max} : temperature of maximum rate of weight loss

3.7. Antimicrobial test of thiol-ene/thiol-epoxy networks

Antibacterial test of the thiol-ene/thiol-epoxy resulting polymer composites was performed on *Staphylococcus aureus* (Gram-positive), *E. coli* (Gram-negative), and *Cronobacter sakazakii* (Gram-negative

bacteria). As a result of the evaluation, contact antibacterial activity was observed only in *S. aureus* (gram-positive bacteria). In the 75A/25E formulation, the antibacterial activity increased in epoxy networks using TSQ oligomer than TSO oligomer and when the oligomer content in the epoxy network was higher. Even after 6 hours, the growth of *S. aureus* was not observed. The cell walls of Gram-positive and Gram-negative bacteria have different structures, compositions, and functions, respectively. The cell walls of bacteria maintain size and shape, and play an important role in preventing cell rupture caused by osmotic pressure and cell division. Gram-positive bacteria consist of 80-90% of peptidoglycan layers, which are polymers of disaccharide, and have thicker cell walls than gram-negative bacteria.

On the other hand, outer membrane is a unique structure observed only in gram-negative bacteria, maintaining the structure of bacteria and acting as a permeability barrier to macromolecules and hydrophobic molecules. The antibacterial properties in this study are due to inhibition of cell wall synthesis, and when synthesis is suppressed at each synthesis stage of cell wall, which functions essential for bacteria to survive, bacteria are destroyed. Long unsaturated fatty acid chains in the triglyceride structure of AESO and ESO-derived from soybean oil exhibit antimicrobial activity mediated by inhibition of fatty acid biosynthesis (Persson, C. et al., 2015).

Unlike Gram-positive bacteria such as *S. aureus*, Gram-negative bacteria such as *E. coli* and *C. Sakazaki* did not show antibacterial properties, especially because the outer membrane stubbornly refuses to penetrate antibacterial substances. On the other hand, Antibacterial substances irreversibly bind to the active site to inhibit the synthesis

of fatty acids in *S. aureus* and interfere with the formation of electrons and RNA in DNA, a process necessary for bacterial proliferation, indicating antibacterial action. The cell wall is then gradually destroyed, and antibacterial substances begin to leak from the cell at this stage (Wang, L. et al., 2017). Additionally, two types of thiol-functionalized polysiloxane oligomers, TSQ and TSO added to the thiol-ene/thiol-epoxy hybrid networks can provide relatively excellent antibacterial activity because they stick to the surface of the substance and prevent Gram-positive bacterial clusters from forming quickly.

Although this study has a relatively narrow antibacterial area that acts only on gram-positive bacteria, it has selective toxicity that affects only microorganisms, inhibiting the synthesis of cell walls that are not present in human cells, so it can be used safely without risk. It is important to select an appropriate application because only *S. aureus* shows sensitive antibacterial properties. Diseases caused by Gram-positive bacteria are mainly human diseases including skin and soft tissue infections caused by direct contacts and are vulnerable to artificial inserts such as catheters, so related applications are expected to be suitable. Furthermore, Gram-positive bacteria have a high carrier rate in diabetic, dialysis, surgical, and AIDS patients. Therefore, the thiol-ene/thiol-epoxy resulting polymer composites are required to be applied only to corresponding applications.

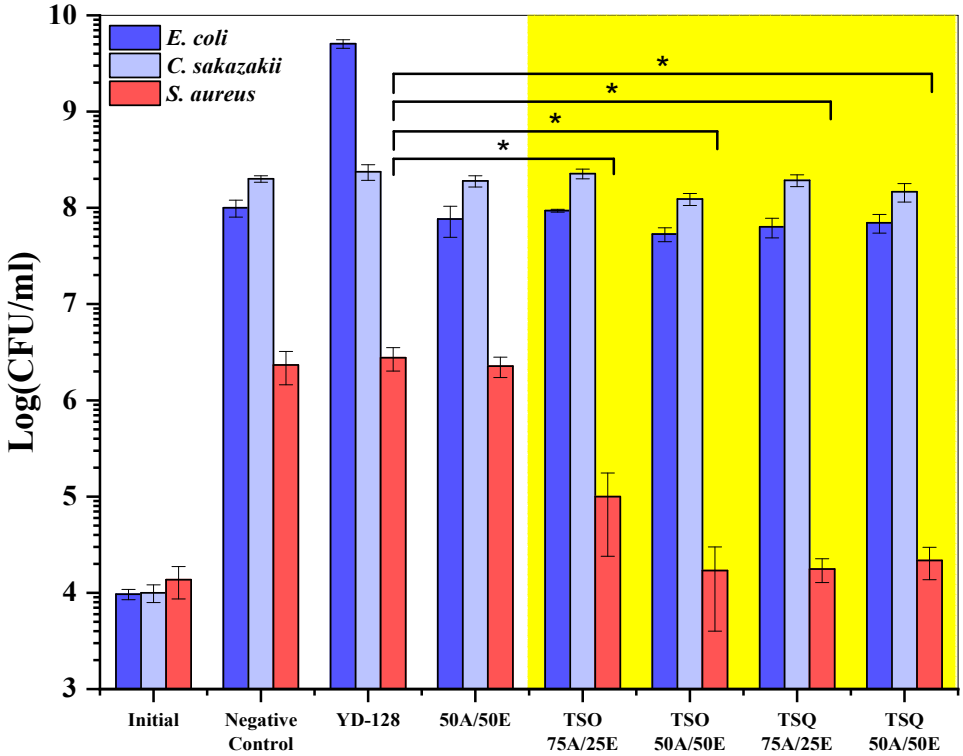

Figure 20. Antimicrobial effect of thiol-ene/thiol-epoxy composites

3.8. VOCs emission analysis

In general, POPD (Poly(oxypropylene)diamine) and PETT (Pentaerythritol tetrakis(3-mercaptopropionate)), commercialized as epoxy hardeners, are over the Ecolabel and CertiPUR Label Requirements (TVOCs standard limits : 500 $\mu g/m^3$). On the other hand, it was confirmed that the TVOCs emissions of the newly synthesized two types of thiol-functionalized polysiloxane oligomers, TSQ and TSO oligomer in this study were very low at 86.79 $\mu g/m^3$ and 118 $\mu g/m^3$, respectively. Furthermore, the TVOCs emissions of TSO 75A/25E and TSQ 75A/25E, the final thiol-ene/thiol-epoxy

resulting polymer composites in this study, are very low at 93.26 $\mu g/m^3$ and 175.9 $\mu g/m^3$, respectively. Therefore, it can be used not only at high temperatures that require heat disinfection, but also in various fields because nothing comes from bisphenol A and industrial oligomers. Similarly, TSO 75A/25E and TSQ 75A/25E initial mixtures, which are thiol-ene/thiol-epoxy prepolymers before curing, can also prevent the health hazards of workers due to strong toxic fumes with TVOCs emissions of 284.3 $\mu g/m^3$ and 508.1 $\mu g/m^3$, respectively.

VOCs are the main odor contributors which detect non-negligible odors even at low ppm concentrations, and most contain irritating and unpleasant odors (Moschandreas, D. J. et al., 1992). Given the correlation between VOCs composition and odor concentration, the thiol-functionalized polysiloxane oligomers with low VOC release contribute to odor reduction compared to other commercial epoxy hardeners despite the presence of thiol groups. The odor properties also depend on various health problems since the VOCs have a toxic potential (Polvara, E. et al., 2020). Therefore, since the oligomers, thiol-ene/thiol-epoxy prepolymers, and composites prevent the occurrence of serious odors, it is believed that vomiting, allergic symptoms, mental neurosis, and poor work efficiency can be prevented (Noguchi, M. et al., 2016).

Table 6. VOCs emission analysis

[$\mu g/m^3$]	POPD	PETT	TSO	TSQ	TSO 75A/25E		TSQ 75A/25E	
					Initial blend	Dual curing	Initial blend	Dual during
TVOCs	11,130	876	86.7	118	284.3	93.2	498.1	175.9
6VOCs	327.3	4.1	3.1	4.7	184.6	3.3	129	10.9
Toluene	311.6	0.41	1.1	1.1	173.8	0.8	116.5	8.7
Benzene	11.7	3.64	2	3.6	3.1	2.5	3.7	2.2
Ethylbenzene	0.6	0	0	0	1.3	0	1.6	0
m,p-Xylene	1.39	0	0	0	5.7	0	6.2	0
Styrene	2	0	0	0	0	0	0	0

* POPD : Poly(oxypropylene)diamine,
* PETT : Pentaerythritol tetrakis(3-mercaptopropionate)
* A : Acrylated epoxidized soybean oil, E : Epoxidized soybean oil

4. Conclusions

In this study, commercially modified soybean oil was used as a substitute for petroleum-based DGEBA. The epoxy networks have been successfully formed without toxic commercial catalysts, reducing the negative impact on health, safety and the environment.

Additionally, Two structures of polysiloxane oligomers were synthesized to improve thermal and mechanical properties. Thiol-functionalized polysiloxane was used as an epoxy curing agent to form an organic-inorganic hybrid network.

The thiol-ene/thiol-epoxy initial mixtures were prepared by incorporating acrylated epoxidized soybean oil (AESO) and epoxidized

soybean oil (ESO) in different composition ratios. All prepolymers targeting the molar ratio of both acrylate/thiol and epoxy/thiol at 1:1 were fabricated from stoichiometric mixtures of AESO, ESO, and thiol-functionalized polysiloxane oligomers. The chemical structure and functionality of two structurally different thiol-functionalized polysiloxane oligomers on the crosslinking and resulting polymer properties of AESO and ESO were investigated in this study.

In the thermal curing system, as the thiol-epoxy ratio increased, the mechanical properties and crosslinking density degraded due to incomplete curing reaction by the internal epoxides with low and non-selective reactivity. Also, the thiol-acrylate network of one-step UV curing has shown lower mechanical properties and crosslinking density than the dual curing network due to the influence of the residual thiol groups. Because a great deal of unreacted thiol groups has dramatically degraded the performance of the cured materials.

On the other hand, among the dual-cured samples, 75A/25E showed optimum performance in terms of mechanical properties and crosslinking density. And the 75A/25E had as short gel time as UV cured samples. Also, TSQ cured samples formed a better crosslink network than those of TSO due to the difference of polysiloxane structure.

In thermal stability analysis, as the degree of the residual mass increased, thermal stability improved gradually. Because as the content of thiol-functionalized polysiloxane oligomer increases, it prevents local thermal decomposition and increases overall thermal stability. However, the thermal decomposition temperature decreases due to low crosslinking density as the epoxy group content increased. Another reason may be the difference in the steric hindrance in the open corner of the POSS structure.

In dual curing conditions, TSO oligomers may be added to reduce the VOCs emission content of the epoxy network and increase compatibility with the bio-based epoxy resins and increase the initial thermal decomposition temperature. TSQ oligomers may be also added to increase crosslinking density, glass transition temperature, and storage modulus. If the thiol-functionalized polysiloxane oligomers with different structures are well controlled, epoxy networks with various performances can be formed.

These attempts to overcome the limitations of vegetable oil-based epoxy resins are expected to have a significant impact on the formation of sustainable epoxy networks in the future.

References

References

Acik, G. (2020). Bio-based poly (□caprolactone) from soybean-oil derived polyol via ring-opening polymerization. *Journal of Polymers and the Environment*, **28**(2), 668-675.

Acocella, M. R., Corcione, C. E., et al. (2016) Graphene oxide as a catalyst for ring opening reactions in amine crosslinking of epoxy resins. *The Royal Society of Chemistry Advances*, **6**(28), 23858-23865.

Altuna, F. I., Espósito, L. H., et al. (2011). Thermal and mechanical properties of anhydride cured epoxy resins with different contents of biobased epoxidized soybean oil. *Journal of Applied Polymer Science*, **120**(2), 789-798.

Andreani, T., Fernandes, P. M., et al. (2020). The critical role of the dispersant agents in the preparation and ecotoxicity of nanomaterial suspensions. *Environmental Science and Pollution Research*, **27**(16), 19845-19857.

Arbenz, A., Perrin, R., & Avérous, L. (2018). Elaboration and properties of innovative biobased PUIR foams from microalgae. *Journal of Polymers and the Environment*, **26**(1), 254-262.

Ayrilmis, N., Lee, Y. K., et al. (2016). Formaldehyde emission and VOCs from LVLs produced with three grades of urea-formaldehyde resin modified with nanocellulose. *Building and Environment*, **97**, 82-87.

Baney, R. H., Itoh, M., Sakakibara, A., & Suzuki, T. (1995). Silsesquioxanes. *Chemical Reviews*, **95**(5), 1409-1430.

Belmonte, A., Fernández-Francos, X., et al. (2017). Phenomenological characterization of sequential dual-curing of off-stoichiometric "thiol-epoxy" systems: Towards applicability. *Materials & Design*, **113**, 116-127.

Bhat, S., Uthappa, U. T., et al. (2021). Functionalized Porous Hydroxyapatite Scaffolds for Tissue Engineering Applications: A Focused Review. *ACS Biomaterials Science & Engineering*.

Boiadjiev, S. E., & Lightner, D. A. (2000). Steric size in conformational analysis. Steric compression analyzed by circular dichroism spectroscopy. *Journal of the American Chemical Society*, **122**(46), 11328-11339.

Cengiz, N., Rao, J., et al. (2013). Designing functionalizable hydrogels through thiol‐epoxy coupling chemistry. *Chemical communications*, **49**(95), 11191-11193.

Chen, Q., Xue, F., & Ding, E. (2019). Preparation of POSS-triol/wollastonite composite particles by Liquid phase mechanochemical method and its application in UV curable coatings. *Science and Engineering of Composite Materials*, **26**(1), 183-196.

Cordes, D. B., Lickiss, P. D., & Rataboul, F. (2010). Recent developments in the chemistry of cubic polyhedral oligosilsesquioxanes. *Chemical Reviews*, **110**(4), 2081-2173.

Das, S., Pandey, P., et al. (2017). Evaluation of biodegradability of green polyurethane/nanosilica composite synthesized from transesterified castor oil and palm oil based isocyanate. *International Biodeterioration & Biodegradation*, **117**, 278-288.

Dernehl, C. U. (1951). Clinical experiences with exposures to ethylene amines. *Industrial Medicine and Surgery*, **20**(12), 541-6.

Doyle, C. D. (1961). Estimating thermal stability of experimental polymers by empirical thermogravimetric analysis. *Analytical Chemistry*, **33**(1), 77-79.

Duchateau, R. (2002). Incompletely condensed silsesquioxanes: versatile tools in developing silica-supported olefin polymerization catalysts. *Chemical Reviews*, **102**(10), 3525-3542.

Espósito, L. H., & Marzocca, A. J. (2020). Silica filled S SBR with epoxidized soybean oil: Influence of the mixing process on rheological and mechanical properties of the compound. *Journal of Applied Polymer Science*, **137**(13), 48504.

Fan, L., Wei, L., et al. (2020). Synthesis of Environmentally Friendly Acrylonitrile Butadiene Styrene Resin with Low VOC. *Materials*, **13**(7), 1663.

Fernández-Francos, X., Konuray, A. O., et al. (2016). Sequential curing of off-stoichiometric thiol‐epoxy thermosets with a custom-tailored structure. *Polymer chemistry*, **7**(12), 2280-2290.

Gerard, J. F., Galy, J., et al. (1991) Viscoelastic response of model epoxy networks in the glass transition region. *Polymer Engineering & Science*, **31**(8), 615-621.

Graiver, D., Farminer, K. W., & Narayan, R. (2003). A review of the fate and effects of silicones in the environment. *Journal of Polymers and the Environment*, **11**(4), 129-136.

Grauzeliene, S., Navaruckiene, A., et al. (2021). Vegetable oil-based thiol-ene/thiol-epoxy resins for laser direct writing 3D micro-/nano-lithography. *Polymers*, **13**(6), 872.

Grzelak, M., Januszewski, R., & Marciniec, B. (2020). Synthesis and Hydrosilylation of Vinyl-Substituted Open-Cage Silsesquioxanes with Phenylsilanes: Regioselective Synthesis of Trifunctional Silsesquioxanes. *Inorganic chemistry*, **59**(11), 7830-7840.

Han, J., Liu, T., et al. (2018). A catalyst-free epoxy vitrimer system based on multifunctional hyperbranched polymer. *Macromolecules*, **51**(17), 6789-6799.

Handke, M., & Kowalewska, A. (2011). Siloxane and silsesquioxane molecules—precursors for silicate materials. *Spectrochimica Acta Part A: Molecular and Biomolecular Spectroscopy*, **79**(4), 749-757.

Hartmann-Thompson, C. (2011). Applications of polyhedral oligomeric silsesquioxanes. *Springer Science & Business Media,* **3**, 25-78

Holmes, R., Yang, X. B., et al. (2017). Thiol-ene photo-click collagen-PEG hydrogels: impact of water-soluble photoinitiators on cell viability, gelation kinetics and rheological properties. *Polymers*, **9**(6), 226.

Horowitz, H. H., & Metzger, G. (1963). A new analysis of thermogravimetric traces. *Analytical Chemistry*, **35**(10), 1464-1468.

Hoyle, C. E., & Bowman, C. N. (2010). Thiol‐ene click chemistry. *Angewandte Chemie International Edition*, **49**(9), 1540-1573.

Ivaldi, C., Miletto, I., et al. (2019). Influence of Silicodactyly in the Preparation of Hybrid Materials. *Molecules*, **24**(5), 848.

Jia, M., Wu, C., et al. (2009). Synthesis and characterization of a silicone resin with silphenylene units in Si-O-Si backbones. *Journal of applied polymer science*, **114**(2), 971-977.

Jian, Y., He, Y., et al. (2013). Thiol‐epoxy/thiol‐acrylate hybrid materials synthesized by photopolymerization. *Journal of Materials Chemistry C*, **1**(29), 4481-4489.

Kalia, S. & Pielichowski, K. (2018) Polymer/POSS nanocomposites and hybrid materials : preparation, properties, applications. *Springer Series on Polymer and Composite Materials*, 1-26.

Kanerva, L., Elsner, P., et al. (2013). Handbook of occupational dermatology. *Springer Science & Business Media*, 570-620.

Kanerva, L., Estlander, T., & Jolanki, R. (1996). Occupational allergic contact dermatitis caused by 2, 4, 6 tris (dimethylaminomethyl) phenol, and review of sensitizing epoxy resin hardeners. *International journal of dermatology*, **35**(12), 852-856.

Kanerva, L., Hyry, H., Jet al. (1997). Delayed and immediate allergy caused by methylhexahydrophthalic anhydride. *Contact Dermatitis*, **36**(1), 34-38.

Karger-Kocsis, J., Grishchuk, S., et al. (2014). Curing, gelling, thermomechanical, and thermal decomposition behaviors of anhydride cured epoxy (DGEBA)/epoxidized soybean oil compositions. *Polymer Engineering & Science*, **54**(4), 747-755.

Keim, W., & Roeper, M. (1981). Terpene amine synthesis via palladium-catalyzed isoprene telomerization with ammonia. *The Journal of Organic Chemistry*, **46**(18), 3702-3707.

Kim, J. S., Yang, S., et al. (2011). Photo-curable siloxane hybrid material fabricated by a thiol‐ene reaction of sol‐gel synthesized oligosiloxanes. *Chemical Communications*, **47**(21), 6051-6053.

Kim, K. R., Lee, J. Y., et al. (2020). Volatile content and VOCs emitted from inks used in the printing industry. *Journal of Odor and Indoor Environment*, **19**(2), 166-176.

Kolb, H. C., Finn, M. G., et al. (2001). Click Chemistry: Diverse Chemical Function from a Few Good Reactions. *Angewandte Chemie International Edition*, **40**(11), 2004-2021.

Krongauz, V. (2010). Diffusion in polymers dependence on crosslink density: Eyring approach to mechanism. *Journal of Thermal Analysis and Calorimetry*, **102**(2), 435-445.

Laine, R. M., & Roll, M. F. (2011). Polyhedral phenylsilsesquioxanes. *Macromolecules*, **44**(5), 1073-1109.

Li, R., Zhang, P., Liu, T., et al. (2018). Use of hempseed-oil-derived polyacid and rosin-derived anhydride acid as cocuring agents for epoxy materials. *ACS Sustainable Chemistry & Engineering*, **6**(3), 4016-4025.

Li, Y., Ren, M., et al. (2019). A robust and flexible bulk superhydrophobic material from silicone rubber/silica gel prepared by thiol‐ene photopolymerization. *Journal of materials chemistry A*, **7**(12), 7242-7255.

Lin, Y., & Song, M. (2018). Effect of polyhedral oligomeric silsesquioxane nanoparticles on thermal decomposition of cyanate ester resin. *Reactive and Functional Polymers*, **129**, 58-63.

Liu, H., Kondo, S. I., et al. (2008). A spectroscopic investigation of incompletely condensed polyhedral oligomeric silsesquioxanes (POSS-mono-ol, POSS-diol and POSS-triol): Hydrogen-bonded interaction and host‐guest complex. *Journal of Organometallic Chemistry*, **693**(7), 1301-1308.

Liu, S. H., Shen, M. Y., et al. (2019) Improving Thermal Stability of Polyurethane through the Addition of Hyperbranched Polysiloxane. *Polymers*, **11**(4), 697.

Liu, X. Q., Huang, W., et al. (2012). Preparation of a bio-based epoxy with comparable properties to those of petroleum-based counterparts. *Express Polymer Letters*, **6**(4).

Liu, X., Xin, W., & Zhang, J. (2009). Rosin-based acid anhydrides as alternatives to petrochemical curing agents. *Green Chemistry*, **11**(7), 1018-1025.

Liu, Z. S., & Erhan, S. Z. (2002). Conversion of soybean oil into ion exchange resins: Removal of copper (II), nickel (II), and cobalt (II) ions from dilute aqueous solution using carboxylate-containing resin. *Journal of Applied Polymer Science*, **84**(13), 2386-2396.

Liu, Z., Xiao, D., et al. (2021). Self-healing and reprocessing of transparent UV-cured polysiloxane elastomer. *Progress in Organic Coatings*, **159**, 106450.

Lorenz, V., Spoida, M., et al. (2001). Silsesquioxane chemistry: Part 5. New silyl-functionalized silsesquioxanes. *Journal of Organometallic Chemistry*, **625**(1), 1-6.

Ma, Y., He, L., Jet al. (2017). Cage and linear structured polysiloxane/epoxy hybrids for coatings: Surface property and film permeability. *Journal of colloid and interface science*, **500**, 349-357.

Mashouf Roudsari, G., Mohanty, A. K., & Misra, M. (2014). Study of the curing kinetics of epoxy resins with biobased hardener and epoxidized soybean oil. *ACS Sustainable Chemistry & Engineering*, **2**(9), 2111-2116.

Materić, D., Bruhn, D., et al. (2015). Methods in plant foliar volatile organic compounds research. *Applications in Plant Sciences*, **3**(12), 1500044.

Miletto, I., Ivaldi, C., et al. (2021). Predicting the Conformation of Organic Catalysts Grafted on Silica Surfaces with Different Numbers of Tethering Chains: The Silicopodality Concept. *The Journal of Physical Chemistry C*, **125**(38), 21199-21210.

Mora, A. S., Tayouo, R., et al. (2019). Synthesis of biobased reactive hydroxyl amines by amination reaction of cardanol-based epoxy monomers. *European Polymer Journal*, **118**, 429-436.

Moschandreas, D. J., & Relwani, S. M. (1992). Perception of environmental tobacco smoke odors: an olfactory and visual response. Atmospheric Environment. *Part B. Urban Atmosphere*, **26**(3), 263-269.

Motahari, A., Rostami, A. A., et al. (2015). On the thermal degradation of a novel epoxy-based nanocomposite cured with tryptophan as an environment-friendly curing agent. *Journal of Macromolecular Science, Part B*, **54**(5), 517-532.

Mustapha, R., Rahmat, A. R., et al. (2019). Vegetable oil-based epoxy resins and their composites with bio-based hardener: a short review. *Polymer-Plastics Technology and Materials*, **58**(12), 1311-1326.

Niemczyk, A., Czaja, K., et al. (2019). Functionalized siloxane silsesquioxane resins and polypropylene based composites: Morphological, structural, thermal, and mechanical properties. *Polymer Composites*, **40**(8), 3101-3114.

Noguchi, M., Tanaka, S., et al. (2016). Correlation between odor concentration and volatile organic compounds (VOC) composition of environmental tobacco smoke (ETS). *International Journal of Environmental Research and Public Health*, **13**(10), 994.

O'Brien, A. K., Cramer, N. B., & Bowman, C. N. (2006). Oxygen inhibition in thiol‐acrylate photopolymerizations. *Journal of Polymer Science Part A: Polymer Chemistry*, **44**(6), 2007-2014.

Pachón, L. D., Gamez, P., et al. (2003) Zinc-catalyzed aminolysis of epoxides. *Tetrahedron Letters*, **44**(32), 6025-6027.

Paramarta, A., & Webster, D. C. (2016). Bio-based high performance epoxy-anhydride thermosets for structural composites: The effect of composition variables. *Reactive and Functional Polymers*, **105**, 140-149.

Pelckmans, M., Renders, T., et al. (2017). Bio-based amines through sustainable heterogeneous catalysis. *Green Chemistry*, **19**(22), 5303-5331.

Persson, C., Robert, E., et al. (2015). The effect of unsaturated fatty acid and triglyceride oil addition on the mechanical and antibacterial properties of acrylic bone cements. *Journal of Biomaterials Applications*, **30**(3), 279-289.

Polvara, E., Capelli, L. M. T., & Sironi, S. (2021). Non-carcinogenic occupational exposure risk related to foundry emissions: focus on the workers involved in olfactometric assessments. *Journal of Environmental Science and Health, Part A*, 1-14.

Quadrelli, E. A., & Basset, J. M. (2010). On silsesquioxanes' accuracy as molecular models for silica-grafted complexes in heterogeneous catalysis. *Coordination Chemistry Reviews*, **254**(5-6), 707-728.

Radojčić, D., Hong, J., et al. (2016) Study on the reaction of amines with internal epoxides. *European Journal of Lipid Science and Technology*, **118**(10), 1507 - 1511.

Radojčić, D., Petrović, Z. S., et al. (2020). Silica-Filled Composites from Epoxidized Natural Oils. *Journal of Polymers and the Environment*, **28**(4), 1292-1301.

Ritzenthaler, S. A. B. C., Court, F., et al. (2003). ABC triblock copolymers/epoxy− diamine blends. 2. Parameters controlling the morphologies and properties. *Macromolecules*, **36**(1), 118-126.

Sahin, M., Ayalur Karunakaran, S., et al. (2017). Thiol Ene versus Binary Thiol - Acrylate Chemistry: Material Properties and Network

Characteristics of Photopolymers. *Advanced Engineering Materials*, **19**(4), 1600620.

Saithai, P., Lecomte, J., et al. (2013). Effects of different epoxidation methods of soybean oil on the characteristics of acrylated epoxidized soybean oil-co-poly(methyl methacrylate) copolymer. *Express Polymer Letters*, **7**(11), 910 - 924.

Sharma, N., & Jha, S. (2020). Amorphous nanosilica induced toxicity, inflammation and innate immune responses: A critical review. *Toxicology*, **441**, 152519.

Shelkovnikov, V. V., Ektova, L. V., et al. (2015). Synthesis and thermomechanical properties of hybrid photopolymer films based on the thiol-siloxane and acrylate oligomers. *Journal of materials science*, **50**(23), 7544-7556.

Sierke, J. K., & Ellis, A. V. (2015). High purity synthesis of a polyhedral oligomeric silsesquioxane modified with an antibacterial. *Inorganic Chemistry Communications*, **60**, 41-43.

Su, Y., Filho, E. B., et al. (2019). High Refractive Index Polymers (n> 1.7), Based on Thiol - Ene Cross-Linking of Polarizable P═S and P═ Se Organic/Inorganic Monomers. *Macromolecules*, **52**(22), 9012-9022.

Szołyga, M., Dutkiewicz, M., & Marciniec, B. (2018). Polyurethane composites based on silsesquioxane derivatives of different structures. *Journal of Thermal Analysis and Calorimetry*, **132**(3), 1693-1706.

Tarvainen, K., Jolanki, R., et al. (1998). Occupational allergic contact dermatitis from isophoronediamine (IPDA) in operative clothing manufacture. *Contact Dermatitis*, **39**(1), 46-47.

Tavakoli, S. M. (2003). An assessment of skin sensitisation by the use of epoxy resin in the construction industry. *HSE Books*, 1-32.

Tran, T. N., Mauro, C. D., et al. (2020). Chemical Reactivity and the Influence of Initiators on the Epoxidized Vegetable Oil/Dicarboxylic Acid System. *Macromolecules*, **53**(7), 2526-2538.

Unsworth, J., & Li, Y. (1992). Thermal degradation of epoxy/silica composites monitored via dynamic mechanical thermal analysis. *Journal of Applied Polymer Science*, **46**(8), 1375-1379.

Vilarinho, F., Sendón, R., et al. (2019). Bisphenol A in food as a result of its migration from food packaging. *Trends in food science & technology*, **91**, 33-65.

Villberg, K., Veijanen, A., et al. (1997). Analysis of odour and taste problems in high-density polyethene. *Journal of Chromatography A*, **791**(1-2), 213-219.

Wang, H., Gao, X., et al. (2012). Effect of amine functionalization of SBA-15 on controlled baicalin drug release. *Ceramics International*, **38**(8), 6931-6935.

Wang, L., Hu, C., & Shao, L. (2017). The antimicrobial activity of nanoparticles: present situation and prospects for the future. *International Journal of Nanomedicine*, **12**, 1227.

Wang, Z., Yuan, L., et al. (2017). Plant Oil-Derived Epoxy Polymers toward Sustainable Biobased Thermosets. *Macromolecular Rapid Communications*, **38**(11), 1700009.

Warwel, S. (1999). Complete and partial epoxidation of plant oils by lipase-catalyzed perhydrolysis. *Industrial Crops and Products*, **9**(2), 125-132.

Wrona, M., Vera, P., et al. (2017). Identification and quantification of odours from oxobiodegradable polyethylene oxidised under a free radical flow by headspace solid-phase microextraction followed by gas chromatography-olfactometry-mass spectrometry. *Talanta*, **172**, 37-44.

Xie, Y., Hill, C. A., et al. (2010). Silane coupling agents used for natural fiber/polymer composites: A review. *Composites Part A: Applied Science and Manufacturing*, **41**(7), 806-819.

Xu, H., Liu, Z., et al. (2018). Impacts of different functional groups on the kinetic rates of α-amine ketoximesilanes hydrolysis in the preparation of room temperature vulcanized silicone rubber. *Materials*, **11**(5), 790.

Xu, Y., Long, J., et al. (2020). Greatly improving thermal stability of silicone resins by modification with POSS. *Polymer Degradation and Stability*, **174**, 109082.

Xue, L., Wang, D., et al. (2013). Facile, versatile and efficient synthesis of functional polysiloxanes via thiol‐ene chemistry. *European polymer journal*, **49**(5), 1050-1056.

국문초록

디글리시딜 에테르 비스페놀 A (DGEBA)는 석유자원을 기반으로 하는 대표적인 에폭시 수지로 내분비계를 교란시키는 물질인 비스페놀 A를 주원료로 하고 있다. 에폭시 수지는 물론 에폭시 수지와 함께 사용되는 에폭시 경화제 역시 독성이 강해 노출 시 인체와 환경에 부정적인 영향을 미치는 것으로 알려져 있다. 이러한 환경 및 건강위해성에 대한 문제가 지속적으로 제기되면서 석유 기반 고분자 재료를 대체할 바이오 기반 고분자에 대한 수요가 증가하고 있다. 따라서 본 연구에서는 지속가능한 에폭시 네트워크를 개발하고자 화학적으로 변형이 가능하고 상업적으로 이용가능한 대두유 기반 에폭시 수지를 DGEBA 대체제로 제시하였다. 더 나아가, 보다 지속가능한 에폭시 경화제의 대안으로, 독성이 없고 석유에 의존하지 않는 새로운 싸이올계 폴리실록산 올리고머를 졸-겔 공법을 이용하여 합성하였다. 합성된 싸이올계 폴리실록산 올리고머는 실록산 (Si-O-Si) 망상구조의 분자로 되어있기 때문에 유-무기 하이브리드 네트워크를 형성하여 식물성 오일의 낮은 반응성과 비선택적인 반응성을 개선시키고자 하였다.

결과적으로 싸이올-앤/싸이올-에폭시 중합체는 아크릴화된 에폭시드 대두유 (AESO)와 에폭시드 대두유 (ESO)에 화학량론적 당량의 싸이올계 폴리실록산 올리고머를 각각 첨가한 다음, UV 및 열경화 반응을 순차적으로 적용하여 얻어졌다. 이중경화 공정에서 광중합과 열중합의 조합은 형성된 싸이올-앤/싸이올-에폭시 네트워크의 기계적 특성과 가교밀도를 향상시킬 수 있었다. 특히, 이중경화 샘플 중 75A/25E 중합체는 단독으로 경화된 싸이올-앤 및 싸이올-에폭시 중합체보다 더 우수한 가교밀도, 유리 전이 온도와 storage modulus 값을 보여주었다.

합성된 에폭시 경화제 중에서는 TSQ 올리고머가 TSO 올리고머에 비해 싸이올-앤 중합 속도뿐만 아니라 가교밀도, 기계적 물성 및 항균성을 더욱 향상시키는 것으로 나타났다. 반면, VOCs 방출량은 TSQ 올리고머보다 TSO 올리고머에서 더 낮은 것으로 관찰되었다.

대두유 기반 에폭시 수지의 한계를 극복하려는 이러한 시도들이 향후 지속가능한 에폭시 네트워크를 구축할 것으로 기대된다.

주요어 : 싸이올-앤/싸이올-에폭시, 이중경화, 폴리실록산, 에폭시화 된 대두유, 유-무기 네트워크, 가교밀도

학 번 : 2020-28661

Appendix. Supplementary data

Appendix. Supplementary data

(A)

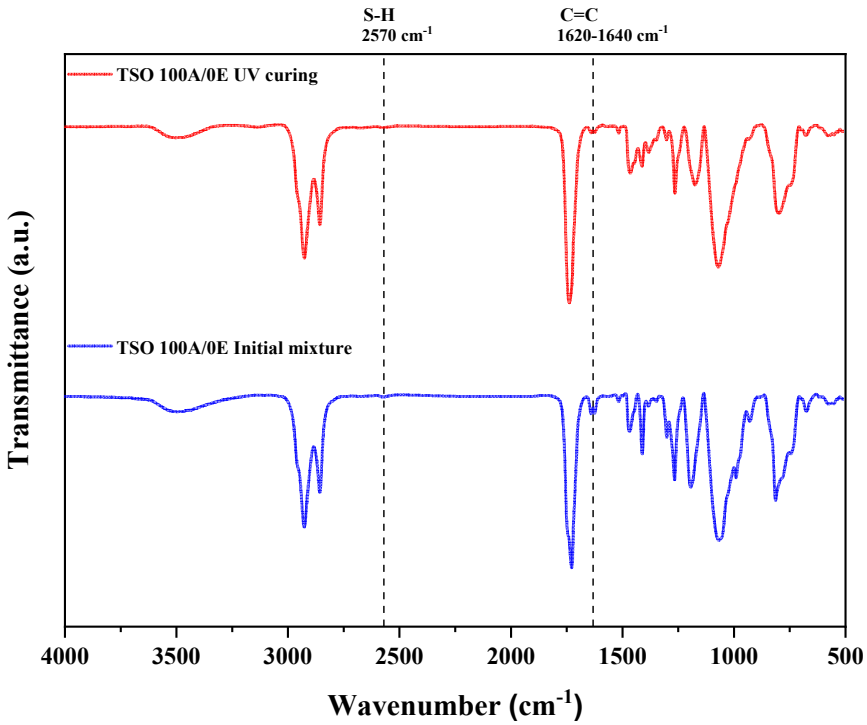
S-H
2570 cm-1
C=C
1620-1640 cm-1
TSO 100A/0E UV curing
TSO 100A/0E Initial mixture
Transmittance (a.u.)
4000
3500
3000
2500
2000
1500
1000
500
Wavenumber (cm-1)

(a)

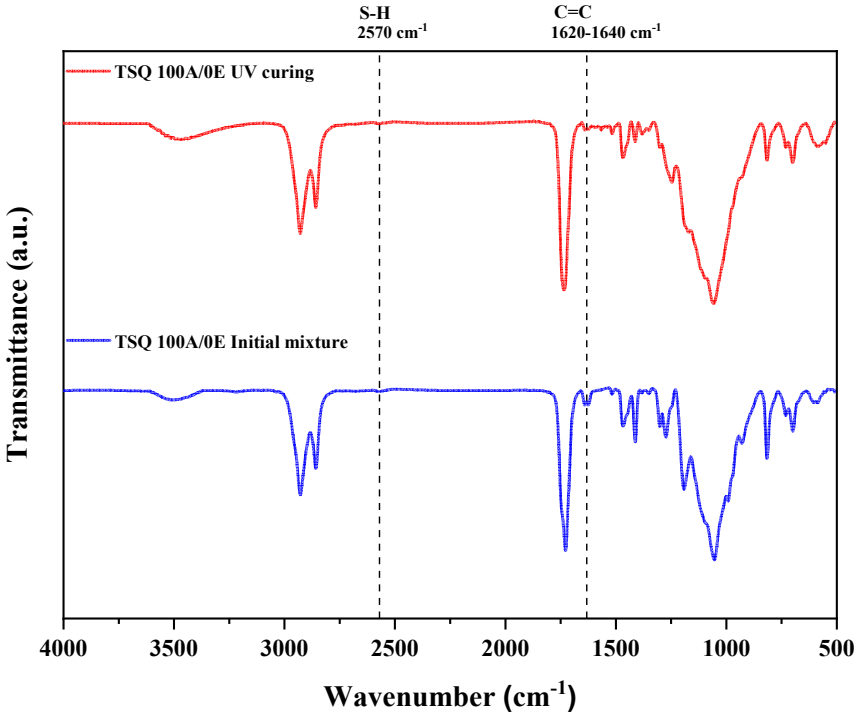
S-H
2570 cm-1
C=C
1620-1640 cm-1
TSQ 100A/0E UV curing
TSQ 100A/0E Initial mixture
Transmittance (a.u.)
4000
3500
3000
2500
2000
1500
1000
500
Wavenumber (cm-1)

(B)

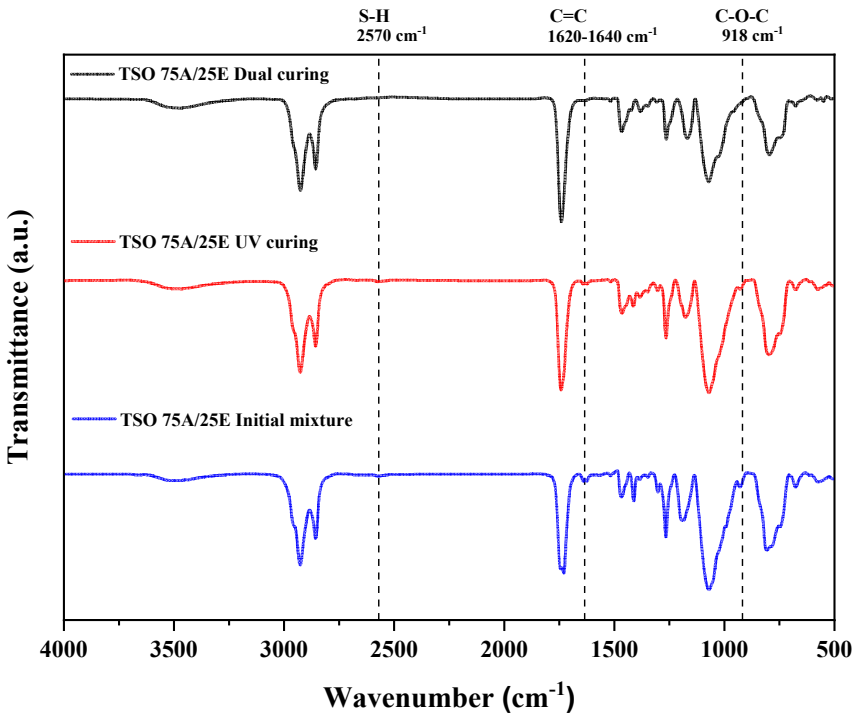
S-H
2570 cm-1
C=C
1620-1640 cm-1
C-O-C
918 cm-1
TSO 75A/25E Dual curing
TSO 75A/25E UV curing
TSO 75A/25E Initial mixture
Transmittance (a.u.)
4000
3500
3000
2500
2000
1500
1000
500
Wavenumber (cm-1)

(b)

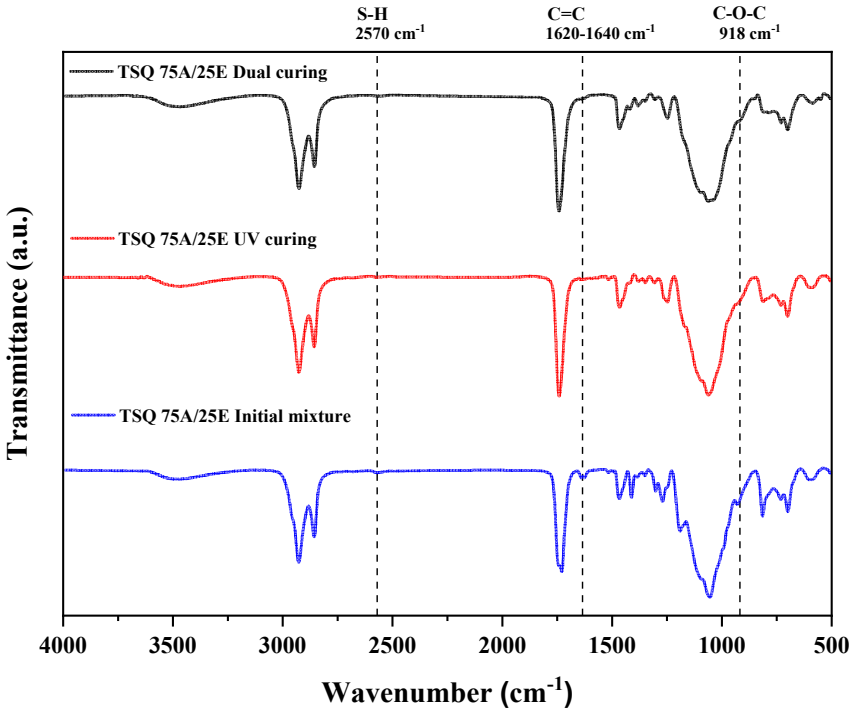
S-H
2570 cm-1
C=C
1620-1640 cm-1
C-O-C
918 cm-1
TSQ 75A/25E Dual curing
TSQ 75A/25E UV curing
TSQ 75A/25E Initial mixture
Transmittance (a.u.)
4000
3500
3000
2500
2000
1500
1000
500
Wavenumber (cm-1)

(C)

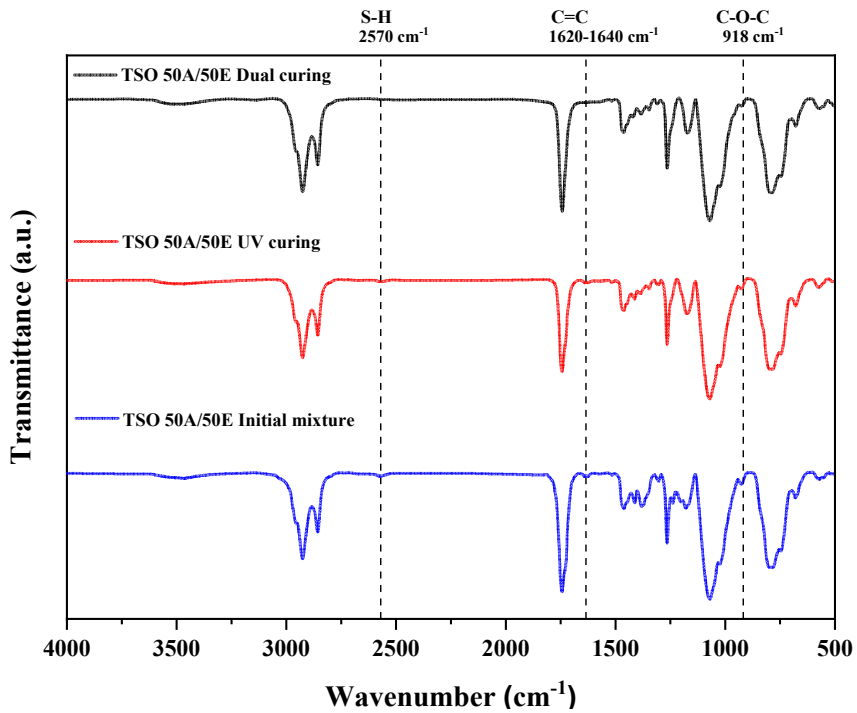
S-H
2570 cm-1
C=C
1620-1640 cm-1
C-O-C
918 cm-1
TSO 50A/50E Dual curing
TSO 50A/50E UV curing
TSO 50A/50E Initial mixture
Transmittance (a.u.)
4000
3500
3000
2500
2000
1500
1000
500
Wavenumber (cm-1)

(c)

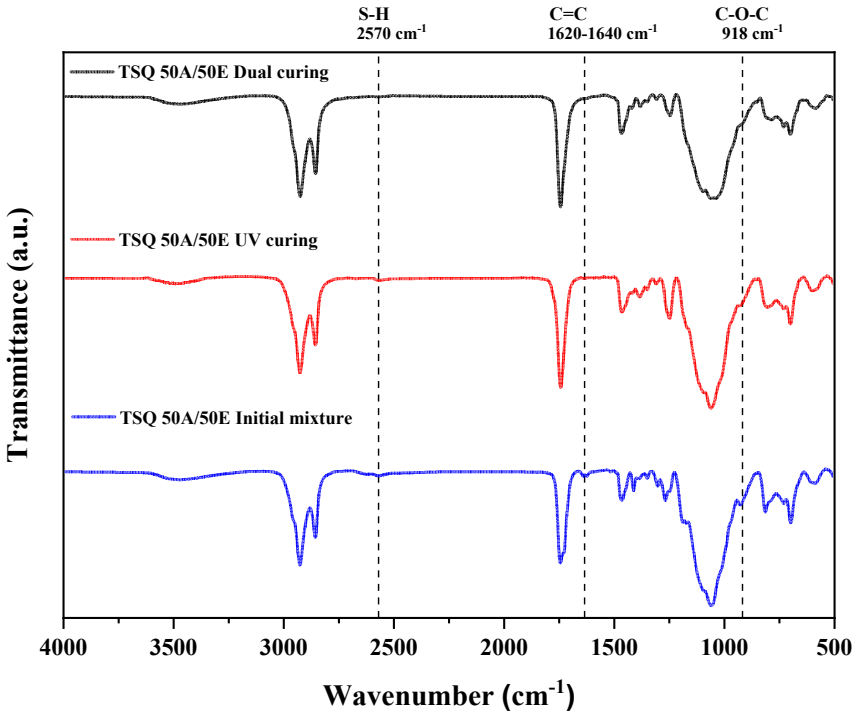
S-H
2570 cm-1
C=C
1620-1640 cm-1
C-O-C
918 cm-1
TSQ 50A/50E Dual curing
TSQ 50A/50E UV curing
TSQ 50A/50E Initial mixture
Transmittance (a.u.)
4000
3500
3000
2500
2000
1500
1000
500
Wavenumber (cm-1)

(D)

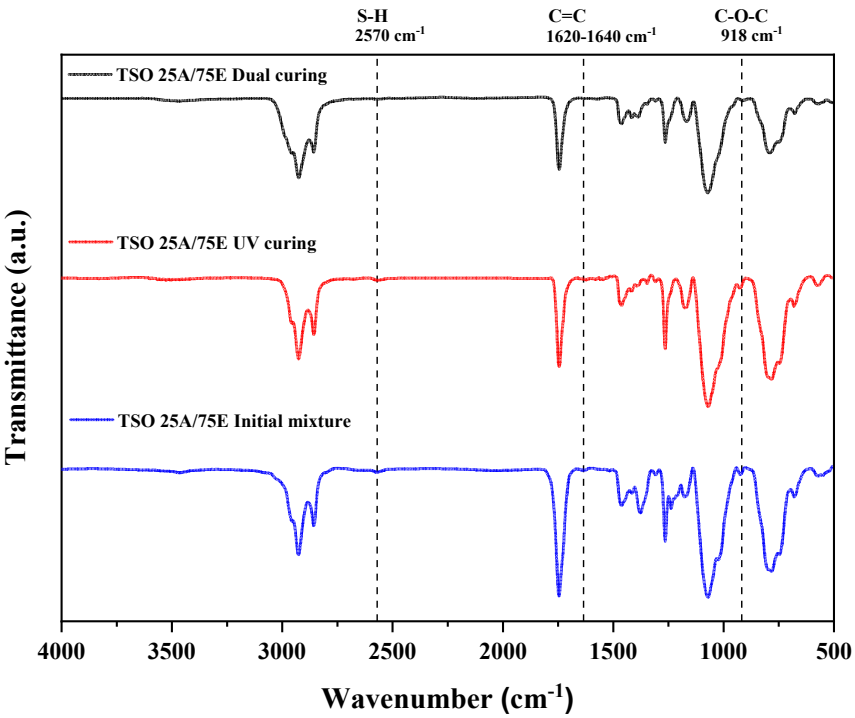
S-H
2570 cm-1
C=C
1620-1640 cm-1
C-O-C
918 cm-1
TSO 25A/75E Dual curing
TSO 25A/75E UV curing
TSO 25A/75E Initial mixture
Transmittance (a.u.)
4000
3500
3000
2500
2000
1500
1000
500
Wavenumber (cm-1)

(d)

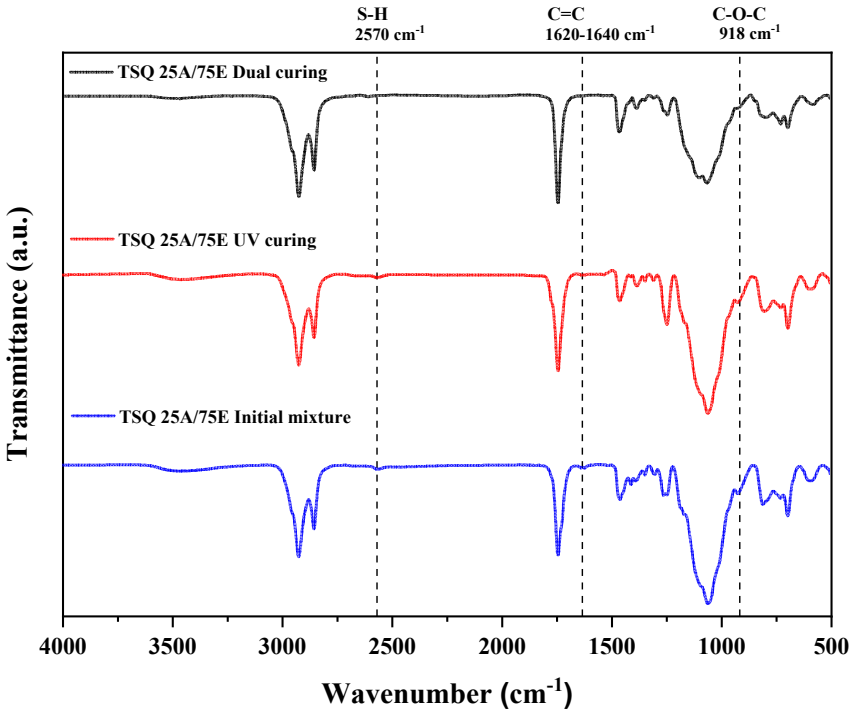
S-H
2570 cm-1
C=C
1620-1640 cm-1
C-O-C
918 cm-1
TSQ 25A/75E Dual curing
TSQ 25A/75E UV curing
TSQ 25A/75E Initial mixture
Transmittance (a.u.)
4000
3500
3000
2500
2000
1500
1000
500
Wavenumber (cm-1)

(E)

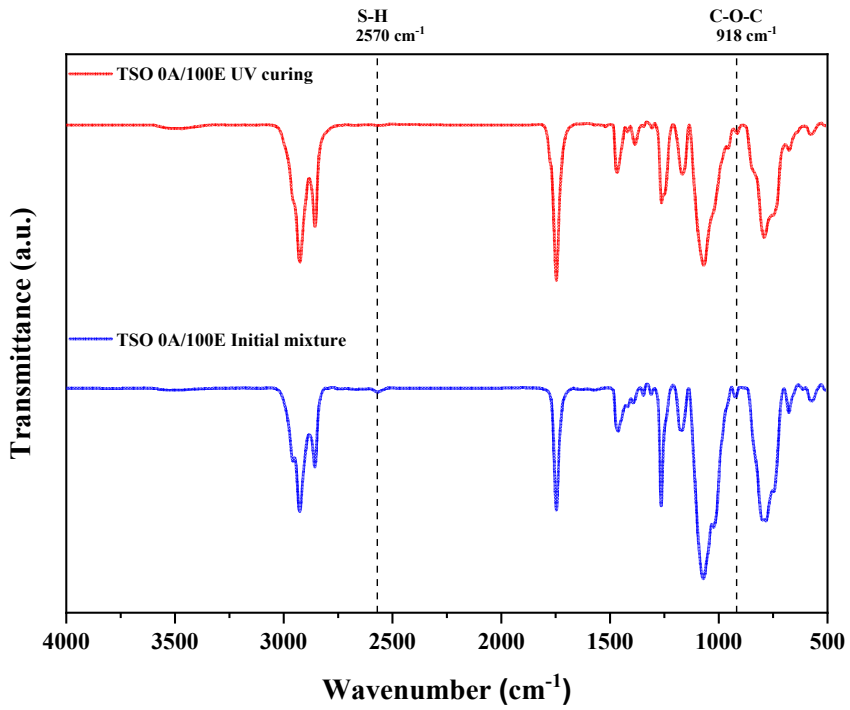
S-H
2570 cm-1
C-O-C
918 cm-1
TSO 0A/100E UV curing
TSO 0A/100E Initial mixture
Transmittance (a.u.)
4000
3500
3000
2500
2000
1500
1000
500
Wavenumber (cm-1)

(e)

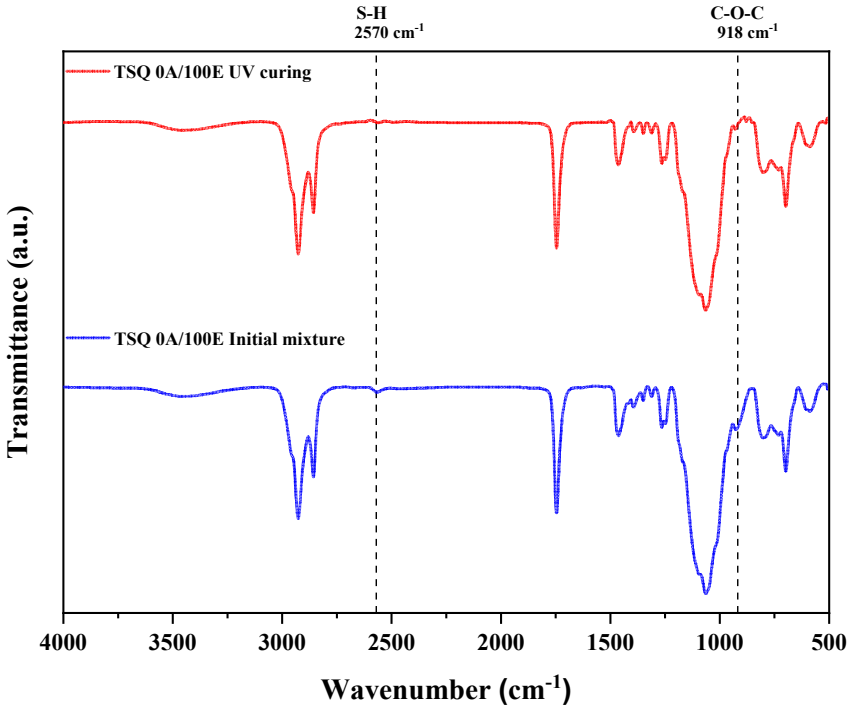

Figure S1. FT-IR spectra according to thiol-ene/thiol-epoxy networks curing behavior (A, a) TSO/TSQ 100A/0E (B, b) TSO/TSQ 75A/25E (C, c) TSO/TSQ 50A/50E (D, d) TSO/TSQ 25A/100E (E, e) TSO/TSQ 0A/100E

(A)

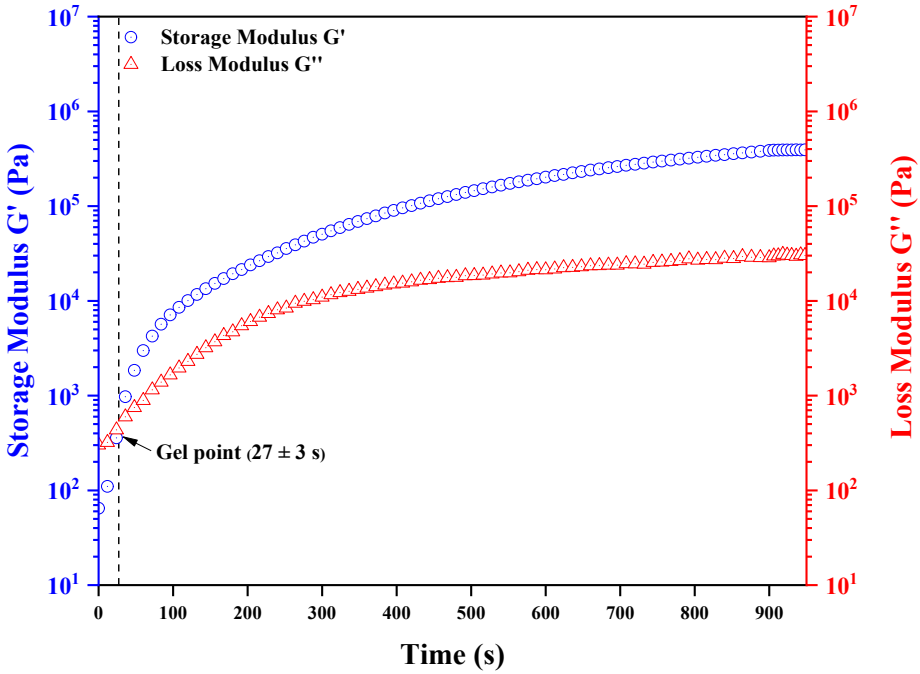
Storage Modulus G'
Loss Modulus G''
Gel point (27 ± 3 s)
Storage Modulus G' (Pa)
Loss Modulus G'' (Pa)
Time (s)

(a)

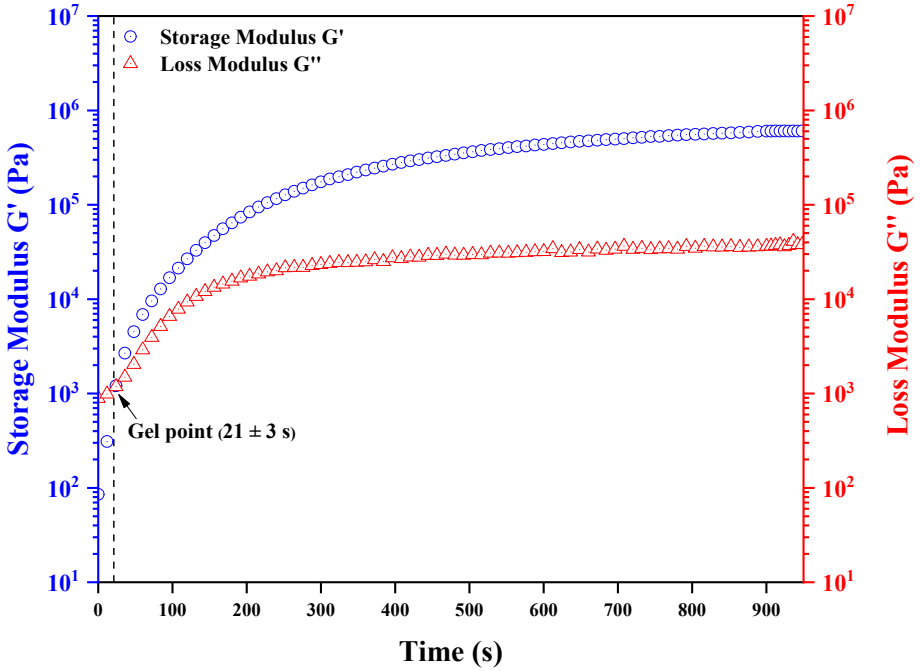
Storage Modulus G'
Loss Modulus G''
Gel point (21 ± 3 s)
Storage Modulus G' (Pa)
Loss Modulus G'' (Pa)
Time (s)

(B)

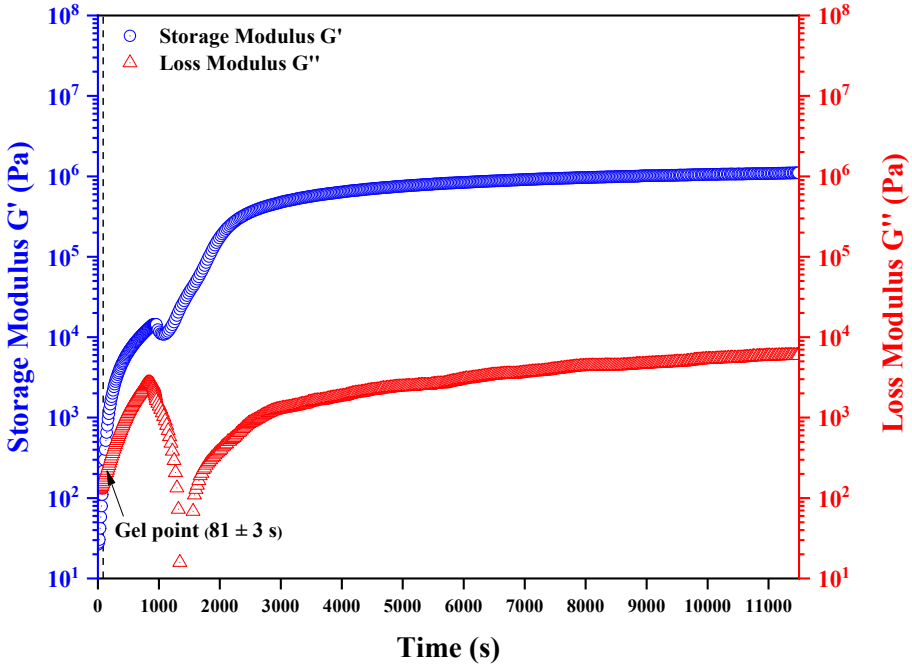
Storage Modulus G'
Loss Modulus G''
Gel point (81 ± 3 s)
Storage Modulus G' (Pa)
Loss Modulus G'' (Pa)
Time (s)

(b)

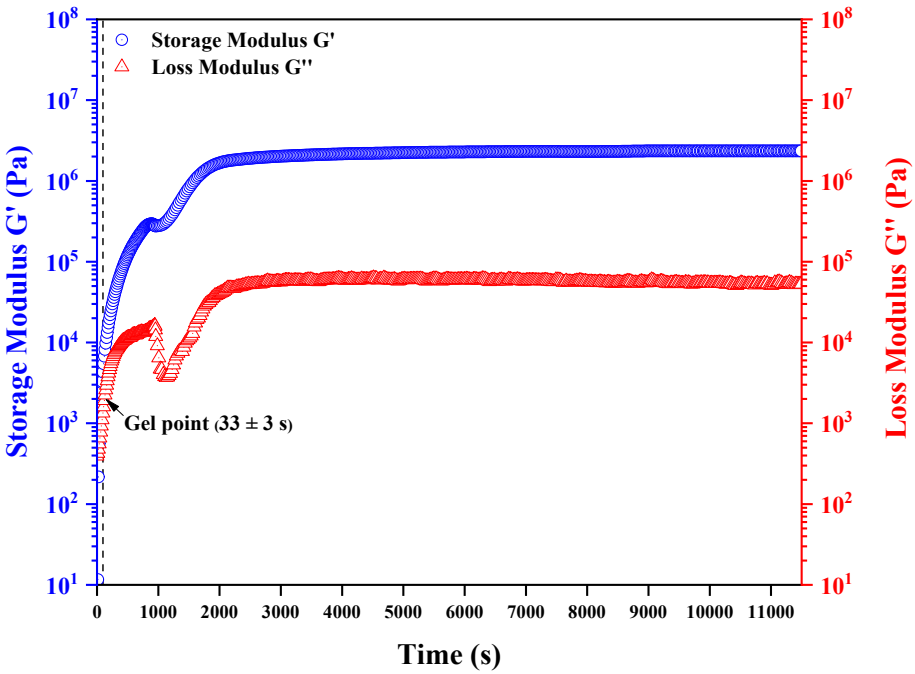
Storage Modulus G'
Loss Modulus G''
Gel point (33 ± 3 s)
Storage Modulus G' (Pa)
Loss Modulus G'' (Pa)
Time (s)

(C)

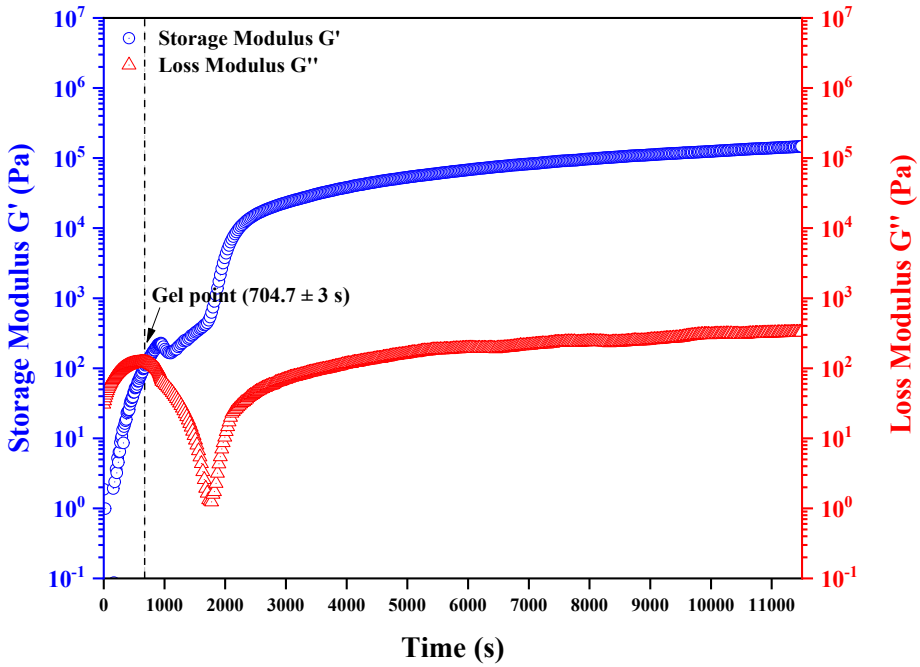
Storage Modulus G'
Loss Modulus G''
Gel point (704.7 ± 3 s)
Storage Modulus G' (Pa)
Loss Modulus G'' (Pa)
Time (s)

(c)

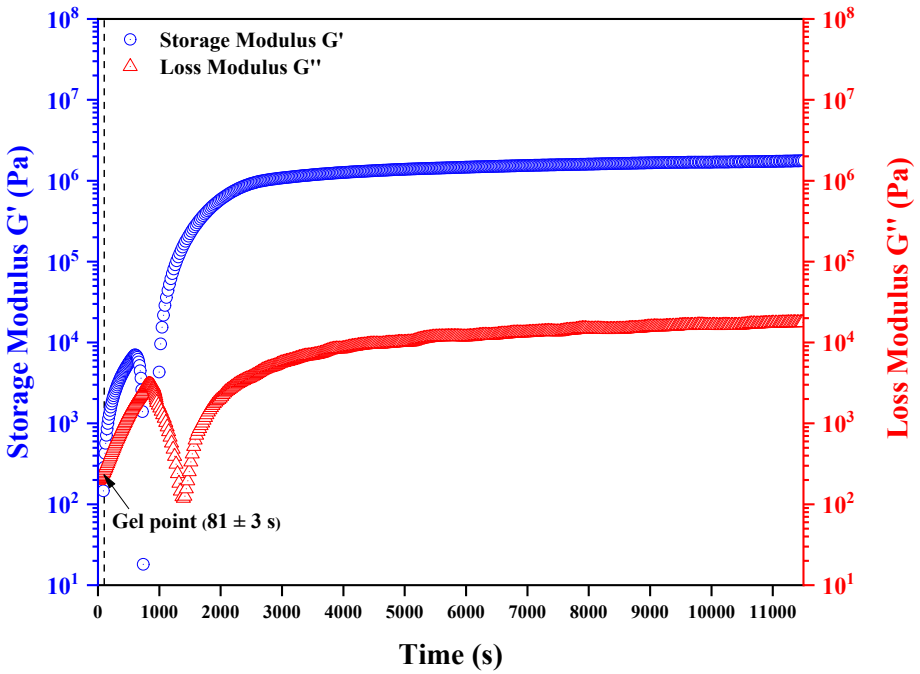
Storage Modulus G'
Loss Modulus G''
Gel point (81 ± 3 s)
Storage Modulus G' (Pa)
Loss Modulus G'' (Pa)
Time (s)

(D)

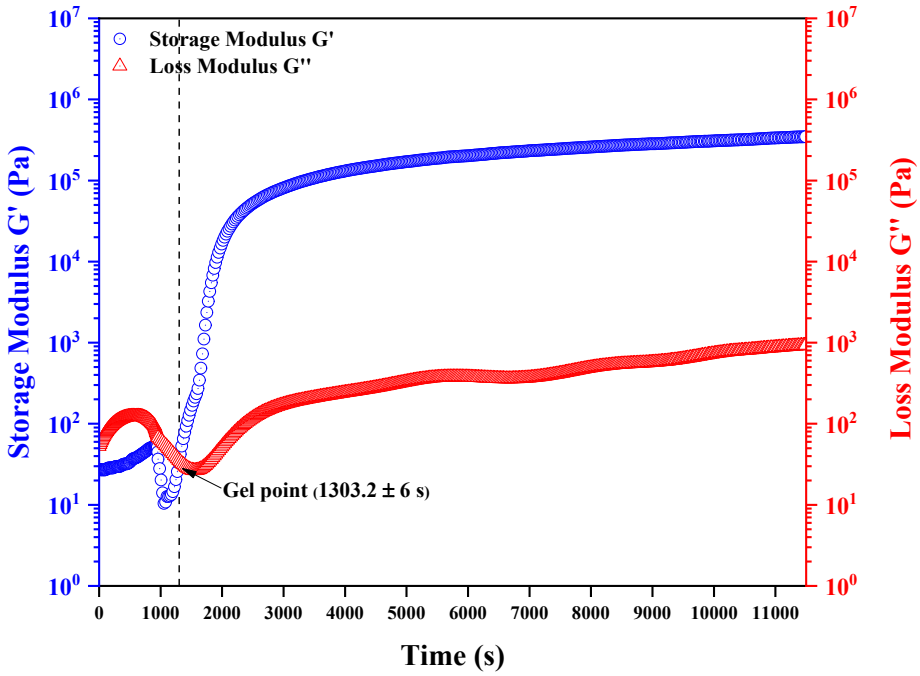
Storage Modulus G'
Loss Modulus G''
Storage Modulus G' (Pa)
Loss Modulus G'' (Pa)
Gel point (1303.2 ± 6 s)
Time (s)

(d)

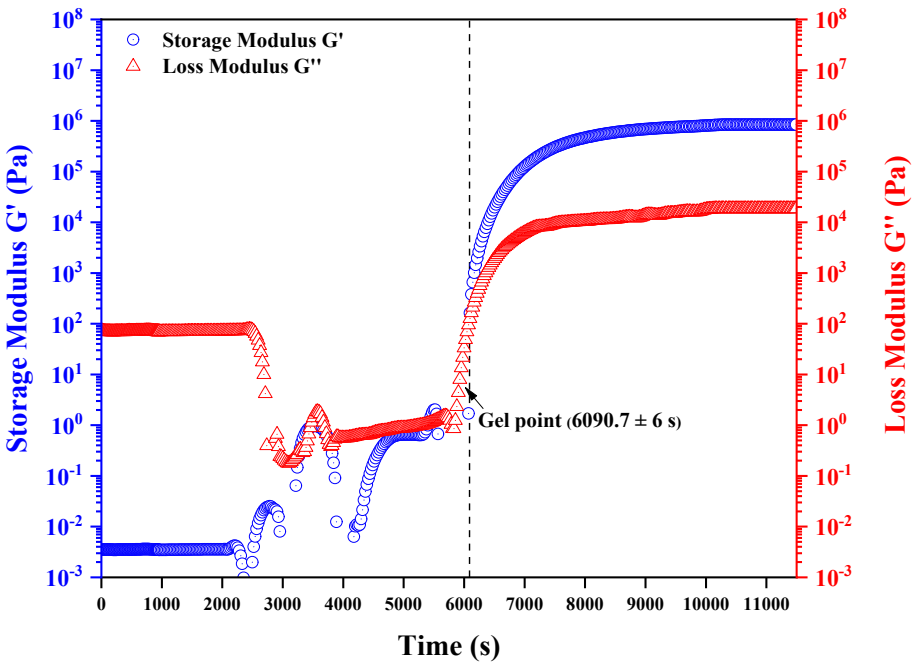
Storage Modulus G'
Loss Modulus G''
Storage Modulus G' (Pa)
Loss Modulus G'' (Pa)
Gel point (6090.7 ± 6 s)
Time (s)

(E)

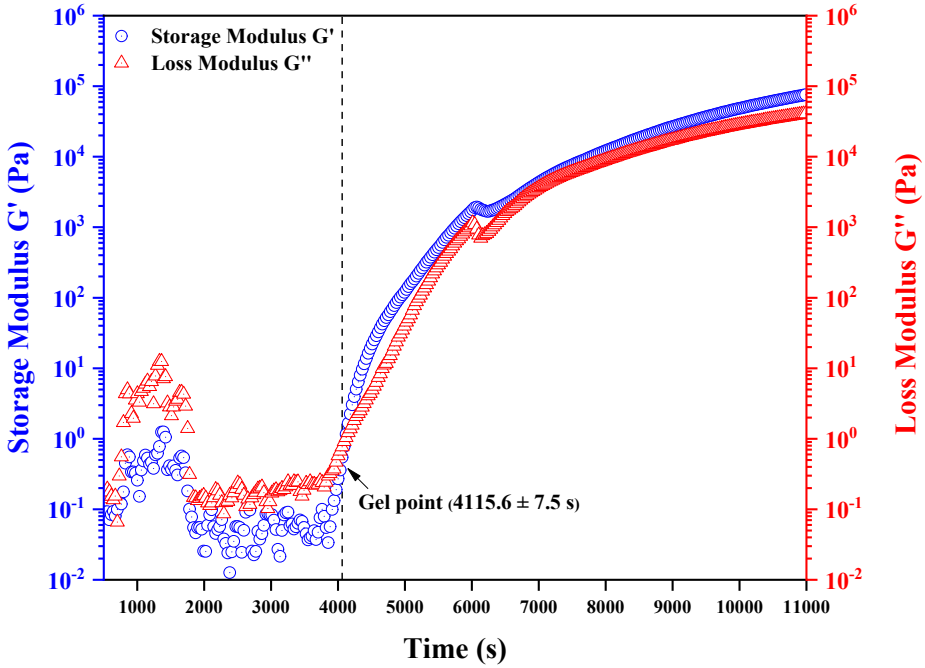
Storage Modulus G'
Loss Modulus G''
Storage Modulus G' (Pa)
Loss Modulus G'' (Pa)
Gel point (4115.6 ± 7.5 s)
Time (s)

(e)

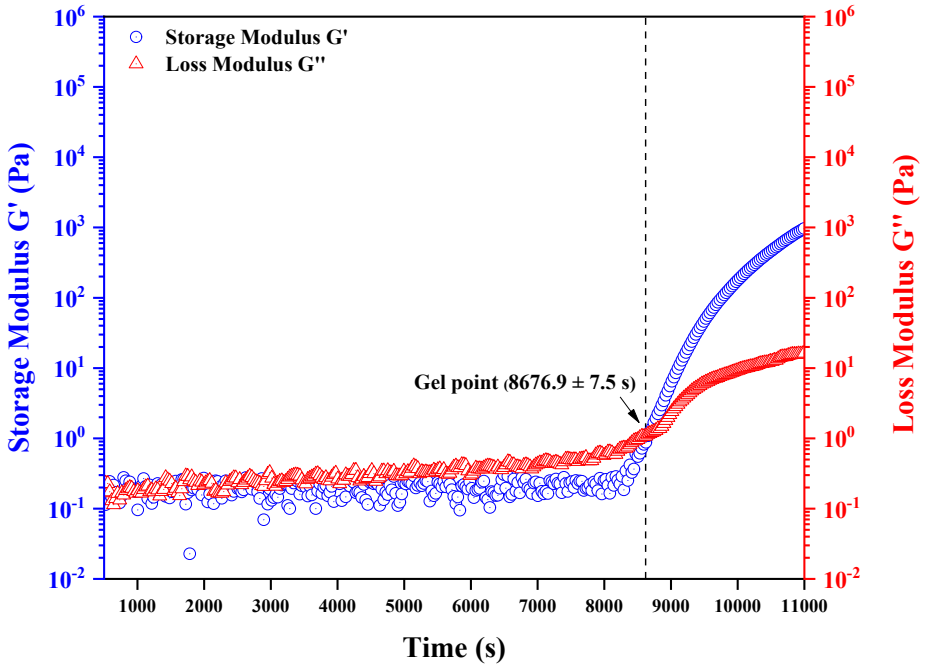
Storage Modulus G'
Loss Modulus G''
Storage Modulus G' (Pa)
Loss Modulus G'' (Pa)
Gel point (8676.9 ± 7.5 s)
Time (s)

Figure S2. Monitoring crosslinking kinetics of thiol-ene/thiol-epoxy networks (A, a) TSO/TSQ 100A/0E (B, b) TSO/TSQ 75A/25E (C, c) TSO/TSQ 50A/50E (D, d) TSO/TSQ 25A/100E (E, e) TSO/TSQ 0A/100E